BINDING AND REPAIR OF DNA

BY SPORE PHOTOPRODUCT LYASE

by

Egidijus Zilinskas

A dissertation submitted in partial fulfillment
of the requirements for the degree

of

Doctor of Philosophy

in

Biochemistry

MONTANA STATE UNIVERSITY
Bozeman, Montana

May 2010

APPROVAL

of a dissertation submitted by

Egidijus Zilinskas

This dissertation has been read by each member of the dissertation committee and has been found to be satisfactory regarding content, English usage, format, citation, bibliographic style, and consistency, and is ready for submission to the Division of Graduate Education.

Dr. Joan B. Broderick

Approved for the Department of Chemistry and Biochemistry

Dr. David Singel

Approved for the Division of Graduate Education

Dr. Carl A. Fox

STATEMENT OF PERMISSION TO USE

In presenting this dissertation in partial fulfillment of the requirements for a doctoral degree at Montana State University, I agree that the Library shall make it available to borrowers under rules of the Library. I further agree that copying of this dissertation is allowable only for scholarly purposes, consistent with "fair use" as prescribed in the U.S. Copyright Law. Requests for extensive copying or reproduction of this dissertation should be referred to ProQuest Information and Learning, 300 North Zeeb Road, Ann Arbor, Michigan 48106, to whom I have granted "the exclusive right to reproduce and distribute my dissertation in and from microform along with the non-exclusive right to reproduce and distribute my abstract in any format in whole or in part."

Egidijus Zilinskas

May 2010

DEDICATION

This work is dedicated to my girlfriend and my parents, who always supported me and helped me.

ACKNOWLEDGEMENTS

I would like to express my gratitude to my advisor Dr. Joan Broderick, who has guided me throughout my graduate career. Without her advice and support, I never would have achieved this goal.

I would also like to acknowledge my graduate committee members, Dr. Brian Bothner, Dr. Martin Teinze, Dr. Valerie Copie, Dr. Bern Kohler, and Dr. Gregory Johnson.

I would like to thank Dr. Gregory Gillispie (Fluorescence Innovations) and Candace Lange for helping me with time-resolved fluorescence experiments.

I would like to thank Dr. Tilak Chandra for making spore photoproduct that was essential for my experiments. I would also like to thank him for all the discussions we had about our project (and not only). I would like to acknowledge Sunshine Silver for providing me with the small, acid soluble protein necessary for the experiments. Also, I would like to thank her for doing the repair assays and for the discussions that we had. I would like to acknowledge Dr. Will Broderick for teaching the anaerobic techniques and inorganic chemistry. I would like to give my thanks to Dr. Eric Shepard and Dr. Robert Szilagiy for doing DFT calculations on spore photoproduct dinucleoside. Also, I would like to thank Eric for teaching me how to use ORIGIN software and helping with me HPLC. Also I would like to thank Dr. Susan Veneziano for helping me with writing my dissertation. I would like to thank all of my lab mates, who also helped me (one way or another) and influenced my research: Kaitlin Duschene, Shourjo Ghose, Rachel Udelhoven, Lexxy Bueling, Adam Crain, Benjamin Duffus.

TABLE OF CONTENTS

TABLE OF CONTENTS - CONTINUED

TABLE OF CONTENTS – CONTINUED

LIST OF TABLES

Table Page

LIST OF SCHEMES

Scheme Page

LIST OF FIGURES

Figure Page

LIST OF FIGURES – CONTINUED

Figure Page

LIST OF FIGURES – CONTINUED

Figure Page

LIST OF ABBREVIATIONS

5’dAdo ..... 5’-deoxyadenosine
AdoCbl ..... adenosylcobalamin
AdoMet ..... S-adenosyl-L-methionine
AnRNR ..... anaerobic ribonucleotide reductase
ATP ..... adenosine triphosphate
APS ..... ammonium persulfate
B. subtilus ..... *Bacillus subtilis*
BER ..... base excision repair
BioB ..... biotin synthase
β-ME ..... β-mercaptoethanol
BSA ..... bovine serum albumin
C. acetobutylicum ..... *Clostridium acetobutylicum*
CPD ..... cyclobutane pyrimidine dimer
CPM ..... counts per minute
DFT ..... density functional theory
D. hafniense ..... *Desulfitobacterium hafniense*
DNA ..... deoxyribonucleic acid
DPM ..... disintegrations per minute
DTT ..... dithiothreitol
EDTA ..... ethylenedinitrolotetra-acetic acid disodium salt dehydrate
EMSA ..... electrophoretic mobility shift assay
ENDOR ..... electron nuclear double resonance
EPR ..... electron paramagnetic resonance
EXAFS ..... extended X-ray absorbtion fine structure
FAD ..... flavin adenine dinucleotide
FPLC ..... fast protein liquid chromatography
HemN ..... oxygen independent coproporphyrinogen-III-oxidase
HEPES ..... 4-(2-hydroxyethyl)-1-piperazineethanesulfonic acid
HhH ..... helix-hairpin-helix
HPLC ..... high performance liquid chromatography
H-T-H ..... helix-turn-helix
E. coli ..... *Escherichia coli*
IMAC ..... immobilized metal affinity chromatography
IPTG ..... isopropyl-β-D-thioglactopyranoside
LAM ..... lysine 2,3 –aminomutase
LB ..... Luria-Bertani
LMCT ..... ligand to metal charge transfer
NER ..... nucleotide excision repair
NMR ..... nuclear magnetic resonance
MM ..... minimal media
MOPS ..... 3-(N-morpholino) propanesulfonic acid
PCR ..... polymerase chain reaction

LIST OF ABBREVIATIONS - CONTINUED

PFL.....pyruvate formate lyase
PFL-AE.....pyruvate formate lyase activating enzyme
PMSF.....phenylmethyl sulfonyl fluoride
RDase.....reductive dehalogenase
RNA.....ribonucleic acid
SAM.....*S*-adenosyl-L-methionine
SDS-PAGE.....sodium dodecyl sulfate-polyacrylamide gel electrophoresis
SP.....spore photoproduct
SPL.....spore photoproduct lyase
SASP.....small acid soluble protein
T.....thymine
TEMED.....N,N,N',N'-tetra-methyl-ethylendiamine
TFA.....triflouroacetic acid
TpT.....thymidylyl (3'-5') thymidine

ABSTRACT

Bacterial spores are extremely resistant to chemical and physical stresses, including UV irradiation, which in spores results in the formation of 5-thyminyl-5,6-dihydrothymine (spore photoproduct, SP). While SP accumulates in UV-irradiated bacterial spores, it is rapidly repaired during germination. Spore photoproduct lyase (SPL) is the enzyme that catalyzes the specific repair of spore photoproduct to two thymines. It utilizes *S*-adenosylmethionine (SAM) and a [4Fe-4S] cluster to catalyze this reaction, and is a member of the radical SAM superfamily. Presented here is an investigation of SPL repair activity towards stereochemically-defined synthetic *R*- and *S*-spore photoproduct dinucleosides and dinucleotides (SP and SPTpT, respectively), utilizing SPL purified from *Clostridium acetobutylicum*. The results of HPLC and Mass Spectrometry analysis of *in vitro* enzymatic assays demonstrate that SPL specifically repairs the *5R*-, but not the 5*S*- isomer. The repair rates were determined to be ~0.4 nmol/min/mg of SPL for the 5*R*-SP dinucleoside and ~7.1 nmol/min/mg of SPL for the 5*R*-SPTpT dinucleotide. Since SPL binding to DNA is a key step in UV damage repair, SPL binding to undamaged DNA, as well as the 5*R*- and the 5*S*-isomers of SP and SPTpT, was also investigated. The binding to different substrates was investigated by carrying out electrophoretic mobility shift assays (EMSA) and time-resolved fluorescence decay experiments. SPL from both *Bacillus subtilis* and *Clostridium acetobutylicum* cooperatively binds the undamaged DNA with relatively high affinity (K_d = 4.7 x 10^{-9} M for *B.s.* SPL and K_d = 1.7 x 10^{-7} M for *C.a.* SPL). The presence of small, acid-soluble proteins (SASP), SAM or the [4Fe-4S] cluster of SPL have little effect on SPL binding to undamaged DNA. Interestingly, SPL is able to bind both the 5*R*- and the 5*S*- diastereomers of the synthetic dinucleoside/dinucleotide spore photoproduct, although only the 5*R*-isomer is repaired. SP lyase binding is stronger to the SPTpT dinucleotide than to the SP dinucleoside, likely due to the dinucleotide more closely resembling the natural substrate in double helical DNA. Also, SPL exhibits higher affinity towards SP and SPTpT than the repair products, thymidine or thymidylyl (3'-5') thymidine (TpT), respectively.

CHAPTER 1

INTRODUCTION

Spores, Spore Photoproduct and Small, Acid-Soluble Proteins

The chemical stability of DNA is one of the prerequisites of life. Even though DNA is a stable molecule, this stability alone is not sufficient for its role as the long-term carrier of genetic information. DNA can undergo spontaneous alterations and also can be damaged by physical and chemical agents. This sensitivity to external factors is a particular challenge for bacterial spores, which may exist for long periods of time under harsh conditions (1-4). Spores can survive for many years in the presence of, for example, heat, UV light, desiccation, radiation and chemicals, by being metabolically dormant; inside of the spore there is very little or no enzymatic activity. As a specific example of spore resistance to external stresses, spores are 10- to 50- times more resistant to UV light at 254 nm than are growing cells. Sporulation occurs in several types of bacteria, including *Bacillus* and *Clostridium* species, and is usually triggered by reduced levels of nutrients or water. Spores can remain dormant for long periods of time and then return to life when nutrients become available. If the DNA inside of spores gets damaged during the dormancy, it has to be repaired during germination to ensure survival of the organism.

The spore structure (Figure 1.1) and chemical composition play very important roles in its resistance and survival. In addition to the contents present in vegetative cells,

the spore core also contains high concentrations of minerals, pyridine-2,6-dicarboxylic acid (or dipicolinic acid, DPA, Figure 1.2) and small, acid-soluble proteins (SASPs)(5,6).

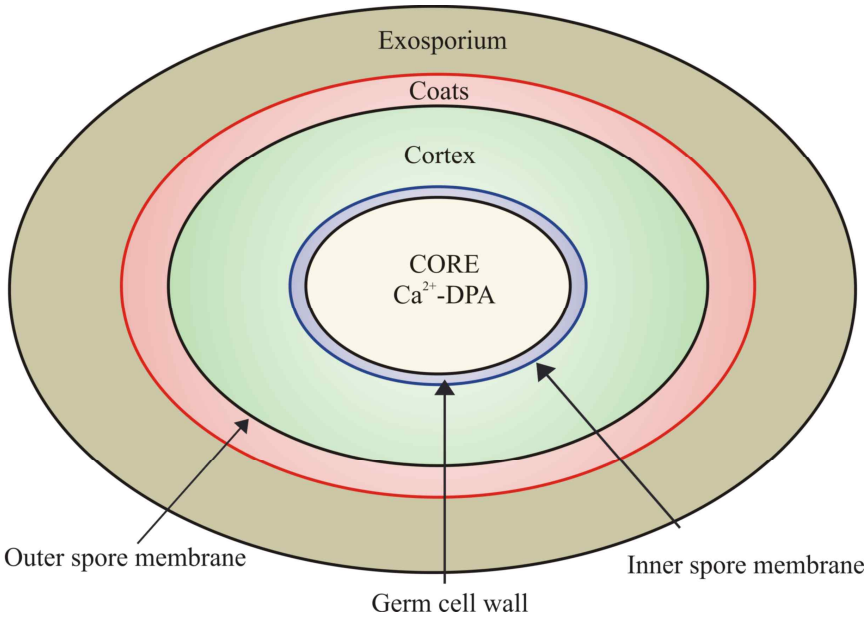

Figure 1.1. The structure of the spore. The spore core consists of the DNA, ribosomes, tRNAs, large amounts of Ca^{2+}, dipicolinic acid (DPA) and the cytoplasm. Cortex contains a peptidoglycan, which is slightly different from vegetative. The coats can consist of more than 50 different proteins. Exosporium might or might not be present in the spores of different bacteria and it usually consists of lipoproteins.

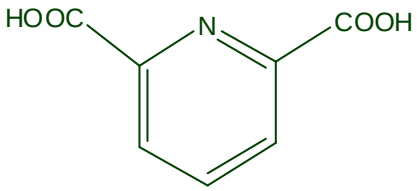

Figure 1.2. The structure of dipicolinic acid (DPA)

The amount of dipicolinic acid can vary from 5 to 15% of the dry weight of the spore and probably chelates divalent cations, most likely Ca^{2+} (7,8). DPA is usually synthesized during sporulation by DPA synthetase and excreted during germination. However, the mechanism of this process is not known. Also, although it is known that the amount of DPA in the core is above its solubility, its precise state is not known (1). DPA plays an important role in DNA protection because it acts as a photosensitizer that promotes formation of spore photoproduct (SP) under UV irradiation, rather than *cys,syn* cyclobutane dimers formed in vegetative cells (Scheme 1.1.) (9-11).

The other unusual properties of the spore core are that it has very low content of water and high-energy compounds like ATP and NADH. The amount of water in the core of the spore, depending on the species, ranges from 27 to 55 % of the wet weight, while in growing cell it comprises 75 to 80 % (1,2). Because of the low hydration levels there is little or almost no enzymatic activity inside the spore. The conformation of the spore DNA is also more A-like than B (Figure 1.3). A-DNA is less common form of DNA, which is observed under low hydration conditions. Compared to B-DNA, A-DNA has a wider minor groove and a narrower, deeper major groove. A-DNA and B-DNA have different patterns of bound cations and water molecules that result in different stability conditions for these structures. It was also found that A-type DNA is more UV resistant than other DNA forms. Interestingly, binding of small, acid-soluble proteins (SASPs) to DNA at least in part could lead to alteration of the DNA conformation from B to A-like as well (12-14), that way contributing to spore resistance to UV light.

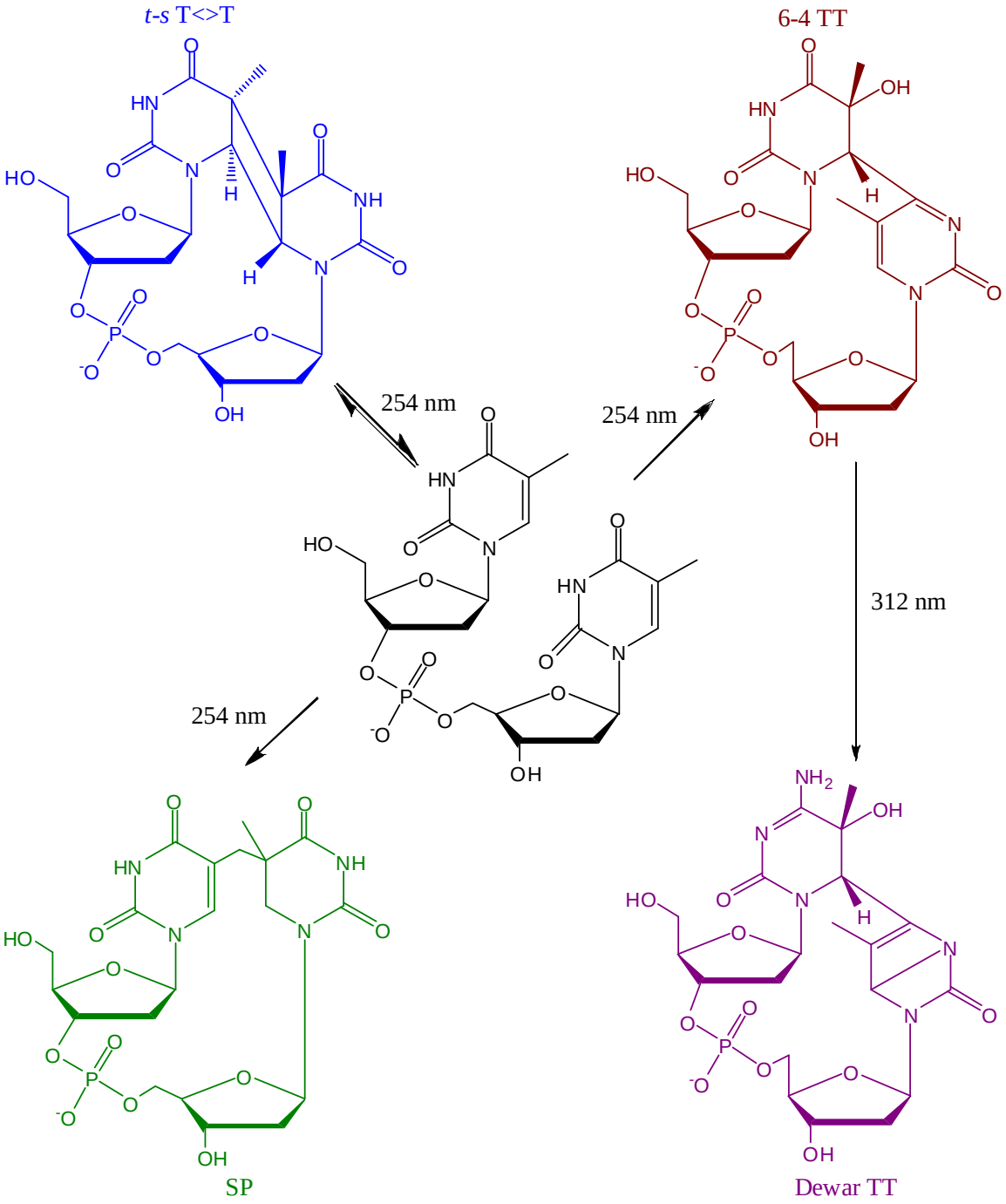

Scheme 1.1. Formation of various thymidine photoproducts under UV radiation. The main UV photoproduct formed in bacterial spores is spore photoproduct. SP – spore photoproduct, *t-s* T<>T – *trans,syn* cyclobutane pyrimidine dimer; 6-4 TT – (6-4) photoproduct, Dewar TT – Dewar photoproduct.

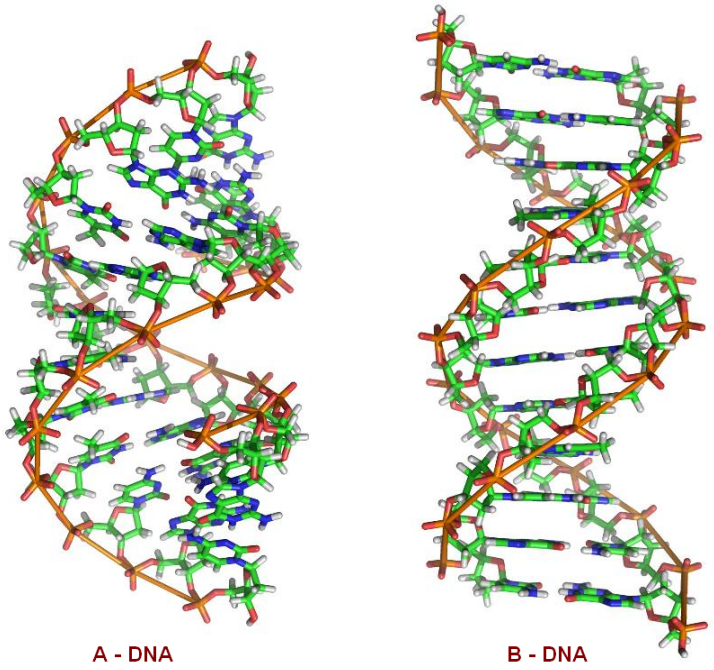

Figure 1.3. Different conformations of DNA

There are two types of SASPs, the γ- and the α/β-type SASPs. The γ-type SASPs are encoded by a single gene in all species (15), have highly conserved amino acid sequences, and are not associated with spore DNA *in vivo*. Their only known role is as an amino acid reserve for spores during germination (15-17).

The α/β-type SASPs are encoded by a family of seven genes and they are associated with spore DNA *in vivo*. They play a major role in determining the properties of spore DNA *in vivo* and resistance of spores to UV light (18). The α/β-type SASPs are synthesized during sporulation and are degraded during germination by spore germination protease (GPR) (16,19). They are small (60-75 amino acids) and present only in bacterial spores. α/β-type SASPs have no homologues in non-spore forming bacteria and their amino acid sequences are highly conserved both within and across

species, including *Bacillus* and *Clostridium* (20). In *Bacillus*, α/β-type SASPs can comprise up to 7 to 20 % of total spore protein. Such a high concentration of protein is enough to saturate the DNA in order to protect it from various kinds of damage (21). SASPs bind to random sequences of DNA with dissociation constants of 15-100 mM (20,22,23). While SASPs are monomers in a solution (24) and have no structure in the absence of DNA (25), recent X-ray crystal structure of SspC (and α/β-type SASP), revealed that it binds as a dimer to 6-bp region of DNA (Figure 1.4) (26). This protein consists of two long helices connected by a turn region, forming a helix-turn-helix (HTH) motif (Figure 1.4) (26). These helices are highly conserved while the amino acids that comprise the turn can vary greatly and the turn can also differ in length (27). Binding of α/β-type SASPs to DNA forms a coat that protects DNA from various type of damage, like heat and chemicals (21) and it also increases the persistent length of DNA, which makes the whole complex more rigid and reduce the bending of the DNA (28,29). While the proteins themselves cannot directly protect DNA from UV irradiation because SASPs contain too few amino acids that can absorb at 260 nm, it was found that their induced DNA conformation change from B to A-like (Figure 1.3) contributes to UV resistance (18,30). SASP significance to the spore resistance was demonstrated by the deletion of or mutations in SASPs, which caused low spore resistance to UV irradiation (18,30).

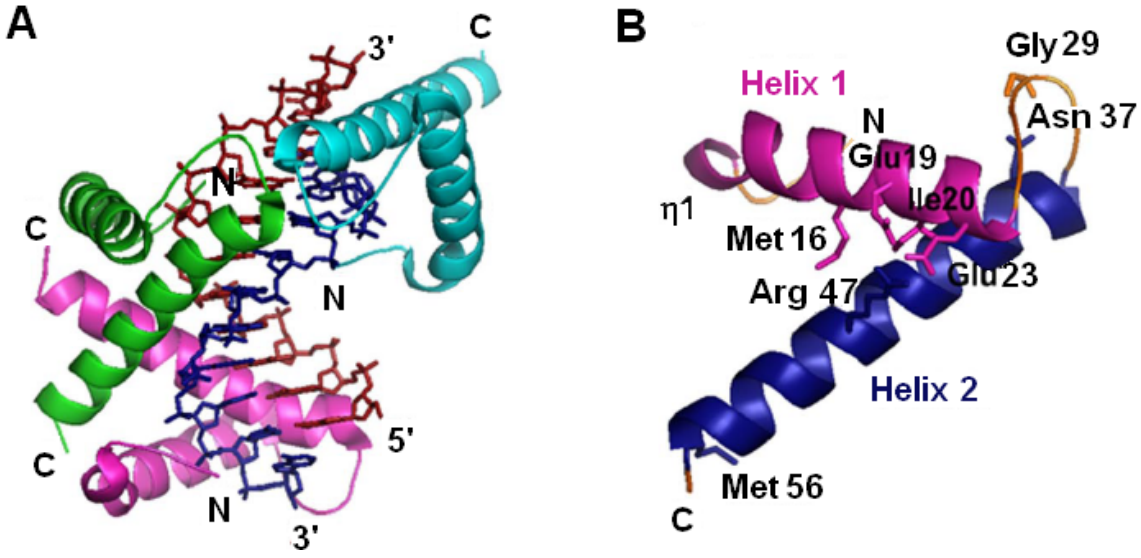

Figure 1.4. Crystal structure of the complex of DNA and 3 molecules of α/β-type SASPs. **A**: Stereo diagram of the complex. N and C termini of each SASP protomer are labeled. Green, magenta, and cyan represent different SASP molecules; red and blue are DNA dG and dC strands, respectively. **B**: Stereo ribbon diagram of an α/β -type SASP that has the orientation present in the protein–DNA complex. Magenta, Helix 1; blue, Helix 2. The N- and C-terminal arms and the loop between Helices 1 and 2 are orange. The amino acids that are essential for DNA binding are also shown. Adapted from reference (26).

While each of spore components, DPA, SASPs and spore hydration, either together or separately, has been found to be essential for spore resistance (31), the central reason for spore resistance to 254 nm UV irradiation is its novel DNA photochemistry. In vegetative cells exposed to UV irradiation the major product is *cis,syn* cyclobutane pyrimidine dimer (CPD) with small amounts of (6-4) photoproduct which are formed between adjacent thymines on the same DNA strand (Scheme 1.1). The case is different in bacterial spores, where the major DNA lesion is 5-thyminyl-5,6-dihydrothymine, also termed spore photoproduct (SP) (Scheme 1.1).

Spore photoproduct is efficiently repaired upon germination, utilizing several repair mechanisms, with one being specific to spores and involving the enzyme spore

photoproduct lyase (SPL). It was found that deletion mutants of the SPL gene (*spl*B) did not have as high of survival capabilities when exposed to UV light (32,33). This enzyme converts spore photoproduct to two thymidines (Scheme 1.2) and is the topic of this dissertation.

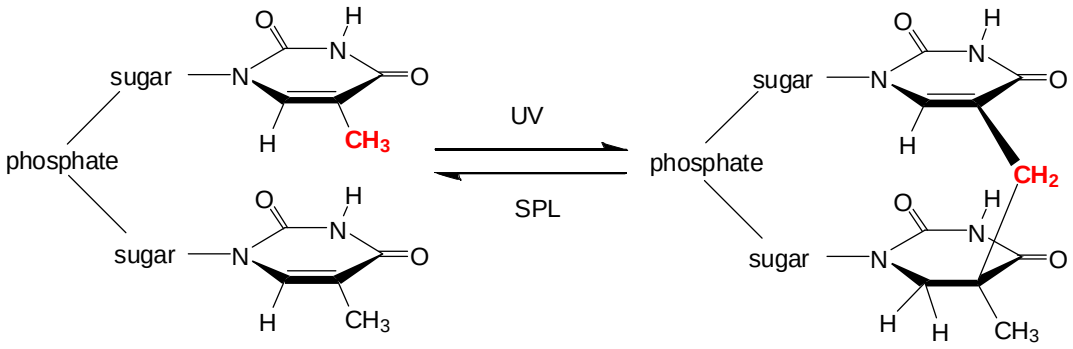

Scheme 1.2. The UV induced spore photoproduct is repaired directly by spore photoproduct lyase. The methyl bridge (shown in red) of SP is cleaved by SPL reverting the thymine dimer back to two adjacent thymines.

Spore Photoproduct Lyase and SP Repair Mechanism

Spore photoproduct lyase (SPL) is a DNA repair enzyme found only in bacterial spores. It is a pyrimidine dimer lyase (Scheme 1.2) that does not require photoactivation to repair damaged DNA, and thus is distinct from DNA photolyases (34). Together with the SASPs, SPL confers on *Bacillus* spores their unusual resistance to UV radiation (32,35).

SPL is synthesized during sporulation and packaged in the spore core (36), but does not repair damaged DNA until germination (32,35). Previous work indicated that SPL utilized *S*-adenosylmethionine (SAM) and contained an iron-sulfur cluster,

suggesting that it was a member of the Fe-S/SAM family of enzymes (37). SPL contains three cysteines in the CX_3CX_2C motif unique to the Fe-S/SAM enzymes, and these are responsible for coordination of the catalytically essential iron-sulfur cluster (38). SPL also shares some C-terminal sequence homology with the members of the DNA photolyase/(6-4) photolyase/blue light photoreceptor protein family (Figure 1.5). Both SPL and photolyase perform the same type of chemistry, the cleavage of nucleotide dimers to monomers, however there are some major differences, including 1) the DNA photolyases, but not SPL, are activated by visible light, 2) the DNA photolyases contain a flavin ($FADH^-$) and either folate or a deazaflavin, while SPL contains an Fe-S cluster, and 3) the DNA photolyases cleave cyclobutane pyrimidine dimers to monomers while SPL cleaves methylene-bridged thymine dimers to monomers (39).

SPL	SPLDKRIEA**A**VKVAKA**GYP**LGFIVAPIYIHE**GW**EEGYRHLF	250
N.c.	WSYNVDHFH**A**WTQGRT**G**F**P**IIDAAMRQVLST**G**YMHNRLRMI	477
S.c.	WENNPVAFEKWCTGNT**G**I**P**IVDAIMRKLLYT**G**YINNRSRMI	454
E.c.	WQSNPAHLQ**A**WQEGKT**GYP**IVDAAMRQLNST**GW**MHNRLRMI	346
H.h.	WRDDPAALQ**A**WKDGET**GYP**IVDAGMRQLRAEAYMHNRVRMI	353
A.n.	WENREALFT**A**WTQAQT**GYP**IVDAAMRQLTET**GW**MHNRCRMI	353
S.g.	WRSDADEMH**A**WKSGLT**GYP**LVDAAMRQLAHE**GW**MHNRARML	334

Figure 1.5. One of the regions of sequence homology between SPL from *Bacillus subtilis* and DNA photolyases from *Neurospora crassa (N.c.), Saccharomyces cerevisiae (S.c.), Escherichia coli (E.c.), Halobacterium halobium (H.h.), Anacystis nidulans (A.n.), Streptomyces griseus (S.g.).* The conserved amino acids are shown in bold. The potential SPL binding site to DNA (helix-turn-helix) is underlined.

The commonly accepted mechanism for photorepair by DNA photolyase involves dimer splitting as a consequence of a single electron transfer from the enzyme to the dimer, a mechanism recently verified by quantum chemical calculations (Scheme 1.4)

(40). Monomerization of the SP by SPL also occurs through an iron-sulfur cluster-mediated radical mechanism (41).

Anaerobically purified spore photoproduct lyase from *Bacillus subtilis* is brown in color, consistent with the presence of an iron-sulfur cluster (42). The UV-visible spectrum further indicated the presence of an iron-sulfur cluster due to broad features at 410 (11.9 $mM^{-1}cm^{-1}$) and 450 nm (10.5 $mM^{-1}cm^{-1}$) (Figure 1.6) (37,42-44), similar to spectra reported for anaerobically purified pyruvate formate lyase-activating enzyme (45) and lipoyl synthase (46). These features decreased in intensity after addition of dithionite, consistent with the reduction of an iron-sulfur cluster (37,42). Anaerobically purified enzyme was found to contain iron (3.1±0.3 mol of iron per mol of SPL) and acid labile sulfide (3.0±0.3 S^{-2} per mol of SPL) (42). Fontecave and co-workers showed that the [Fe-S] cluster could be reconstituted from aerobically purified SPL to contain ~3.5-3.9 irons and sulfurs per enzyme (43).

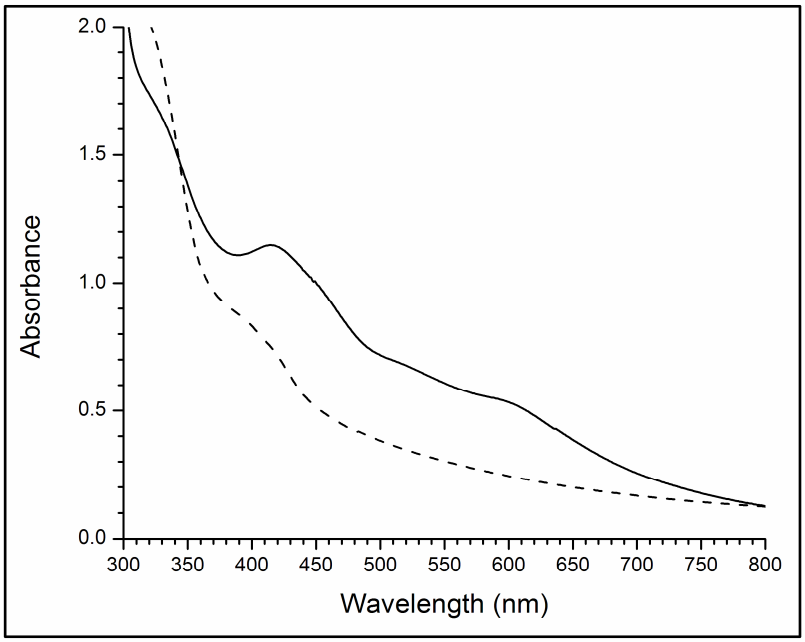

Figure 1.6. UV-visible absorption spectra of SPL as isolated (solid line) and reduced with dithionite (dashed line). For both spectra, the protein was 150 μM in 20 mM sodium phosphate, 350 mM NaCl, 5 mM dithiothreitol, 5% glycerol, pH 7.5. The reduced protein also contained 100 μM 5-deazariboflavin. The spectra were recorded in a 1 cm pathlength cuvette under anaerobic conditions at room temperature. Taken from reference (44).

The iron-sulfur clusters present in SPL were further investigated by electron paramagnetic resonance (EPR) spectroscopy (42,43,47). The EPR spectrum of as-isolated SPL demonstrated a strong, nearly isotropic signal at g = 2.02, observable only below 35 K (Figure 1.7). This indicates the presence of a $[3Fe\text{-}4S]^{1+}$ cluster (42). Under anaerobic conditions SPL can be reduced in the presence of sodium dithionite to give a nearly axial EPR signal characteristic of a $[4Fe\text{-}4S]^{1+}$ cluster with g_z = 2.03, g_y = 1.93, and g_x = 1.89 (Figure 1.7) (42). After adding SAM to dithionite-reduced SPL, the EPR signal decreased in intensity, but the g values remain almost identical (Figure 1.7) (42). Similarly, the EPR

of *C.a.* SPL revealed that EPR signal characteristic to $[4Fe\text{-}4S]^{1+}$ cluster, which is then reduced in the presence of SAM and changed into a rhombic signal with g-values of 2.02, 1.93 and 1.82. While addition of SAM cleavage products 5'-deoxyadenosine and L-methionine or SAM analog *S*-adenosyl-L-homocysteine (SAH), also reduced EPR signal, it didn't change the shape of it, indicating the specific interaction of $[4Fe\text{-}4S]^{1+}$ cluster with SAM (44).

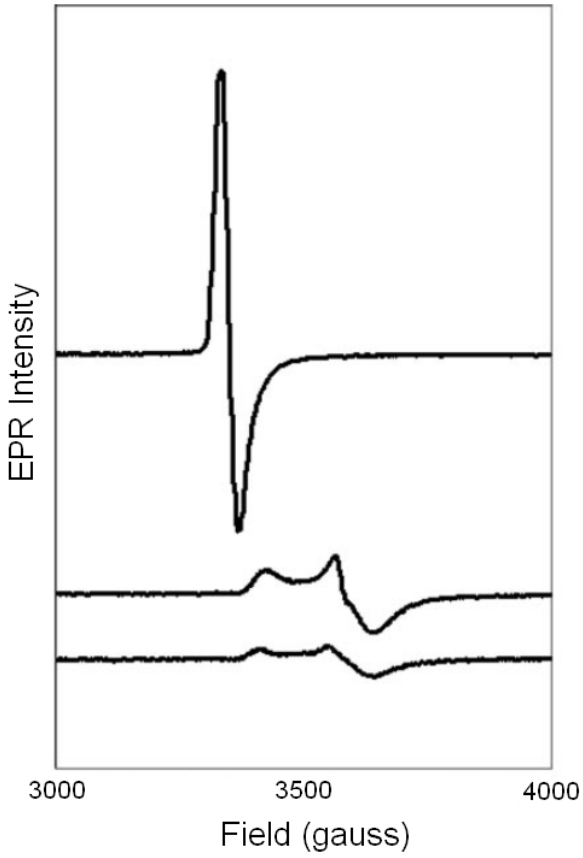

Figure 1.7. X-band EPR of spore photoproduct lyase. *Top* – as isolated enzyme, *middle* – reduced with 5 mM dithionite and *bottom* – reduced with dithionite followed by addition of 2 mM SAM (42). The protein was 350 mM in 20 mM sodium phosphate, 500 mM NaCl, 10 mM dithiothreitol, 5 % glycerol (pH 8.0). Conditions for the EPR were T = 12 K, microwave power 2 mW, microwave frequency 9.4841 GHz, modulation amplitude 10.084 and receiver gain 2 x 10^4, 1 scan accumulated. Taken from reference (42).

The early studies on SPL pointed to a novel mechanism of repair of UV-induced DNA damage, which involved an Fe-S cluster and SAM (37,39). This mechanism was initially proposed by Mehl and Begley (48), and further supported by Cheek and Broderick (39). The latter work showed that a 5'-dAdo radical was involved in the SPL enzymatic mechanism (Scheme 1.3). During repair, ^{3}H-label was transferred from C-6-tritiated spore photoproduct to SAM (39). This label transfer suggested that SP repair is initiated by C-6 H atom abstraction, with the resulting substrate radical presumably undergoing β-scission to provide the monomeric products (39). The mechanism was further confirmed by the Hartree-Fock density functional theory (DFT) calculations by Himo and co-workers (40). Their proposed mechanism also had an additional step whereby inter-thymine hydrogen transfer took place before it was abstracted back by 5-deoxyadenosine, with the last step being rate-determining (40). In this mechanism SAM acts as a catalytic cofactor during repair to reversibly generate the putative adenosyl radical intermediate (Scheme 1.3) (39,42). This role for SAM was supported by experiments where SPL and SAM were incubated in the presence of the substrate, but no production of 5'deoxyadenosine, the SAM cleavage product, was observed (Figure 1.8) (42). Further it was shown that only catalytic amounts of SAM were required in repair assays (Table 1.1) (42).

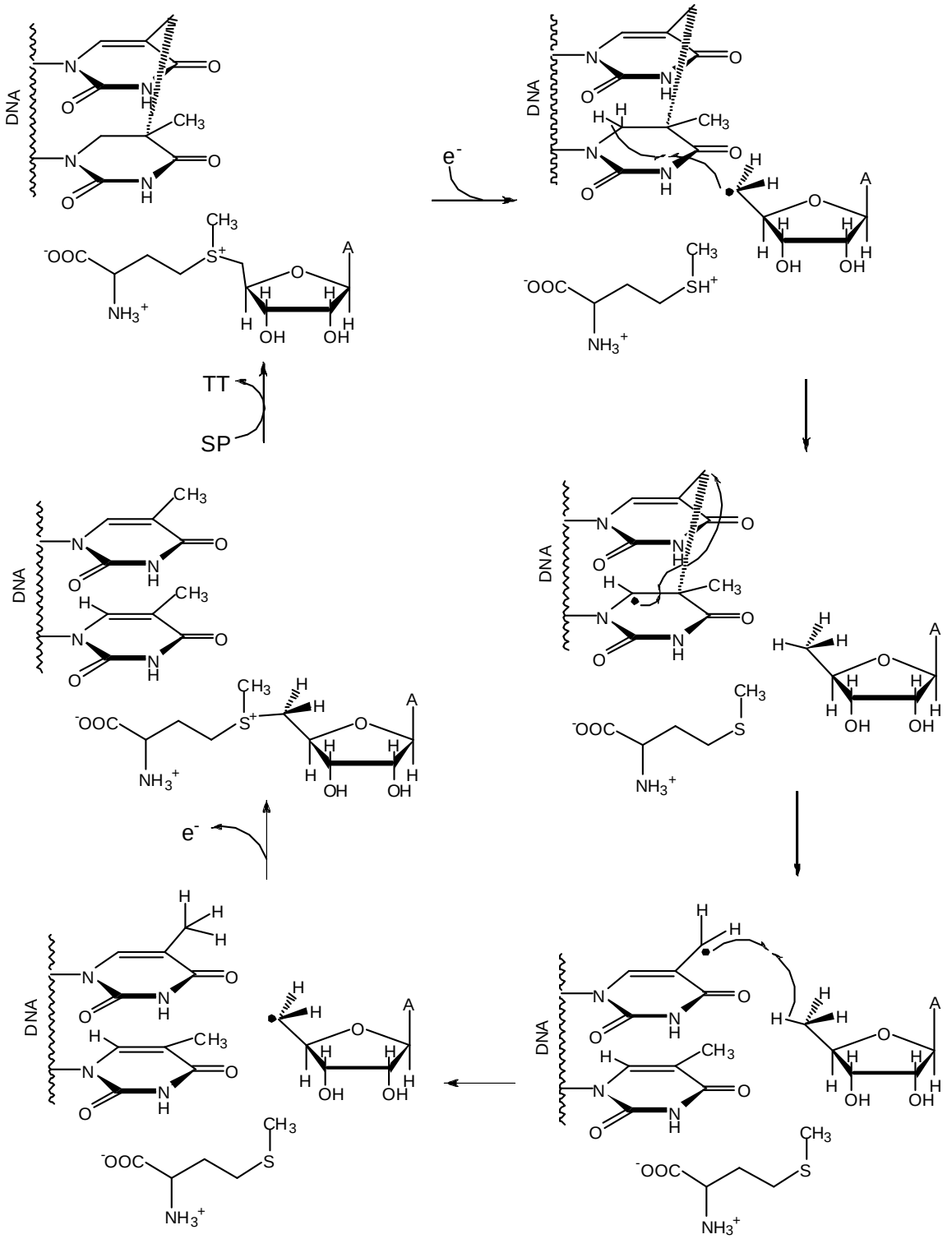

Scheme 1.3. Proposed spore photoproduct repair mechanism by SPL with SAM as a cofactor, present in the reaction mix, suggesting that SAM must act as cofactor, but not substrate. Adapted from reference (42).

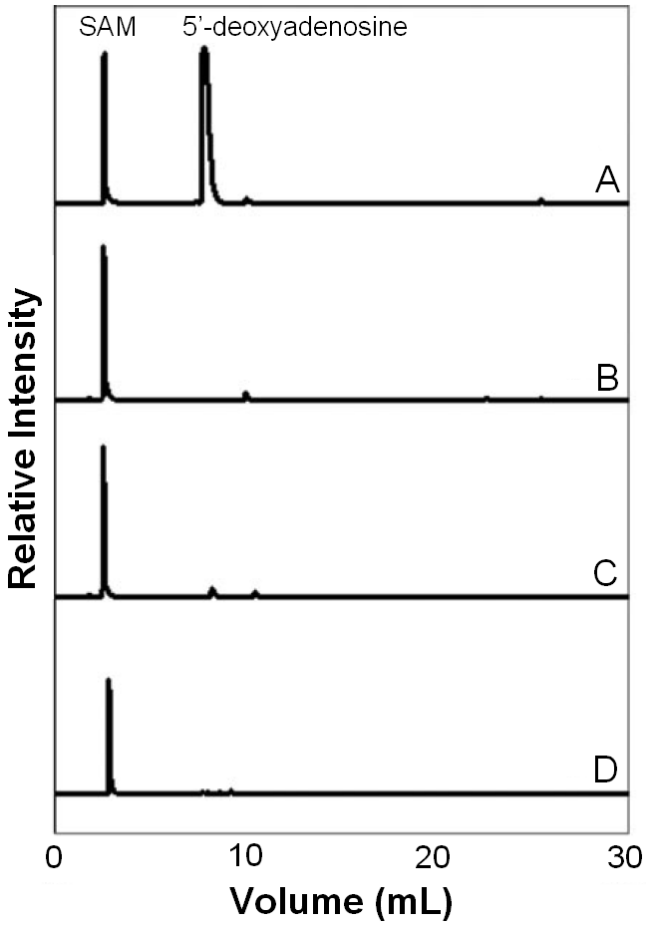

Figure 1.8. HPLC analysis of SAM cleavage to 5'-deoxyadenosine by SPL. HPLC chromatograms of (A) standard sample, containing SAM and 5'-deoxyadenosine; (B) control sample containing SAM under assay conditions with no SPL; (C) SAM assay mix after 90 minutes of incubation; (D) SAM assay mix after overnight incubation. Samples (B-D) contained 3 mM sodium dithionite, 4 mM dithiothreitol, 30 mM KCl, 25 mM Tris acetate, and 36 μM SAM, pH 7.0. Samples C and D also contained 200 μg of SP-containing pUC18 DNA and 36 μM spore photoproduct lyase. Taken from reference (42).

Table 1.1. Amounts of spore photoproduct repaired by spore photoproduct lyase (0.2 nmol) in 1 hr in the presence varying quantities of SAM. Taken from reference (42).

nmol of SAM	nmol of SP repaired
0.23	130 ± 10
0.46	130 ± 10
2.3	180 ± 10

Earlier work done by Nicholson and co-workers suggested that SAM was cleaved and 5'deoxyadenosine was produced (47). However, in their work SAM cleavage was observed even in the absence of substrate, and the rates of SAM cleavage, were ~8% and ~10% in the absence and in the presence, respectively, of SP-containing DNA (47). Carell and Fontecave also reported similar SAM cleavage (49). Based on work in our laboratory, however, we now believe that these early observations and SAM cleavage may have resulted from the use and/or reconstituted enzyme.

Radical SAM Superfamily

The radical SAM superfamily consists of over 2800 different enzymes that have very broad functions (50-52). This superfamily of enzymes utilizes iron-sulfur clusters and *S*-adenosyl-L-methionine (SAM) to carry out radical reactions (52). One unique feature of this superfamily is the nearly universally conserved CX_3CX_2C motif (Figure 1.9), which is responsible for the coordination of the iron-sulfur cluster.

All radical SAM enzymes, depending on their function, contain one or more iron sulfur clusters. Iron sulfur clusters (Scheme 1.4) are ubiquitous metal-containing structures found in biology (53-55). Their functions include roles in electron transport, protein structural stabilization, sulfur donation and others (56). The flexible protein environment surrounding the cluster can provide a range of redox potentials in different proteins, varying from –500 to 600 mV (57,58). Iron sulfur clusters also can be involved in redox (nitrogenase, hydrogenase, carbon monoxide dehydrogenase) and non-redox catalysis (aconitase). They can also have a regulatory role by turning on or off gene

expression in response to the levels of oxygen (the fumarate-nitrate reduction protein) (59,60) or superoxide (SoxR) (54). Iron-sulfur clusters can also have a structural role, such as in the DNA repair enzymes MutY and Endonuclease III (55). They can also serve as electron transporters in ferrodoxin, rubredoxin, and in photosynthesis proteins.

• SPL	86	IPFATG**C**MGH**C**HY**C**YLQTT
• PFL-AE	24	ITFFQG**C**LMR**C**LY**C**HNRDT
• aRNR-AE	20	VLFVTG**C**LHK**C**EG**C**YNRST
• BioB	47	SIKTGA**C**PQD**C**KY**C**PQTSR
• LipA	48	MILGAI**C**TRR**C**PF**C**DVAHG
• LAM	132	LLITDM**C**SMY**C**RH**C**TRRRF
• HemN	53	YFHIPF**C**QSM**C**LY**C**GCSIH
• ThiH	90	LYLSNY**C**NSK**C**VY**C**GFQIL
• MoaA	15	IAVTPE**C**NLD**C**FF**C**HMEFK
• BssD	68	TIFLKG**C**NYK**C**GF**C**FHTIN

Figure 1.9. CX_3CX_2C conserved binding motif of the radical SAM superfamily.

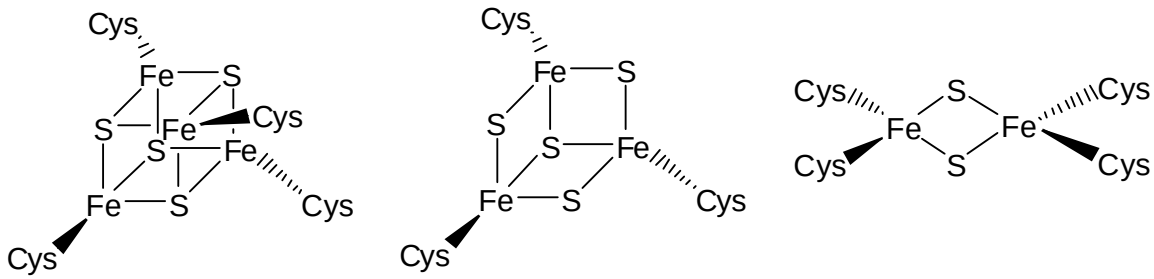

Scheme 1.4. The three major categories of iron sulfur clusters are illustrated including the [4Fe-4S], [3Fe-4S], [2Fe-2S].

The most common types of iron-sulfur clusters include $[2Fe\text{-}2S]^{2+/1+}$, $[3Fe\text{-}4S]^{1+/0}$ and $[4Fe\text{-}4S]^{3+/2+/1+}$ (Scheme 1.4). The iron atoms in these clusters are ligated to proteins via cysteine thiols and inorganic sulfide ions, and have tetrahedral geometry (61). Histidine and arginine can serve as ligands to iron as well. The other types of iron-sulfur clusters found in enzymes include heteroatomic clusters (nitrogenase FeMo-cofactor, carbon monoxide dehydrogenase) and ones that contain different ligands around specialized iron centers ([FeFe] hydrogenase H-cluster, [NiFe] hydrogenase) (62-70).

Radical SAM enzymes are believed to reductively cleave *S*-adenosylmethionine to form a 5'-deoxyadenosyl radical intermediate with the electron provided by oxidation of a $[4Fe\text{-}4S]^{+}$ cluster to a $[4Fe\text{-}4S]^{2+}$ cluster (Scheme 1.5) (71-73). This 5'-deoxyadenosyl radical then abstracts a hydrogen atom from a substrate molecule, generating a substrate radical (Scheme 1.5), which can then be involved in a series of reactions (Scheme 1.6). The B_{12} enzymes utilize a similar mechanism by generating 5'-deoxyadenosyl radical from 5'-deoxyadenosylcobalamin (AdoCbl) (74). B_{12} enzymes use AdoCbl to generate 5'deoxyadenosyl radical by homolytically cleaving the Co-carbon bond of the cofactor, which leads to the formation of a 5'deoxyadenosyl radical (74,75). One of the unique features of radical SAM superfamily enzymes is that they utilize an iron-sulfur cluster and SAM in place of AdoCbl to initiate radical chemistry. In some cases SAM acts as a cofactor and is regenerated after substrate turnover (SPL, LAM) (42,76,77), while in other cases it is a co-substrate and is consumed stoichiometrically with the substrate (PFL-AE, BioB) (45,78).

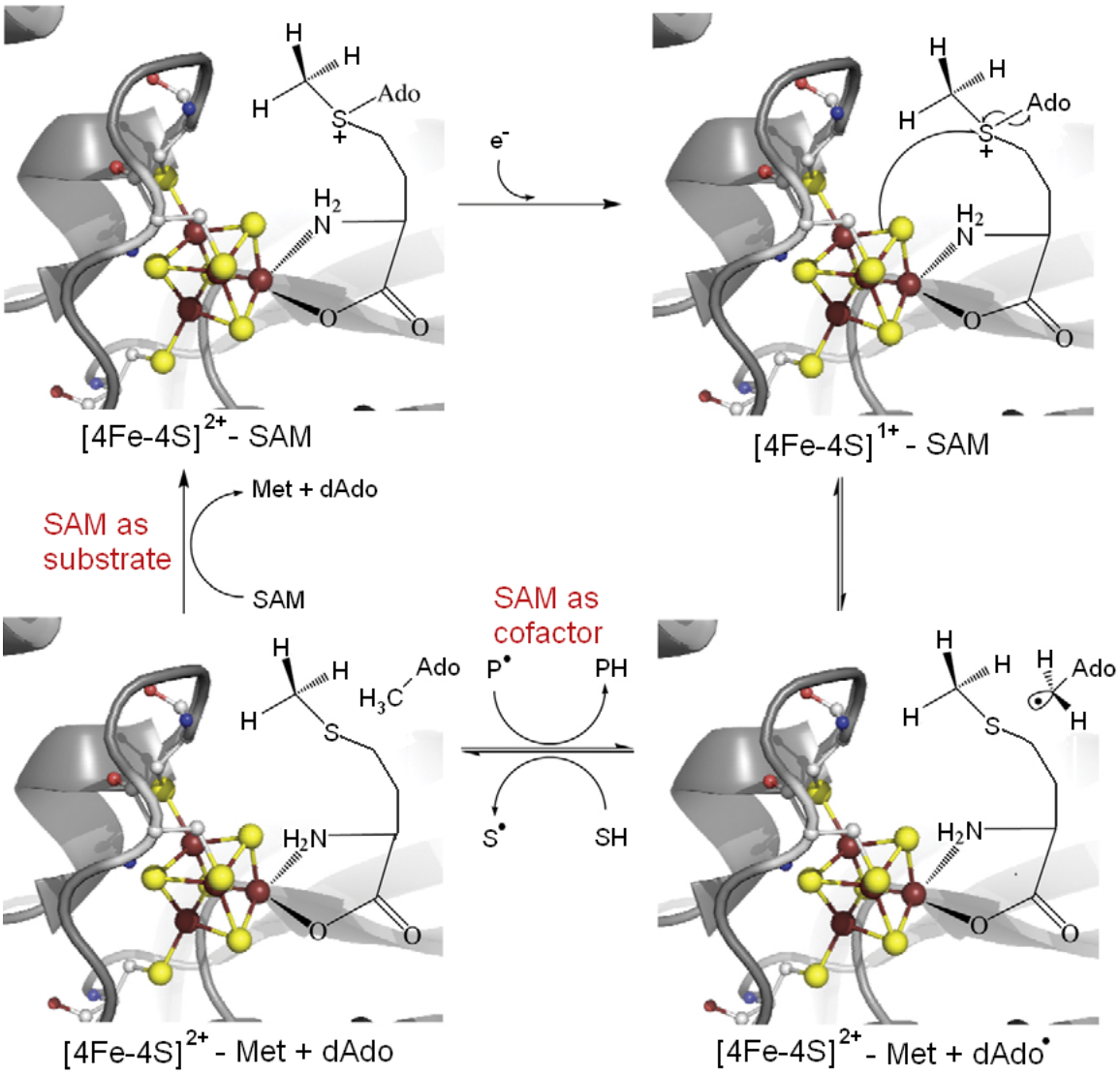

Scheme 1.5. Proposed mechanistic steps involved in SAM cleavage by the radical SAM enzymes. Adapted from reference (79).

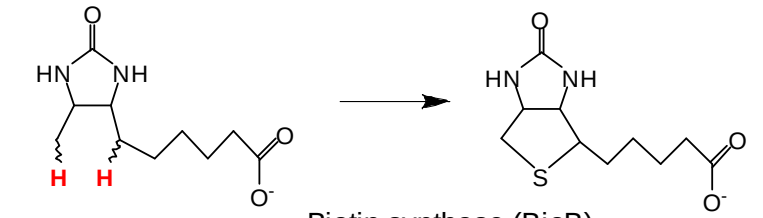

Biotin synthase (BioB)

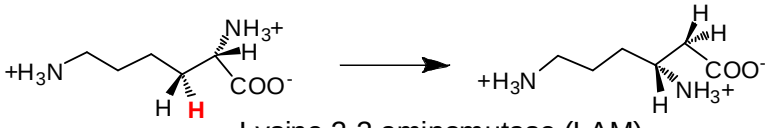

Lysine 2,3 aminomutase (LAM)

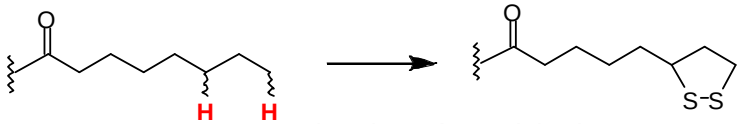

Lipoyl synthase (LipA)

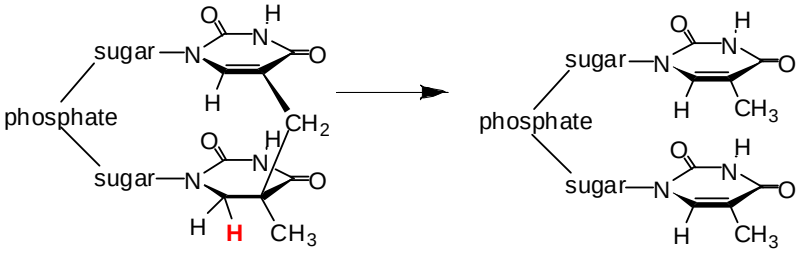

Spore photoproduct lyase (SPL)

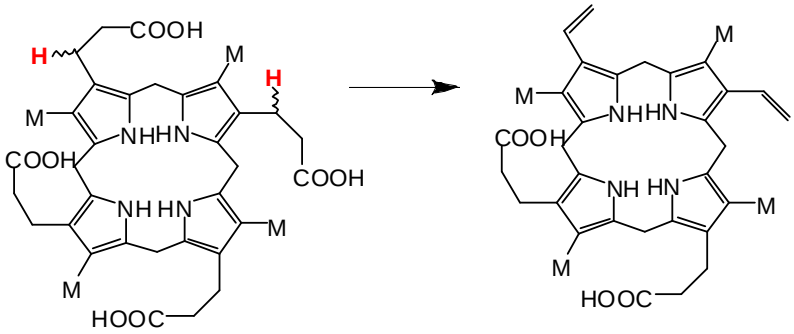

Oxygen-independent coproporphyrinogen-III oxidase (HemN)

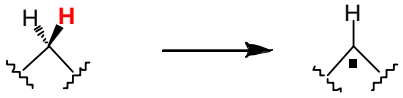

Activating Enzymes (PFL-AE, ARR-AE)

Scheme 1.6. Examples of the reactions catalyzed by radical SAM superfamily enzymes. PFL-AE is pyruvate formate lyase-activating enzyme, ARR-AE – anaerobic ribonucleotide reductase-activating enzyme. The hydrogen atom that gets abstracted is shown in red.

S-adenosylmethionine (SAM) is a naturally abundant molecule, which is involved in a number of biochemical reactions (80-82) and is synthesized from methionine and ATP by SAM synthetase. SAM can serve as a methyl group donor involved in methylation reaction of DNA, proteins and phospholipids (80,83). SAM is also involved in transsulfuration reaction and can serve as a precursor to form glutathione (GSH) (84). SAM can be utilized as a source of methylene groups in the synthesis of cyclopropyl fatty acids, ribosyl groups in synthesis of epoxyquinone (a modified nucleoside in tRNAs) and aminopropyl groups in the synthesis of polyamines (80). Therefore it is intriguing to find that SAM is also involved in radical chemistry (Scheme 1.5).

The early work on radical SAM enzymes started with Knappe's discovery that pyruvate formate lyase (PFL) needed another enzyme, later termed pyruvate formate lyase-activating enzyme (PFL-AE), to be activated (85). This activation reaction was dependent on the presence of flavodoxin, *S*-adenosylmethionine and iron. It was also discovered that PFL-AE had a CX_3CX_2C motif, contained an iron-sulfur cluster (86) and was involved in the hydrogen atom abstraction from G734 on PFL by using SAM as a co-substrate (87). Later it was discovered that there was another enzyme, class III anaerobic ribonucleotide reductase-activating enzyme (ARR-AE), which also performed hydrogen abstraction in order to form a glycyl radical on its substrate protein anaerobic ribonucleotide reductase (Scheme 1.6) (88,89).

The other early research on radical SAM enzymes was done by Barker and co-workers as well Frey and co-workers on lysine 2,3-aminomutase (90). This enzyme catalyzes the isomerization of L-lysine to L-β-lysine (Scheme 1.6) by migrating the α-

amino group from L-lysine to the β-carbon to form L-β-lysine (91). This conversion was shown to require SAM as a cofactor, rather than AdoCbl, which is the most common cofactor among isomerases (92). This reaction was also dependent on reducing conditions, presence of the iron and pyridoxal-5'-phosphate (PLP). Work carried out by Frey and co-workers directly detected the putative 5'-deoxyadenosyl radical by using the SAM analog 3',4'-anhydroadenosylmethionine (anSAM) (93,94).

More recent discoveries of radical SAM superfamily enzymes were followed biotin synthase (BioB) and lipoate synthase (LipA), which are involved in sulfur insertion in C-H bond (Scheme 1.6) (95,96). Biotin synthase contains two clusters, [4Fe-4S] and [2Fe-2S] and 2 molecules of SAM. BioB uses [4Fe-4S] cluster to generate 5'dAdo radical, while [2Fe-2S] cluster most likely is used as sulfur source to synthesize biotin from dethiobiotin (Scheme 1.6) (95). Lipoate synthase performs sulfur insertion to form lipoic acid, but differently from BioB, it inserts two sulfurs (Scheme 1.6) (97).

Radical SAM enzymes can also be involved in synthesis of complex organic cofactors. MoaA was found to be involved in molybdenum cofactor synthesis (98), HemN – in heme biosynthesis (Scheme 1.6) (99), while enzymes ThiH and ThiC are involved in synthesis of thiamine pyrophosphate (79).

Benzylsuccinate synthase (BSS) and anaerobic ribonucleotide reductase-activating enzyme (ARR-AE) are another two enzymes from larger group of enzymes that are involved in formation of glycyl radicals (GRE). They are involved in hydrogen abstraction from glycine, just like pyruvate formate lyase-activating enzyme, PFL-AE,

and are thought to function by transferring glycyl radical to a thiol in the active site, resulting thyil radical, which then participates in catalysis (50).

Radical SAM enzymes were also found to be involved in synthesis of complex metal centers, like iron-molybdenum cofactor (FeMoCo) of enzyme nitrogenase (100) and H-cluster of enzyme hydrogenase (101). The assembly of these clusters is a very complex process that involves a number of proteins, some of which are radical SAM enzymes, like NifB or HydE and HydG (100,101).

The other functions of radical SAM enzymes include DNA repair (spore photoproduct lyase, SPL), modifications of tRNA (MiaB), formylglycine generation (AtsB) (79).

The conserved CX_3CX_2C sequence in radical SAM enzymes gives three cysteinal ligands that coordinate an iron-sulfur cluster and is unique among the iron-sulfur cluster bearing enzymes (Scheme 1.7), which in most cases coordinate all four irons (102,103). As isolated enzymes usually have a combination of $[3Fe\text{-}4S]^{1+}$ and $[4Fe\text{-}4S]^{2+}$ clusters that can be reduced to $[4Fe\text{-}4S]^{1+}$ clusters (76,104-106). The presence of $[4Fe\text{-}4S]^{1+}$ was shown by electron paramagnetic resonance (EPR) in many different enzymes and these results suggested that this state of this cluster was the active one. This was subsequently demonstrated by Broderick and co-workers where disappearance of the EPR signal of $[4Fe\text{-}4S]^{1+}$ cluster was correlated with the formation of the product PFL glycyl radical (107).

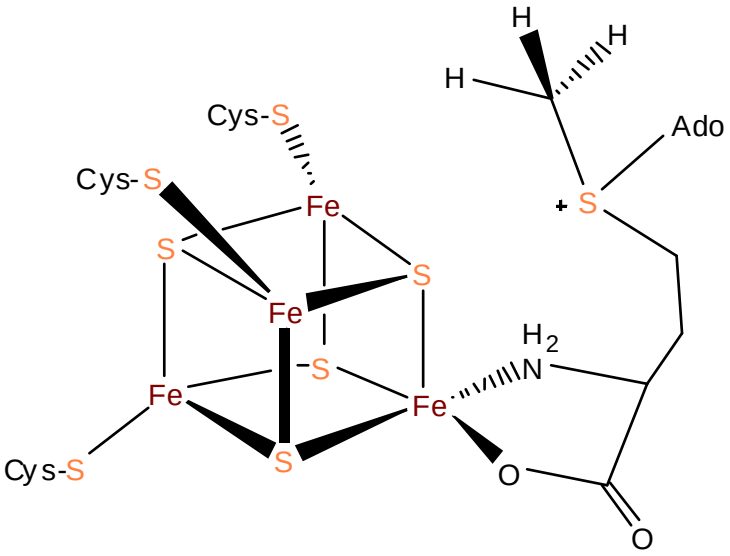

Scheme 1.7. ENDOR based model of SAM binding to the [4Fe-4S] cluster of PFL-AE. Taken from references (108,109).

Enzyme aconitase, just like radical SAM superfamily enzymes, contains a [4Fe-4S] cluster that is coordinated by 3 cysteines (110). Aconitase is involved in non-redox catalysis in the citric acid cycle and it does the dehydration/hydration reactions to convert citrate to isocitrate (110). It utilizes site-differentiated [4Fe-4S] cluster as a Lewis acid, and it was found that the fourth, unique, iron in the [4Fe-4S] cluster is coordinated by the substrate citrate via the carboxyl oxygens (110-112). Initial ENDOR studies carried out by Broderick and co-workers on PFL-AE by utilizing labeled SAM demonstrated that the unique iron of the [4Fe-4S] cluster binds SAM (Scheme 1.7) (109). Later ENDOR studies showed that the unique iron of the [4Fe-4S] cluster is ligated to the amino nitrogen and carboxyl oxygen of *S*-adenosylmethionine (Scheme 1.7) (71,108,109,113,114). Recent crystal structures of radical SAM enzymes, like biotin

synthase and PFL-AE, further support the interaction between *S*-adenosyl-L-methionine and the unique iron of the [4Fe-4S] cluster (Figure 1.10) (115-117).

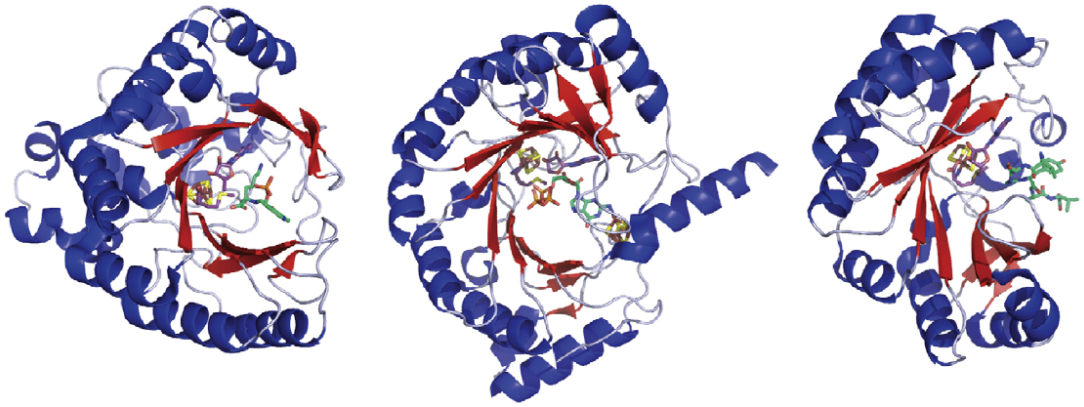

Figure 1.10. X-ray crystal structures of radical SAM enzymes. Left, lysine 2,3-aminomutase (LAM, left, minus its C-terminus); center, MoaA; right, pyruvate formate lyase-activating enzyme (PFL-AE), each with both SAM and substrate bound. The location of the radical SAM cluster is at one end of the TIM barrel, with SAM (carbons in purple) and substrate effectively sealing off the active site. As the substrate (carbons in teal) size increases from left to right, the size of the lateral opening in the TIM barrel also increases. Taken from reference (79).

Several crystal structures of these interesting enzymes, including PFL-AE, LAM, BioB, MoaA and HemN, have been recently reported (98,99,115,117,118). The interesting feature from these structures became clear - the similarity of their crystal structures despite very different amino acid sequences and very different chemistries carried out among this family of enzymes (99,116,119). All the radical SAM enzymes seems to have a partial or full TIM barrel (Figure 1.10) (116). Also it was found that the loop bearing the cysteine motif CX_3CX_2C is on the N-terminus (116,119). The orientation of the SAM molecule and the [4Fe-4S] cluster is similar in all the structures as well, although some bonds distances are different (119). Even though the crystal

structure of SPL is not known, considering the fact that it is a radical SAM enzyme and it carries a [4Fe-4S] cluster and binds SAM, it is likely to have a similar structure to these enzymes.

DNA Binding, Base Flipping Proteins and DNA Photolyase

Double-stranded DNA is a polymer, which consists of a negatively charged sugar-phosphate backbone and a core of stacked base pairs. The edges of these base pairs are exposed to either major or minor grooves. DNA repair proteins usually recognize a particular sequence or structure with a surface that is chemically complimentary to that of the DNA. Further, protein and DNA base pairs can form a number of favorable electrostatic and van der Waals interactions. In addition, protein-DNA complexes might contain a number of contacts between the negatively charged phosphates that include salt bridges with positively charged side chains. It can also have hydrogen bonds with uncharged main chain or side chain atoms in the protein (120). The great majority of DNA-protein structures contain DNA that is in B-form, with only a moderate degree of bending and deformation. Typically the binding domain of the protein interacts with 4-10 base pairs of the DNA (120). In some cases DNA binding motifs might span larger sites due to multiple independently folding protein domains. There are proteins, which simply bind to DNA without deforming the structure of the latter. However, there are also proteins that distort the structure of DNA by binding to it, but still are able to form base contacts (121). That kind of deformation of the DNA requires energy, which usually is compensated for by a sufficient number of favorable contacts with the protein. Some

proteins are capable of opening specific base pairs to perform chemical reactions on the target base.

The α-helix is the most common protein structural element used for recognition of DNA bases (120). The contacts between the protein α-helix and DNA are usually established through the major groove of DNA, and, in some cases, in the minor groove, which occurs in the *lac* repressor family (122). Even though the crystal structure of spore photoproduct lyase is not known, it has a potential helix-turn-helix (HTH) motif based on the results from protein sequence analysis (123). The putative helix-turn-helix motif of SPL is highly conserved among the *Bacillus* and *Clostridium* species (Figure 1.11), suggesting that it could be a potential DNA binding site.

The helix-turn-helix motif is present among many proteins that bind DNA, as well in proteins of different function (124,125). The HTH motif is utilized by transcription factors, is involved in DNA repair and replication, RNA metabolism, and protein-protein interactions (125). The basic HTH motif is comprised of three helices that can vary in length among different proteins (124). One of the helices, termed helix-3, is usually a recognition helix that forms both base and sugar-phosphate backbone contacts with the major groove of the DNA (120,124). The amino acids from this helix that are involved in DNA binding vary across the fold (125). Helix-2 might make additional DNA contacts, although it is not bound to the major groove (124,126). This helix frequently contains the "phs" motif, where p is charged residue (usually glutamate), h is a hydrophobic residue and s is a small residue (125). Helix-3 and helix-2 are connected by the characteristic sharp turn (120,124), which contains the "shs" pattern, where s is a small residue, with

glycine often being in the first position (125). The loop between helix-1 and helix-2 can differ among the different classes of HTH motifs. Additional secondary contacts between the DNA and the protein, outside of this helix-turn-helix motif, can also be formed (126).

212	EAAVKVAKAGYPLGFIVAPI	*B. subtilis*
219	EAAVKVA**E**AGYPLGFIVAPI	*B. halodurans* (88 % similarity)
273	EAA**R**KVA**G**AGYPLGFIVA	*B. thuringiensis* (strain Al Hakam) (88% similarity)
218	EAAVKVA**E**AGYPLGFI**I**API	*B. amyloliquefaciens* (88% similarity)
217	EAA**R**KVAKA**N**YPLGFIVA	*B. weihenstephanensis* (KBAB4) (83% similarity)
217	EAA**E**KVAKA**D**YPLGF**VI**A	*B. clausii* (strain KSM-K16) (77% similarity)
218	EAAVKVA**E**AGYPLGFI**I**A	*B. lichenformis* (strain DSM13) (88%)
217	EAA**R**KVA**G**AGYPLGFIVA	*B. cereus* (ZK/E 33L) (88% similarity)
217	EAA**R**KVA**G**AGYPLGFIVAP**L**	*B. anthracis* (88% similarity)
215	E**S**A**YNILNS**GY**KT**GFIV**G**P**F**	*C. acetobutylicum* (42% similarity)
215	EAA**L**KV**S**K**S**GY**K**IGFI**I**A	*C. noviy* (strain NT) (66% similarity)
216	E**S**AVK**L**A**R**AGY**QI**GFI**I**A	*C. difficile* (strain 630) (66% similarity)
216	EA**SI**K**A**AKAGYP**I**GF**L**VA	*C. beijerinski* (strain NCIMB 8052) (72% similarity)
217	A**SI**K**V**AKAGYPLGFI**I**API	*C. tetani* (82% similarity)
219	A**S**VK**I**AKA**N**YPLGFI**I**AP**V**	*C. perfringens* (76% similarity)

Figure 1.11. Amino acid alignment of the predicted helix-turn-helix regions in different SPL proteins from *Bacillus* and *Clostridium*. The amino acids that do not match with SPL from *Bacillus subtilis* are shown in bold. The proteins overexpressed in our lab were from *Bacillus subtilis* and *Clostridium acetobutylicum*.

Structurally, there can be different HTH configurations, including tetra-helical bundle, winged-helix, or ribbon-helix-helix (125). Also, these proteins can have very different structures outside of the helix-turn-helix region (125). One of the enzymes

containing a HTH motif is β-D-xylosidase, which catalyze the release of xylose from xylooligosaccharides (125,127). Interestingly, this enzyme also contains a TIM barrel $(\beta/\alpha)_8$ (127). Another enzyme that contains a HTH motif is O^6-alkylguanine-DNA-alkyltransferase (AGT) (128). AGT repairs mutagenic lesions in DNA by direct damage reversal of *O*-alkylguanines by selectively transferring the *O*-alkyl adduct to an internal cysteine residue. First, AGT uses its helix-turn-helix motif to bind to substrate DNA via the minor groove. Then alkylated guanine is flipped out from the base stack into the AGT active site for the repair, which occurs by covalent transfer of the alkyl adduct to cysteine (128). This enzyme could be of interest due to the fact that it repairs DNA and it flips out DNA base, something that SPL also is hypothesized to do.

Usually, when a protein binds to its preferred sequence, it can form an optimal number of contacts with the base pairs and backbone. Most proteins bind to the major groove of DNA due to easier recognition of the functional groups, where each base pair can be uniquely distinguished. In the minor groove, however, the pattern of hydrogen bond donors and acceptors is less varied and because of that CG is similar to GC and TA is similar to AT.

The way proteins recognize DNA bases seems to be even more complicated because one side chain of the protein can bind all four bases. As single side chain can form either a single hydrogen bond or two hydrogen bonds with DNA, with the later one having a higher degree of specificity. However, that might have no any predictive power or uniqueness. Van der Waals interactions are less significant due to their lack of directionality, but can play an important role in sequence specificity when the methyl

groups of thymine and the protein side chains are involved. Also, specificity of binding might depend on the orientation at which protein side chains approach the DNA bases.

Numerous ways of side chains contacting DNA bases are possible – through one or two hydrogen bonds, through a water molecule, or even through contacts to the DNA backbone. The surroundings of the protein side chains might also influence the binding by making additional contacts either with DNA bases or to each other. Therefore understanding of how proteins recognize and bind DNA can be difficult. Also, each family of enzymes can have completely different ways of approaching and binding to DNA and which particular amino acids are involved in base recognition. Hydrogen bonds mediated by water are also common in protein-DNA complexes, but most likely might have no effect on SPL binding or specificity of binding due to the low water content in bacterial spores (1). Therefore, the ways each organism evolves a protein to recognize and bind specific sequence of DNA can vary greatly and depends on the conditions.

DNA photolyase and some other DNA repair enzymes are structure specific (129). Their binding does not depend on sequence, but rather on a DNA structural change caused by the damaged site, like *cis,syn* cyclobutane pyrimidine dimer (CPD) (121). It has been shown that UV damage induces a DNA bend, which could be a different degree for a different photodimer. Also, since DNA damage by UV light can occur randomly on two adjacent thymines, the DNA repair enzymes must be able to find that damage and repair it before replication starts. And while it is known that DNA photolyase is structure specific (130), there is almost no information on how SPL recognizes and binds to either damaged or undamaged DNA, and most likely is structure specific as well.

How exactly SPL access the spore photoproduct to repair it, is also not known. Based on how DNA photolyase repairs the *cis,syn* cyclobutane pyrimidine dimer we could predict that SP is being flipped out of the DNA helix before the repair. Base flipping is fundamental to the function of many DNA-binding proteins (131,132). There is variety of proteins that use DNA base flipping in their interactions with DNA, including methyltransferases (DNA methyltransferases *HhaI* and *HaeIII*) and DNA glycosylases, (bacteriophage T4 pyrimidine dimer glycosylase, 3-methyladenine DNA glycosylase, and endonuclease VIII among others) (133-135). An important aspect of the action of all these enzymes is their ability to act on particular sites on DNA. While methyltransferases are involved in bacterial restriction systems that target specific DNA sequences, DNA repair enzymes have to identify the site of damage first.

It is proposed that there are three steps to base flipping – 1) recognition of the target site, 2) the increase of the interstrand phosphate-phosphate distance, which initiates base flipping by protein invasion of the DNA and 3) trapping the flipped base (131). There are several reasons why proteins might be flipping out bases. Some enzymes flip out bases on the complementary strand in order to gain access to the target site. For example, the T4 endonuclease V excises thymine dimers by flipping out one of the complementary adenines, which are not modified but provide space for the dimer to be reached by the catalytic side chains of the enzyme (131,135). The other reason is to have chemical modification within a catalytic pocket; the mechanism employed by methyltransferases, DNA glycosylases, AlkB oxygenases and DNA photolyases (121,135,136). The common feature among these enzymes is that they have contacts with

the phosphates on DNA. The interactions usually involve two to three phosphates on one or both sides of the target site, as well as phosphates on the complementary strand (DNA methyltransferases *HhaI* and *HaeIII,* DNA photolyase)(121). Binding to the phosphates on a particular strand can increase the interstrand phosphate-phosphate distance, which could lead to disruption of the target base pair and provide the path for one of the bases to rotate out of the double helix. This could also happen due to the already weakened hydrogen bonds that are a result of mismatched or damaged bases. The next step of the mechanism is the actual flipping of the base, where the enzyme could play either a passive or an active role (131). The enzyme could actively facilitate the flipping or bind to the base that already flipped out of the helix spontaneously. The empty space of flipped out nucleoside in some cases gets partially occupied with the protein side-chains. DNA photolyase kinks DNA in order to flip out out *cis,syn* cyclobutane dimer (Figure 1.10) and the cavity is partially filled with residues Gly397 and Phe406 (121). After the target base is flip out of the double helix, it is stabilized by interactions with the protein binding pocket as well as additional phosphate contacts. The common feature with all these enzymes is that they flip out only one base, while DNA photolyase flips out two. If SPL is repairing spore photoproduct in a way similar to DNA photolyase, it potentially is flipping out two bases.

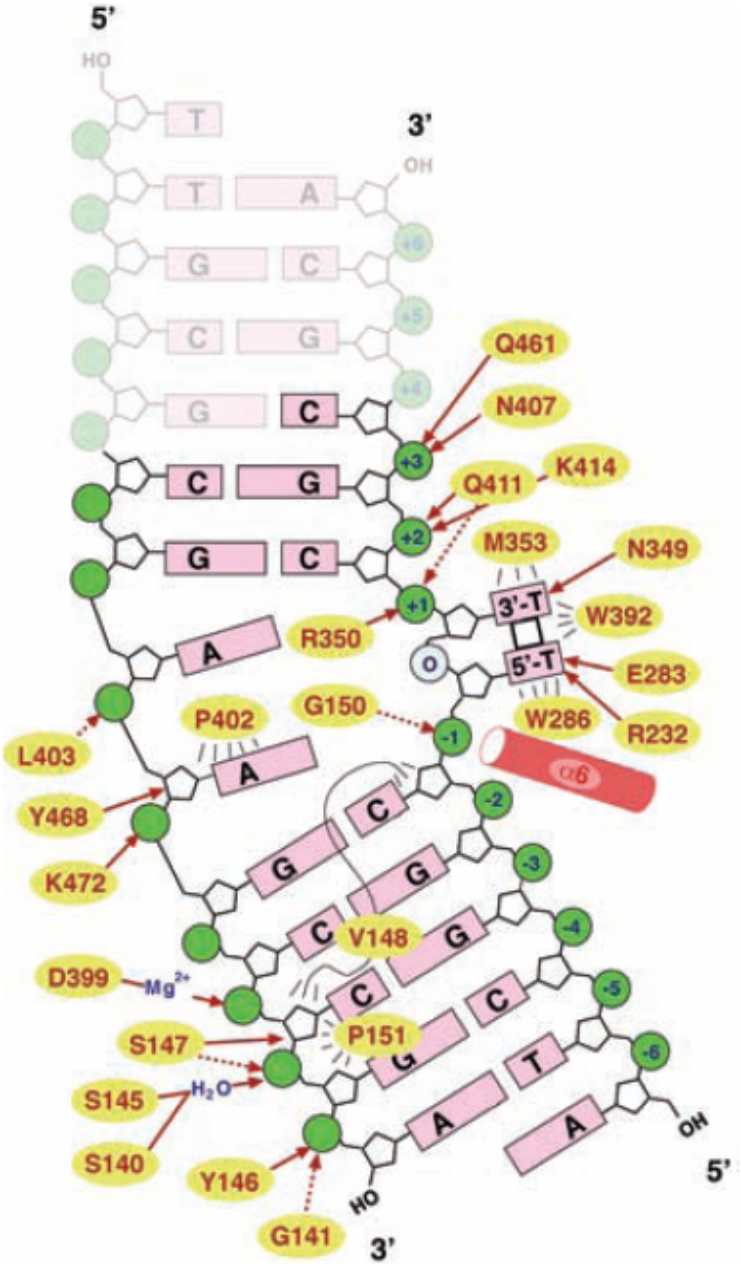

Figure 1.12. Interactions between CPD-containing DNA and DNA photolyase. Nucleotides not defined by electron density are shown faded. Dashed arrows indicate interactions with the protein backbone; solid arrows with side chains. Numbering of the phosphate groups starts from intradimer formacetal group (0). Interactions between enzyme and the complementary strand may stabilize the bending of duplex DNA, because there are no major differences in the affinities toward CPD-comprising single- and double-stranded DNA. Taken from reference (121).

Base flipping enzymes might also form base contacts. However, methyltransferases are sequence-dependent, while T4 endonuclease V and DNA photolyase are not. Methyltransferases within themselves can have different base contacts in the sequence they recognize. Interestingly, DNA methyltransferases show little binding specificity for the specific base itself, which could be due to the need to leave this base unaltered by binding contacts. Other important thing about base flipping enzymes is that DNA-interacting regions in methyltransferases and glycosylases are highly conserved.

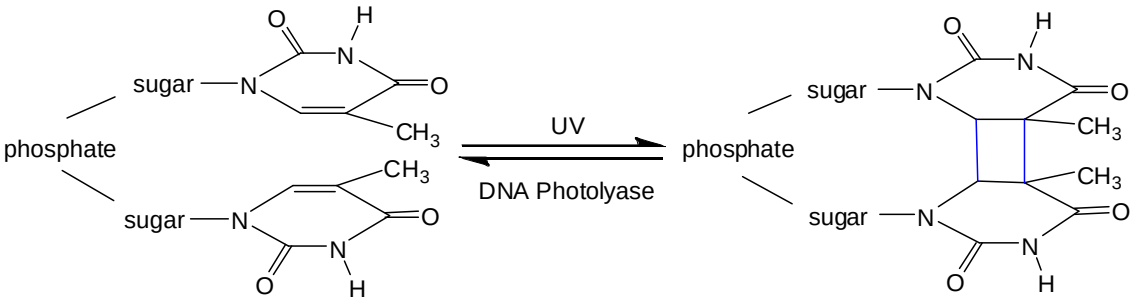

Scheme 1.8. The UV induced *cis, syn* cyclobutane pyrimidine dimer is repaired by DNA photolyase back to two adjacent thymines.

DNA photolyase is a widely studied DNA repair enzyme, which converts *cis, syn* cyclobutane pyrimidine dimers (CPD) to two thymines (Scheme 1.8) (137-140). This light-activated enzyme utilizes two cofactors; one is a flavin-adenine dinucleotide (FAD) and the other one is either folate (methenyltetrahydrofolate, MTHF) or a deazaflavin(8-hydroxy-7,8-didemetheyl-5-deazariboflavin, 8-HDF) (141). Due to the last two cofactors, these enzymes are classified into folate photolyases or deazaflavin photolyases. It was found that DNA photolyase binds to the DNA first and then flips out the damaged bases outside the DNA helix to its active site for repair (121). Then folate/deazariboflavin

absorbs a blue light photon and transfers the excitation energy to the flavin, which transfers an electron through the amino acid residues (tryptophan-tyrosine 'wire') to the cyclobutane ring, which is split to form two thymines (141). Consequently, an electron from radical anion is transferred back to the FADH to regenerate $FADH^{-}$. DNA photolyase binds to DNA with several regions. Even though SPL and DNA photolyase share sequence similarities (Figure 1.11) and both repair UV damaged DNA, the DNA photolyase binding region (121,140) is different from the predicted SPL helix-turn-helix motif. The binding regions of photolyase have no match with any part of the SPL sequence. That could mean that despite some sequence similarities these two enzymes have different binding sites. Also, most of DNA binding enzymes and radical SAM superfamily enzymes have very different sequences but very similar structures (within the same family). SPL specifically repairs spore photoproduct (SP), but not *cis,syn* cyclobutane pyrimidine dimers (142), and it presumably recognizes an SP-specific helical distortion in DNA which differs in its geometry from the distortion caused by *cis,syn* cyclobutane pyrimidine dimers (121). Once SP-specific binding occurs, the [4Fe-4S] cluster of SPL interacts with *S*-adenosylmethionine (SAM), resulting in the creation of a 5'-adenosyl radical, which participates in the reversal of SP to two thymines by radical fragmentation (Scheme 1.2) (39).

CHAPTER 2

SPORE PHOTOPRODUCT LYASE AND THE REPAIR OF SPORE PHOTOPRODUCT

Introduction

Spore photoproduct lyase catalyzes the specific repair of 5-thyminyl-5,6-dihydrothymine (spore photoproduct, or SP) to two thymines and, unlike DNA photolyase, does not need photoactivation. Instead it utilizes *S*-adenosylmethionine as a cofactor and a $[4Fe\text{-}4S]^{1+}$ cluster as an electron donor.

Several groups previously described the formation and the repair of spore photoproduct (35,37,39,142). Most of the research done previously focused on repair by using UV-irradiated DNA as a substrate. The drawback of this type of experiment was that only 3-5% of all thymines were converted to spore photoproduct (143). Also, the spore photoproduct usually is not homogenous and might have other photoproducts, such as *cis,trans* cyclobutane photodimers (143). Also, the previous work did not investigate if the spore photoproduct that was formed on DNA was either 5*S*- or 5*R*-isomer (Schemes 2.1 and 2.2). The early work of Begley had proposed that the formation *R*-isomer of SP should be more favored due the steric constrains in double helical DNA (144). The *S*-isomer potentially could be formed between two interstrand thymidines although only ~1% of spore photoproduct is generated as interstrand cross-link (18). Begley's work, however, provided no evidence as to which isomer is formed on DNA and repaired by SPL.

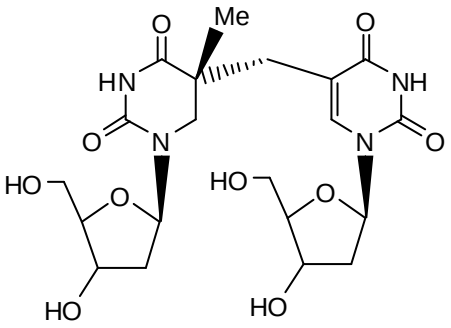

5*R*-SP

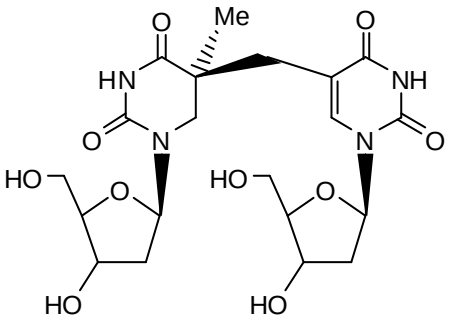

5*S*-SP

Scheme 2.1. The 5*R*- and 5*S*-spore photoproduct dinucleosides

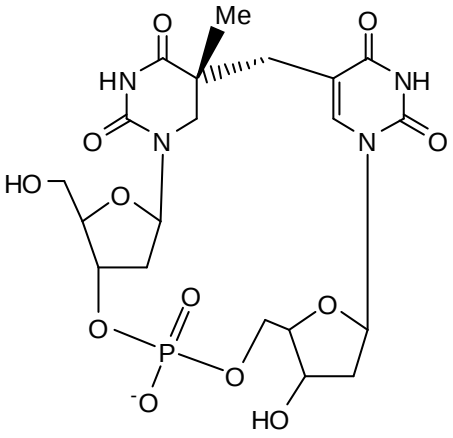

5*R*-SPTpT

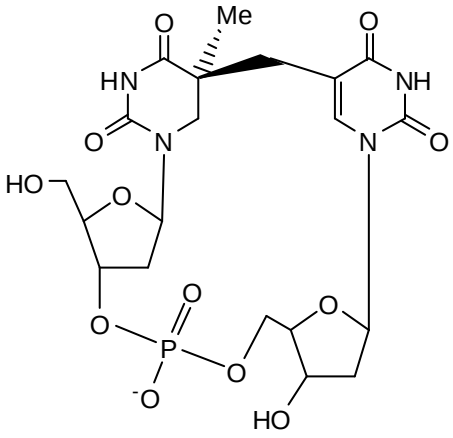

5*S*-SPTpT

Scheme 2.2. The 5*R*- and 5*S*-spore photoproduct dinucleotides

Recent work from the Fontecave and Carell groups investigated SPL chemistry involving spore photoproduct dinucleoside (SP, Scheme 2.1) or dinucleotide (SPTpT, Scheme 2.2). These smaller substrates can be made by either organic synthesis starting with thymidine (144-146) or by UV-irradiating thymidilyl-(3'-5')-thymidine (TpT) (43,147). Fontecave and co-workers showed that SPTpT generated by UV-irradiation of

TpT was a good substrate for SPL (43). Their work, however, lacked the full characterization of the spore photoproduct. Carell and co-workers were able to synthesize the *S*-isomer and *R*-isomer of spore photoproduct dinucleoside from thymidine and carry out the repair assays with *Geobacillus stearothermophilus* SPL (49,148). They reported the repair of only the *S*-SP, although the amount of SP repaired was very small (49,148). Carell and co-workers also incorporated 5*R*-SP and 5*S*-SP dinucleoside analogs into an oligonucleotide and measured their melting temperatures. They proposed that due to lower melting temperature of the *R*-isomer containing oligonucleotide, the *S*-isomer containing oligonucleotide should be the more stable and predominant one after the UV irradiation (149). However, no repair assays on these synthetic oligonucleotides have been reported. Instead, Carell and co-workers used UV-irradiated oligonucleotide, for which SP identity had been only confirmed by mass spectrometry (49).

Only recently NMR and DFT calculations demonstrated that spore photoproduct formed during the UV irradiation of thymidilyl-(3'-5')-thymidine (TpT) was 5*R*-SPTpT, and not 5*S*-SPTpT (150). This result would then suggest that the *R*-isomer would be repaired by SPL, contrary to the findings of Carell, Fontecave, and co-workers.

In this chapter SPL purification from *Clostridium acetobutylicum* and its repair activity towards SP and SPTpT (both 5*R*- and 5*S*-) will be discussed. Also, insight as to which of the isomers, *R*- or *S*-, is repaired by SPL, will be provided. The substrate molecules were synthesized and characterized in our lab by Dr. T. Chandra (146,151). The SP repair assays were developed and carried out by S.Silver and myself.

Experimental Methods

Materials

All chemicals, used in this work, unless otherwise indicated, were purchased commercially and were of the highest purity available. Tuner(DE3)pLysS competent cells were purchased from Novagen™. The Ni-sepharose™ column was purchased from GE Healthcare. Thymidine (T) and thymidylyl (3'-5') thymidine (or thymidine dinucleotide, TpT) were purchased from Sigma-Aldrich. Spore photoproduct dinucleoside and dinucleotide, both *R*- and *S*- isomers, were synthesized and characterized by Dr. T. Chandra (146,151). *S*-adenosylmethionine was according to published procedures as described below.

Purification and Dialysis of SPL

Spore photoproduct lyase from *Clostridium acetobutylicum* was grown and purified as described previously (42). Briefly, a single colony of the overexpression strain pET14b-SPL17 was transformed into *E. coli* Tuner(DE3)pLysS competent cells and used to inoculate 50 ml of LB medium containing 50 μg/mL of ampicillin. This culture was grown at 37 ^{o}C for ~15 hr and used to inoculate a 10 L flask of minimal media, also containing ampicillin (42). This culture was grown at 37 ^{o}C in a New Brunswick fermentor (250 rpm, 5 p.s.i. O_2) and was induced with isopropyl β-D-thiogalacto-pyranoside (IPTG, final concentration 0.5 mM) when an OD_{600} = 0.6. The medium was also supplemented with 750 mg $Fe(NH_4)_2(SO_4)_2$. The culture was grown for an additional 2 hours, and then was cooled to 25 ^{o}C and placed under nitrogen (5 p.s.i.). The culture was further cooled to 15 ^{o}C, moved to a 4 ^{o}C refrigerator, and was left under nitrogen for

12 hours. The cells were harvested by centrifugation at 4°C and stored under nitrogen at –80 ^{o}C until the purification was carried out.

The purification was performed under strictly anaerobic conditions in a Coy anaerobic chamber (Coy Laboratories, Grass Lake, MI) at 16 °C. Solutions and buffers used in the purification were deoxygenated by sparging with nitrogen prior to bringing them into the Coy chamber. The pelleted cells (13 to 19 grams) were brought into the anaerobic chamber and resuspended in 20-30 mL of pH 8.0 lysis buffer containing 20 mM sodium phosphate, 500 mM NaCl, 1% Triton X-100, 5% glycerol, 10 mM $MgCl_2$, 20 mM imidazole, 1 mM PMSF, 1 mg lysozyme per gram of cells, and 0.2 mg DNAse I and RNAse A. This suspension was agitated for one hour and then centrifuged at 27,000 x g for 30 min at 4 ^{o}C. The resulting crude extract was loaded directly onto a HisTrap HP^{TM} affinity column prepacked with Ni Sepharose^{TM} High Performance resin (0.7 X 2.5 cm, 1mL) that had been previously equilibrated with buffer A (20 mM sodium phosphate, 500 mM NaCl, 10 mM imidazole, 5% glycerol, pH 8.0). The column was washed with 15 mL of buffer A, and then a 25 mL step gradient (5 mL steps at 10%, 20%, 50%, 70%, 100% buffer B) from buffer A to buffer B (20 mM sodium phosphate, 500 mM NaCl, 500 mM imidazole, 5% glycerol, pH 8.0) was run to elute the adsorbed proteins. SP lyase eluted as a sharp brownish band at 50% buffer B in the step gradient. The fractions were analyzed by SDS-PAGE, and those judged to be ≥95% pure were pooled and concentrated at 16 ^{o}C using an Amicon concentrator equipped with the YM-10 membrane. The protein was flash-frozen and stored at –80 ^{o}C.

Protein concentrations were determined by the method of Bradford (152), using a kit sold by Bio-Rad and bovine serum albumin as a standard. Iron assays were performed using the methods of Fish or Beinert (153,154).

Dialysis of the protein was performed in order to remove imidazole. Dialysis was done anaerobically at +16 ^{o}C in Buffer A (50mM HEPES, 500 mM NaCl, 5% glycerol, pH 8).

Synthesis of *S*-Adenosylmethionine

S-adenosylmethionine was synthesized enzymatically by using the procedure described previously (Scheme 2.3) (109). A 10mL reaction contained 100 mM Tris-HCl (pH 8.0), 50 mM KCl, 26 mM $MgCl_2$, 13.0 mM adenosine triphosphate, 8% β-mercaptoethanol, 1mM EDTA, 10.0 mM methionine, 2.5 μL inorganic pyrophosphatase (0.25 U) and 1 mL SAM synthetase. The reaction was carried out at room temperature for 15 hrs while stirring. When the reaction was completed it was quenched with 1 mL 1M HCl and purified by loading onto a Source 15S cation exchange column (Pharmacia, 1 cm x 10 cm) charged with 1M HCl and equilibrated with MQ water. A linear gradient of MQ H_2O to 1 M HCl was used to elute the SAM. The fractions containing SAM were lyophilized and redissolved anaerobically in 50 mM HEPES, 200 mM NaCl (pH 8.0).

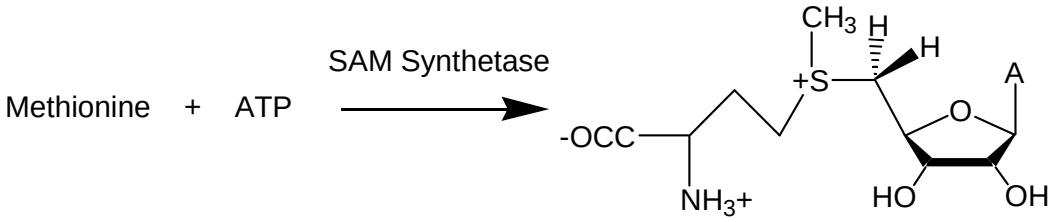

Scheme 2.3. Generalized reaction scheme for the enzymatic synthesis of SAM.

Repair of Spore Photoproduct Dinucleoside (SP) by SPL

The SP repair assays were carried out under anaerobic conditions in an MBraun glove box with O_2 < 1 ppm. The assays included 1 mM of *R*-SP or *S*-SP, 1 mM SAM, 5 mM DTT, 1 mM dithionite, and 50 μM of *C.a.* SPL in 50 mM HEPES buffer, which also contained 362 mM NaCl, 30 mM KCl (pH 7.5). SPL was photoreduced for 1 hour in the presence of 50 μM of 5-deazariboflavin prior to the assay. The assay was done at 37 ^{o}C and aliquots were taken after 1 hour, 6 hours and 20 hours. These aliquots were boiled for 45 s to further precipitate the protein and diluted 1:3 in water prior to injection to the HPLC. However, significant protein precipitation was observed in these assays due to higher temperature and prolonged incubation times at 37 ^{o}C. Under these conditions 100% repair of *R*-SP was observed, although the results were not reproducible due to the protein precipitation. For the next set of assays a few conditions were changed. The repair of both 5*R*- and 5*S*-isomers of spore photoproduct was carried out using the method developed by S. Silver (146). The assays were done at 30 ^{o}C under the same anaerobic conditions and included 1mM of either *R*-SP or *S*-SP, 1 mM SAM, 5 mM DTT, 1 mM dithionite in 45 mM HEPES buffer, which also contained 362 mM NaCl, 30 mM KCl (pH 7.5). SPL (50 μM, photoreduced with 5-deazariboflavin) was added to the reaction

mix and aliquots were taken at specific time points. These aliquots were boiled for 45 s to precipitate the protein and centrifuged briefly to separate the samples from the protein. These samples were then diluted 1:3 in water and used for further analysis by HPLC.

Identical conditions were used to carry out the *R*- and *S*-SP repair assays in phosphate buffer. The only difference was that SPL was purified using 50 mM phosphate buffer instead of 50 mM HEPES (see Purification and dialysis of SPL). The reaction mix also contained 45 mM sodium phosphate instead of 45 mM HEPES.

Repair of Spore Photoproduct Dinucleotide (SPTpT) by SPL

The conditions for assaying the repair of spore photoproduct dinucleotide were similar to those for assaying the repair of SP dinucleoside (see above). The difference was that SP dinucleotide (*S*-SPTpT or *R*-SPTpT) was used. The assays were done at 30 ^{o}C under anaerobic conditions in an MBraun glove box with O_2 < 1ppm. Assays included 500 μM of either *R*-SPTpT or *S*-SPTpT, 1 mM SAM, 5 mM DTT, 1 mM dithionite in 45 mM HEPES buffer, which also contained 362 mM NaCl, 30 mM KCl (pH 7.5). SPL (50 μM, photoreduced with 5-deazariboflavin) was added to the reaction mix and aliquots were taken at specific time points. These aliquots were boiled for 45 s to precipitate the protein and centrifuged briefly to separate the samples from the protein. Then these samples were diluted 1:3 in water and used for further analysis by HPLC.

HPLC Analysis of Repair Assays

To analyze SP dinucleoside repair assays, 20 μl of the diluted reaction mix (see above) was injected onto an HPLC reverse-phase Waters Spherisorb ODS2 column (4.6 x 150mm, 5 μm). The samples were eluted using a gradient of acetonitrile in water (0% to 10% acetonitrile from 2 min to 20 min, then to 20% in the next 5 min). The buffers were filtered through 0.22 μm membrane and de-gassed before using. The flow rate was 0.6 ml/min and column temperature was 35 ^{o}C. Under these conditions *R*-SP elutes at 18.5 min, *S*-SP elutes at 20 min and thymidine, which is the repair product, elutes at 14.5 min.

SPTpT dinucleotide repair assays were analyzed in a similar way. The diluted reaction mix (20 μl) was injected onto the same HPLC reverse-phase Waters Spherisorb ODS2 column (4.6 x 150mm, 5 μm). The samples were eluted using a gradient of acetonitrile in 2mM triethylammonium acetate (0% to 10% acetonitrile from 0 min to 25 min, then to 20% in the next 5 min). The flow rate was 1 ml/min and column temperature was 28 ^{o}C. Under these conditions *R*-SPTpT elutes at 8.5 min and TpT, which is the repair product, elutes at 16.5 min.

Identification and Characterization of the Repair Products

For the SP dinucleoside repair assays, the peaks from the HPLC chromatograms were identified using the following techniques (see also Figure 2.4). First, the assays were run on HPLC by co-injecting the following standard compounds – 5*R*-SP, 5*S*-SP, thymidine, thymine, *S*-adenosylmethionine (SAM), 5'-deoxyadenosine (dAdo), methylthioadenosine (MTA), and S-adenosylhomocysteine (SAH). For further identification, the fractions from HPLC were collected, pooled, concentrated, and ESI-

MS of these samples were carried out at Noyes Laboratory, University of Illinois Urbana-Champaign.

For the SPTpT dinucleotide repair assays, the peaks from HPLC were identified using the same techniques as for SP. The assays were run on HPLC by co-injecting following compounds – 5*R*-SPTpT, TpT, *S*-adenosylmethionine (SAM), 5'-deoxyadenosine (dAdo), methylthioadenosine (MTA), and S-adenosylhomocysteine (SAH). The ESI-MS of the pooled fractions was also carried out.

Results and Discussion

Purification of Spore Photoproduct Lyase

The SPL expression vector, pET14b-SPL17, was used to transform *E. coli* Tuner(DE3)pLysS for overproduction of N-terminal 6 histidine-tagged SPL (SPL-His_6). The resulting cells were lysed using an enzymatic lysis procedure. The crude extract was then passed through a nickel HisTrap HP^{TM} affinity column; pure fractions (>95 %) were identified by SDS-PAGE, pooled, concentrated, and stored under nitrogen at –80 ^{o}C. Approximately 25 mg of *B.s.* SPL and 100 mg *C.a.* SPL is typically obtained from 10 L of growth media. SPL elutes as a dark brown band from the nickel HisTrap HP^{TM} affinity column, consistent with the presence of an iron-sulfur cluster in the protein.

The anaerobically purified *Clostridium acetobutylicum* SPL was found to contain iron (2.9 Fe / SPL) and had a concentration of 0.104 mM. The amount of iron present in the purified SPL is dependent on the precise growth and purification conditions.

The Repair of Spore Photoproduct Dinucleoside by Spore Photoproduct Lyase

It is known that SPL repairs spore photoproduct, but not any other UV-photoproducts, such as cyclobutane photodimers (142). Previous experiments in our lab involved only the repair of UV-damaged DNA (39,42). For these assays, pUC18 DNA was labeled with tritium and then irradiated under UV light under certain conditions to create spore photoproduct (39,42). However, this method yielded very low amounts of spore photoproduct (only 3-5%) and it was not very reliable. To have better substrate for the enzymatic assays, the open form spore photoproduct, in both *R*- and *S*- forms, was synthesized by Dr. Tilak Chandra in our lab (Scheme 2.1).

To investigate SPL activity towards the 5*R*- and 5*S*- spore photoproduct dinucleosides, repair assays were performed. The procedure involved photoreducing spore photoproduct lyase in the presence of 5-deazariboflavin and small amounts of dithionite. The assays were performed under anaerobic conditions and were incubated at 30 ^{0}C for up to 4 hours. The repair assay that included 5*R*-SP as a substrate yielded thymidine (Scheme 2.4, Figure 2.1) and started to "slow down" after 3 hours and stopped after 4 hours. The repair assay of 5*S*-SP yielded no thymidine (Scheme 2.4, Figure 2.2).

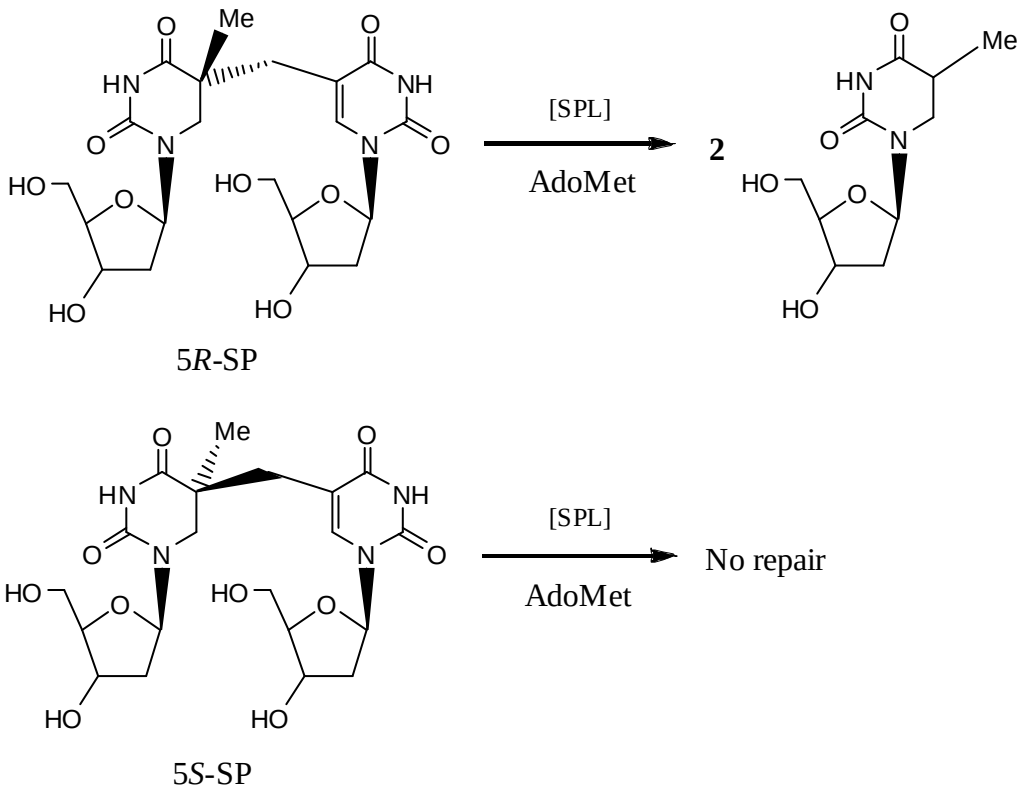

Scheme 2.4. The repair of 5*R*- and 5*S*- spore photoproduct dinucleosides (5*R*-SP and 5*S*-SP) by spore photoproduct lyase

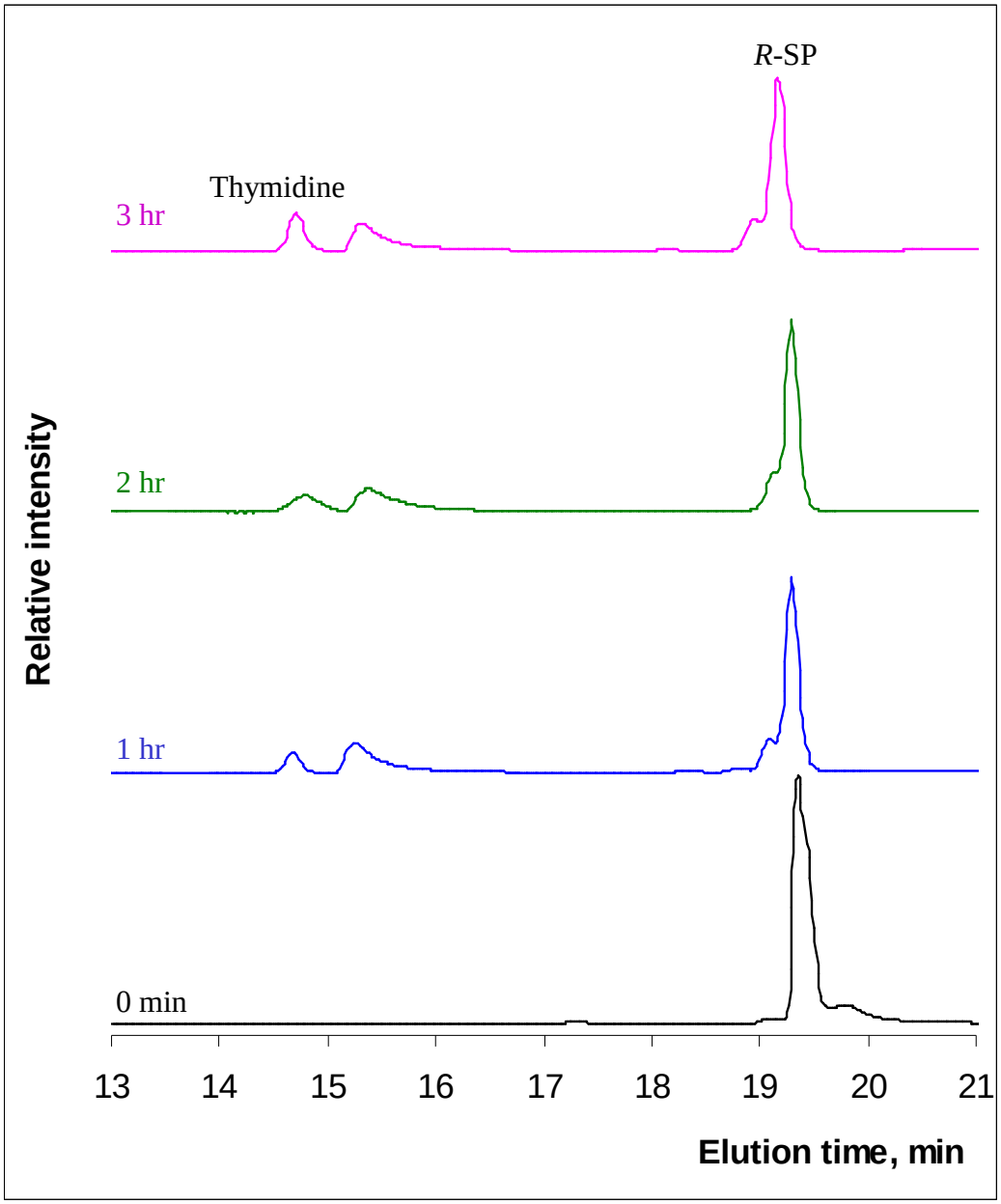

Figure 2.1. HPLC chromatogram of 5*R*-SP repair and thymidine formation over time. The diluted reaction mix (20 µl) was injected onto an Spherisorb ODS2 column (4.6 x 150mm, 5 µm, Waters). The samples were eluted using a gradient of acetonitrile in water (0% to 10% acetonitrile from 2 min to 20 min, then to 20% in the next 5 min. The flow rate was 0.6 ml/min and column temperature was 35 ^{o}C. Thymidine elutes at 14.5 min, amino acid residues at 15.5 min, 5*R*-SP at 19 min (146).

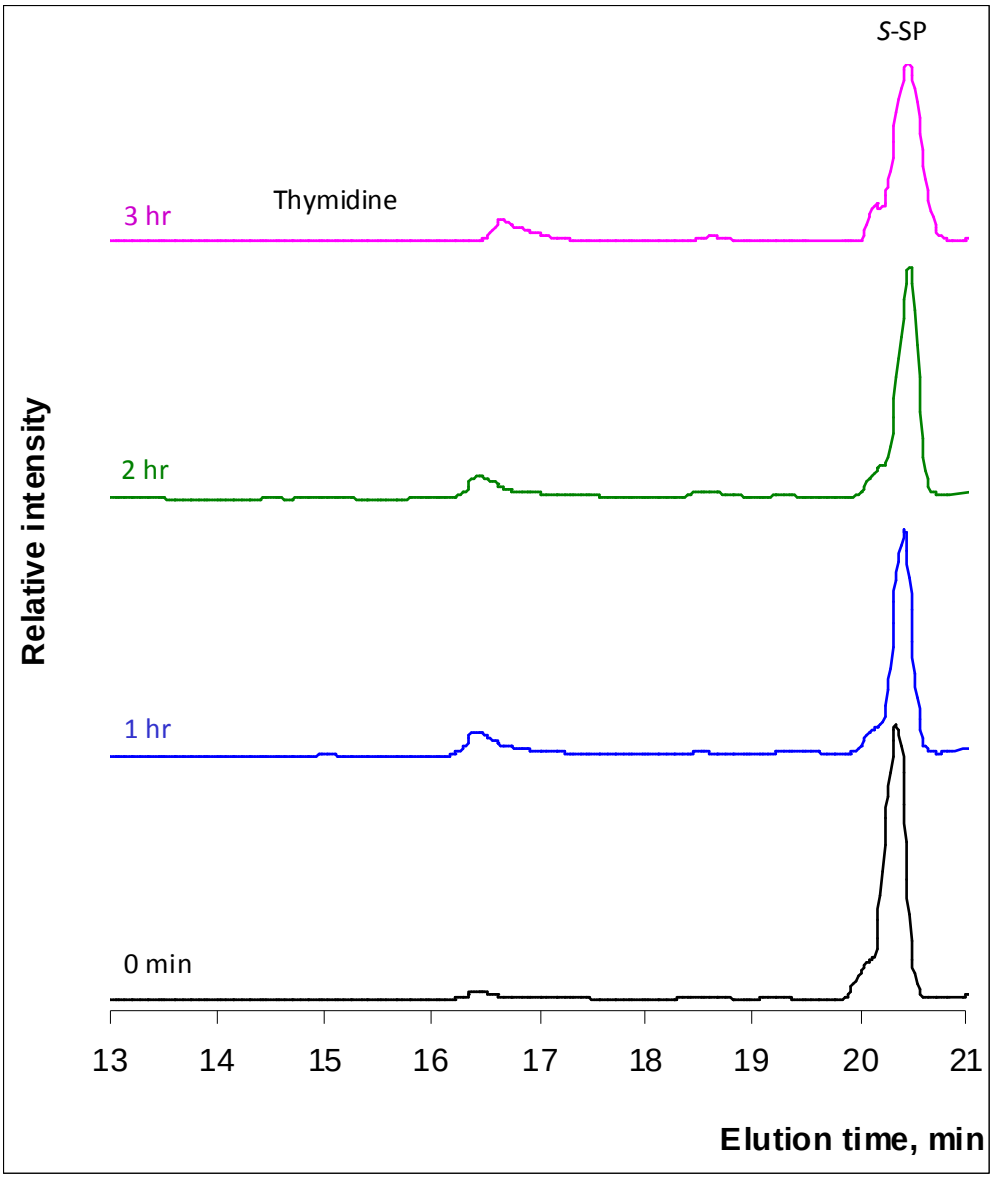

Figure 2.2. HPLC chromatogram of 5*S*-SP repair and thymidine formation over time. The diluted reaction mix (20 µl) was injected onto an Spherisorb ODS2 column (4.6 x 150mm, 5 µm, Waters). The samples were eluted using a gradient of acetonitrile in water (0% to 10% acetonitrile from 2 min to 20 min, then to 20% in the next 5 min. The flow rate was 0.6 ml/min and column temperature was 35 ^{o}C. Thymidine elutes at 14.5 min, amino acid residues – at 16.5 min, 5*S*-SP at 20.5 min (146).

Characterization of the Peaks from HPLC (5*R*-SP Repair Assay - Dinucleoside)

The products of 5R-SP repair assay were identified by both co-injection of authentic compounds on HPLC and by ESI-MS of isolated fractions (Figure 2.3). For the co-injections, one of the repair assay samples (5*R*-SP repair after 3 hours) was spiked with each of the following standard compounds in separate experiments – thymine, thymidine, *R*-SP, *S*-adenosylmethionine (SAM), methylthioadenosine (MTA), *S*-adenosylhomocysteine (SAH) and 5'-deoxyadenosine (dAdo) (Table 2.1). Then HPLC was run under standard conditions and the increase in one peak intensity was used to identify specific HPLC peaks. From these results we were able to show that peak eluting at 14.5 minutes was thymidine, at 18.5 minutes 5*R*-SP, 21 minutes *S*-adenosylmethionine, at 24 minutes 5'-deoxyadenosine, at 28 minutes methylthioadenosine (Figures 2.4 and 2.5) (Table 2.1).

Table 2.1. HPLC elution times of standard compounds. For HPLC, a reverse-phase Waters Spherisorb ODS2 column (4.6 x 150mm, 5 μm) was used. The samples were eluted using a gradient of acetonitrile in water (0% to 10% acetonitrile from 2 min to 20 min, then to 20% in the next 5 min). The buffers were filtered through 0.22 μm membrane and de-gassed before using. The flow rate was 0.6 ml/min and column temperature was 35 ^{o}C.

Compound	**Elution time, min**
Thymine	10.5
Thymidine	14.5
5*R*-spore photoproduct	18.5
5*S*-spore photoproduct	20.0
S-Adenosylmethionine (SAM)	22.0
5'-Deoxyadenosine (dAdo)	24.0
Methylthioadenosine (MTA)	28.0
S-adenosylhomocycteine (SAH)	18.0

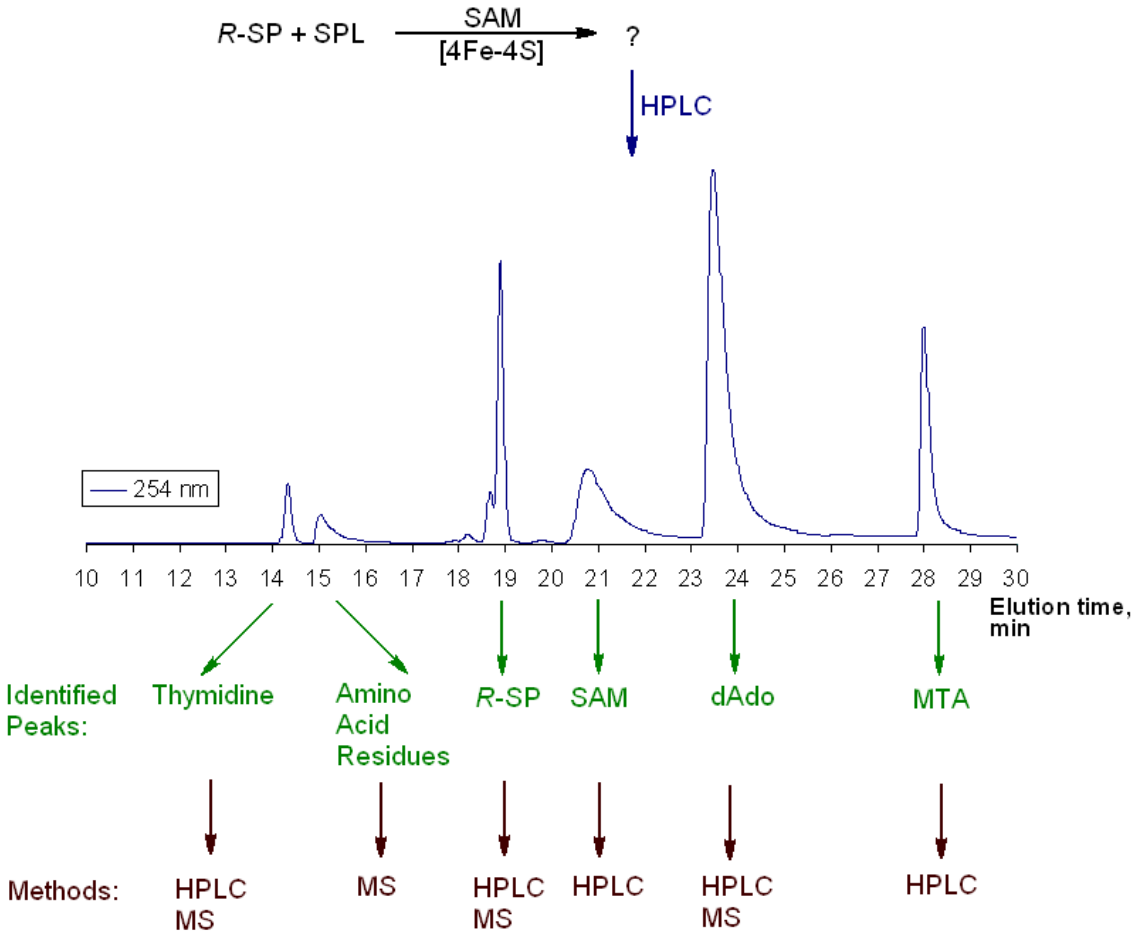

Figure 2.3. The separation of 5*R*-SP repair assay products by HPLC. The peaks that eluted from HPLC C-18 ODS-2 column (Waters) were further analyzed by co-injecting the standards and doing ESI-MS. SP – spore photoproduct, SAM - *S*-adenosylmethionine (AdoMet), dAdo- 5'-deoxyadenosine, MTA – methylthioadenosine.

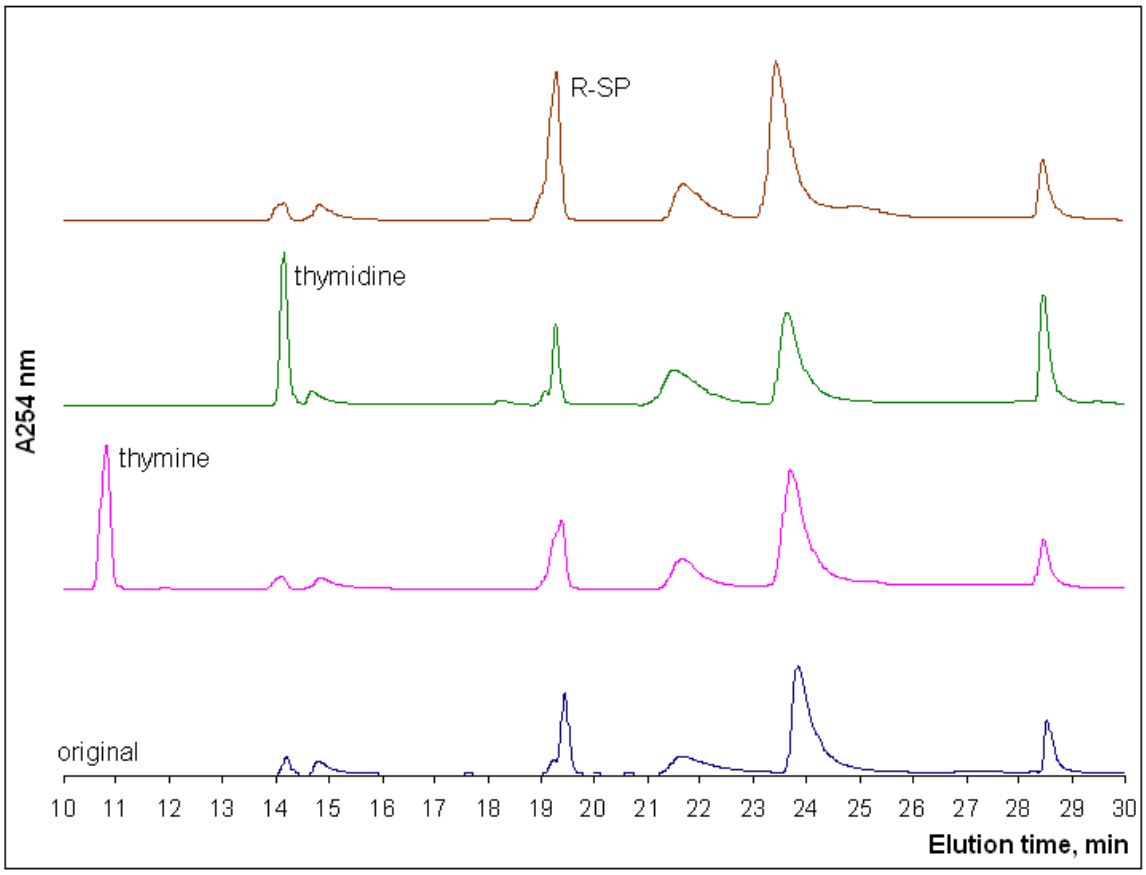

Figure 2.4. Co-injections of 5*R*-SP, thymidine and thymine in the original 5*R*-SP repair assay (3 hr). The diluted reaction mix (20 μl) was injected onto an Spherisorb ODS2 column (4.6 x 150mm, 5 μm, Waters). The samples were eluted using a gradient of acetonitrile in water (0% to 10% acetonitrile from 2 min to 20 min, then to 20% in the next 5 min. The flow rate was 0.6 ml/min and column temperature was 35 ^{o}C. Some shifting of the peaks was observed.

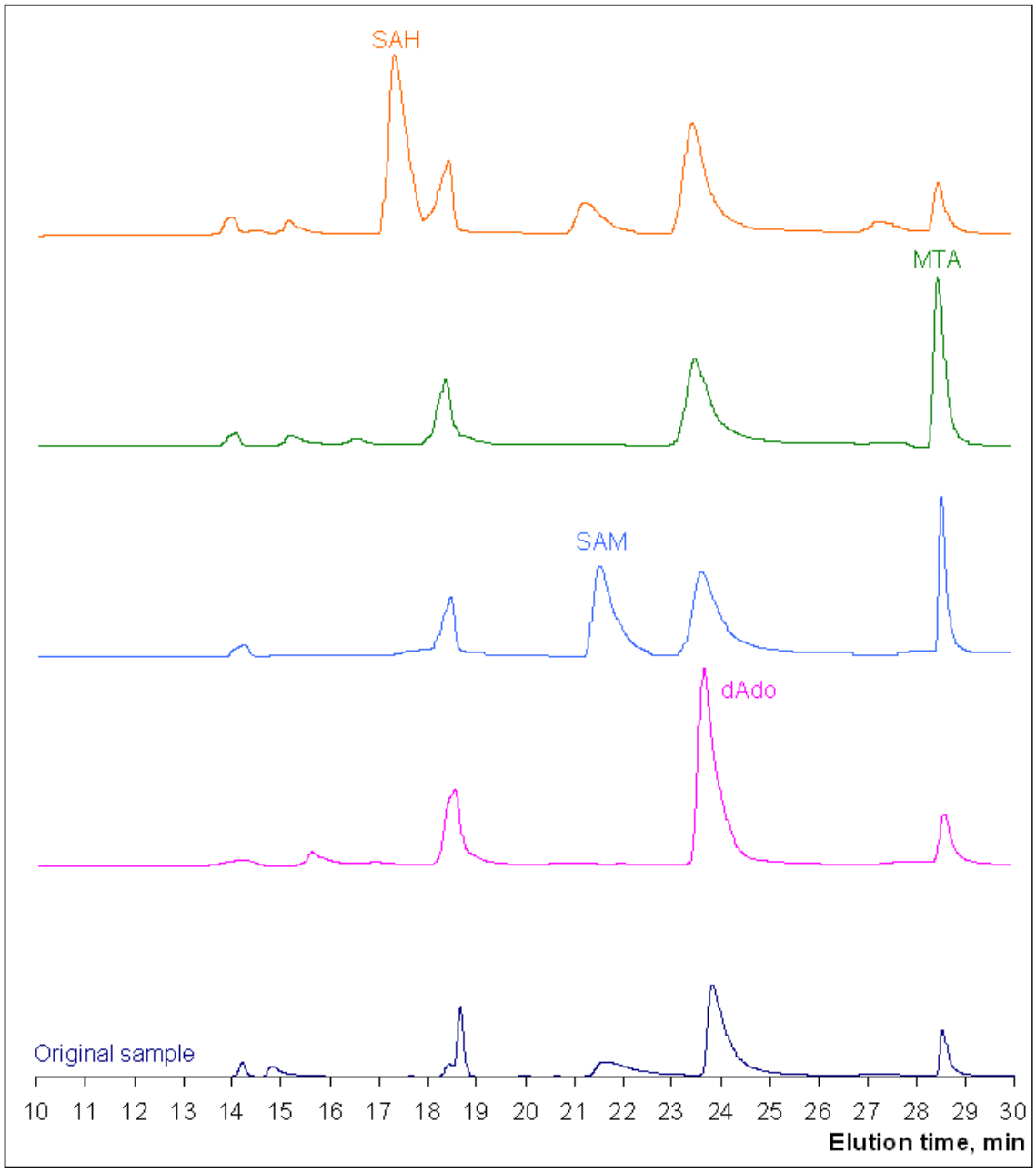

Figure 2.5. Co-injection of standards – S-adenosylhomocycteine (SAH), methylthioadenosine (MTA), *S*-adenosylmethionine (SAM), 5'-deoxyadenosine (dAdo) – in the original repair assay mix (3 hr). The diluted reaction mix (20 µl) was injected onto an Spherisorb ODS2 column (4.6 x 150mm, 5 µm, Waters). The samples were eluted using a gradient of acetonitrile in water (0% to 10% acetonitrile from 2 min to 20 min, then to 20% in the next 5 min. The flow rate was 0.6 ml/min and column temperature was 35 ^{o}C. In some spectra SAM peak was absent most likely due to SAM degradation.

To further confirm this data, the fractions were collected after HPLC of the 5*R*-SP repair assays were concentrated using a SpeedVac and were identified by ESI-MS (Figures 2.6 to 2.11). The fraction at 12 minutes from the 100% repair assay (see above) was also tested to confirm that the product is thymidine. The MS of the known/standard compounds (thymidine and 5*R*-SP) were also done for comparison (Figure 2.7 for thymidine and Figure 2.9 for 5*R*-SP). The mass spectrometry further confirmed the information suggested by HPLC spiking. The fraction that eluted at 24 minutes contained 5'-deoxyadenosine (Figure 2.10). ESI-MS also showed that the peak at 15.5 minutes likely contains amino acids and the fragments of several amino acids, presumably resulting from protein degradation during the sample preparation (data not shown).

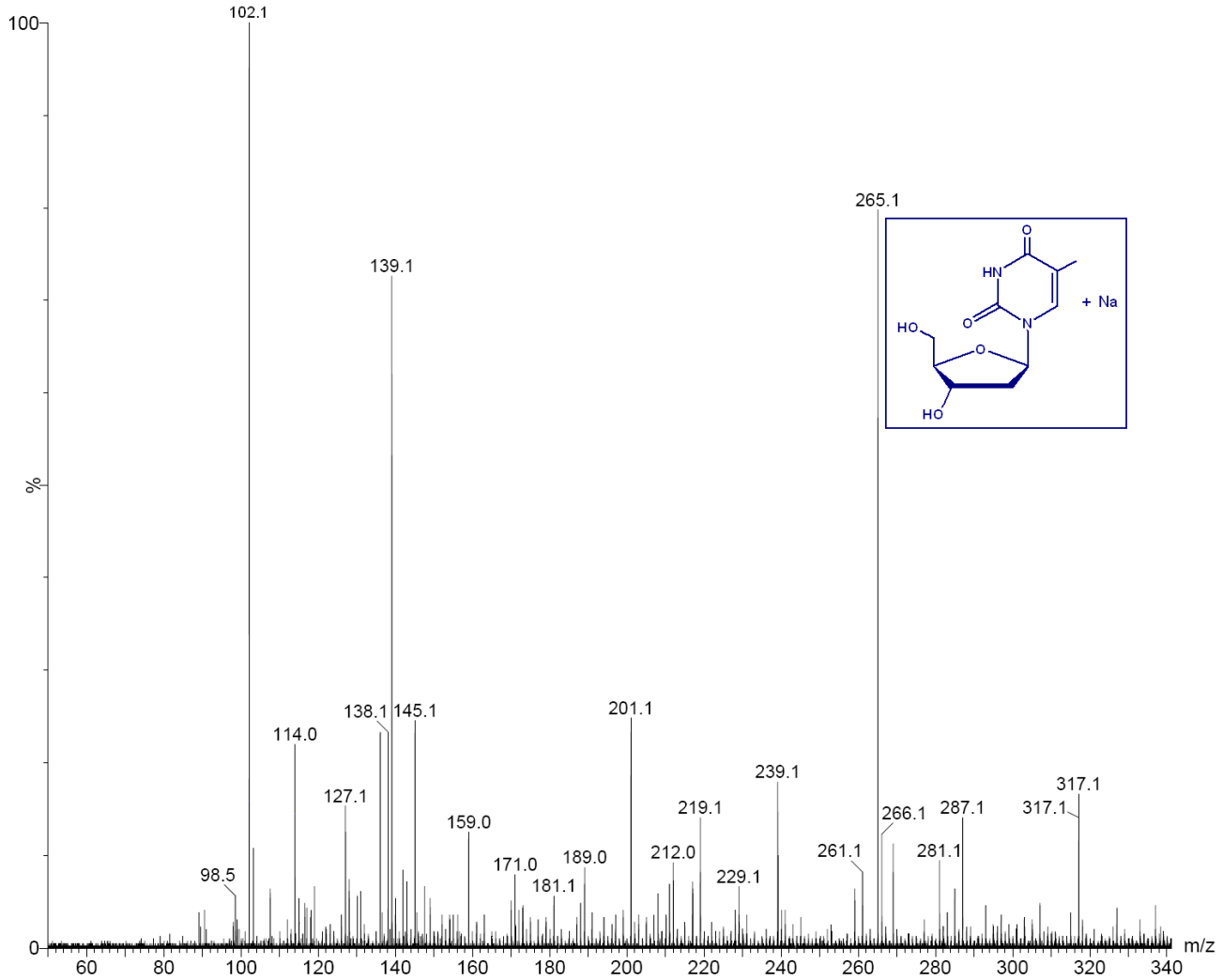

Figure 2.6. The mass spectrum of the fraction that eluted at 14.5 minutes after the 5*R*-SP repair assay. The molecular ion peak at 265.1 m/z matches thymidine + Na.

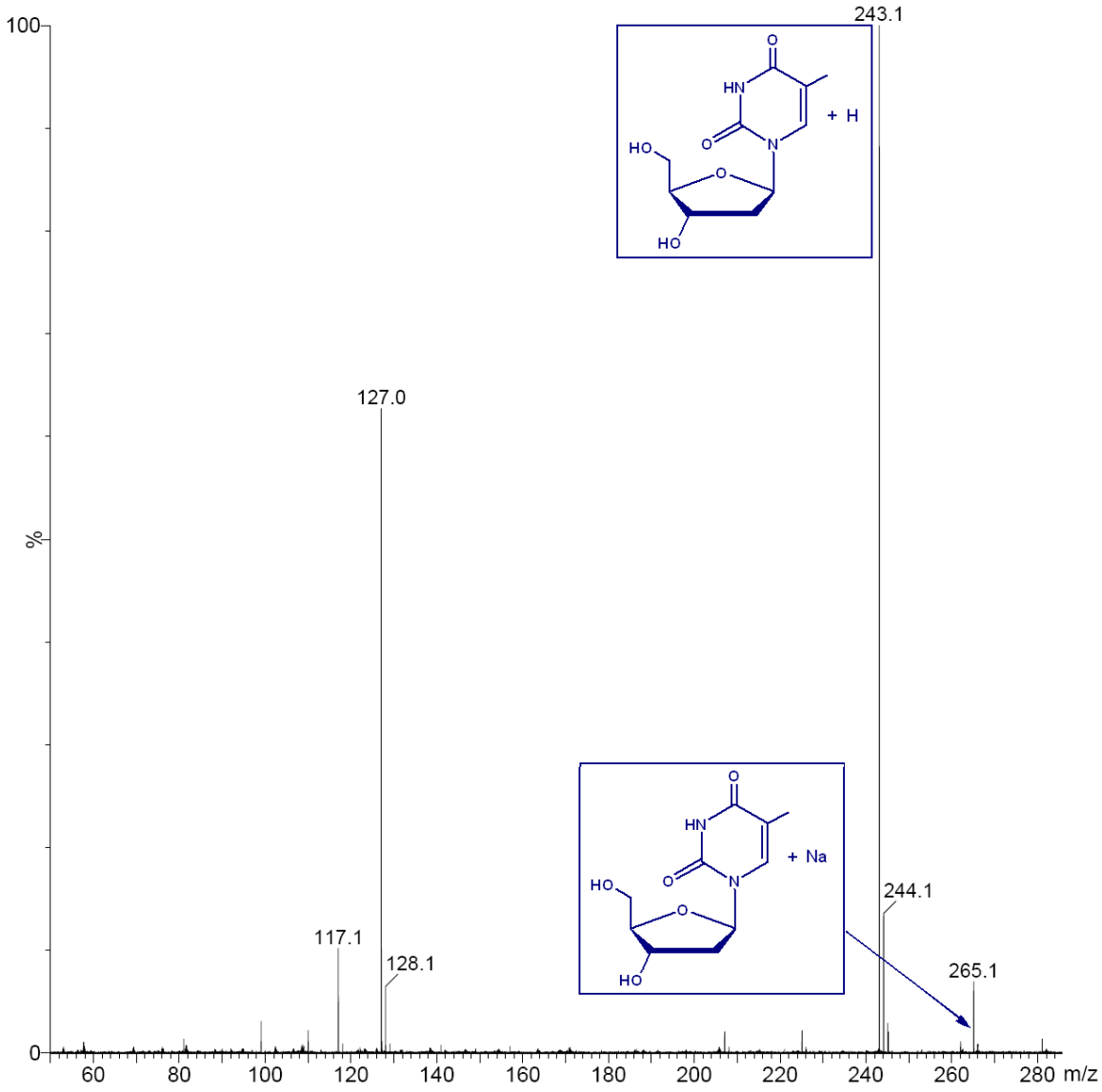

Figure 2.7. The mass spectrum of thymidine standard. The molecular ion peak at 243.3 m/z matches thymidine + H and peak at 265.3 m/z – thymidine + Na.

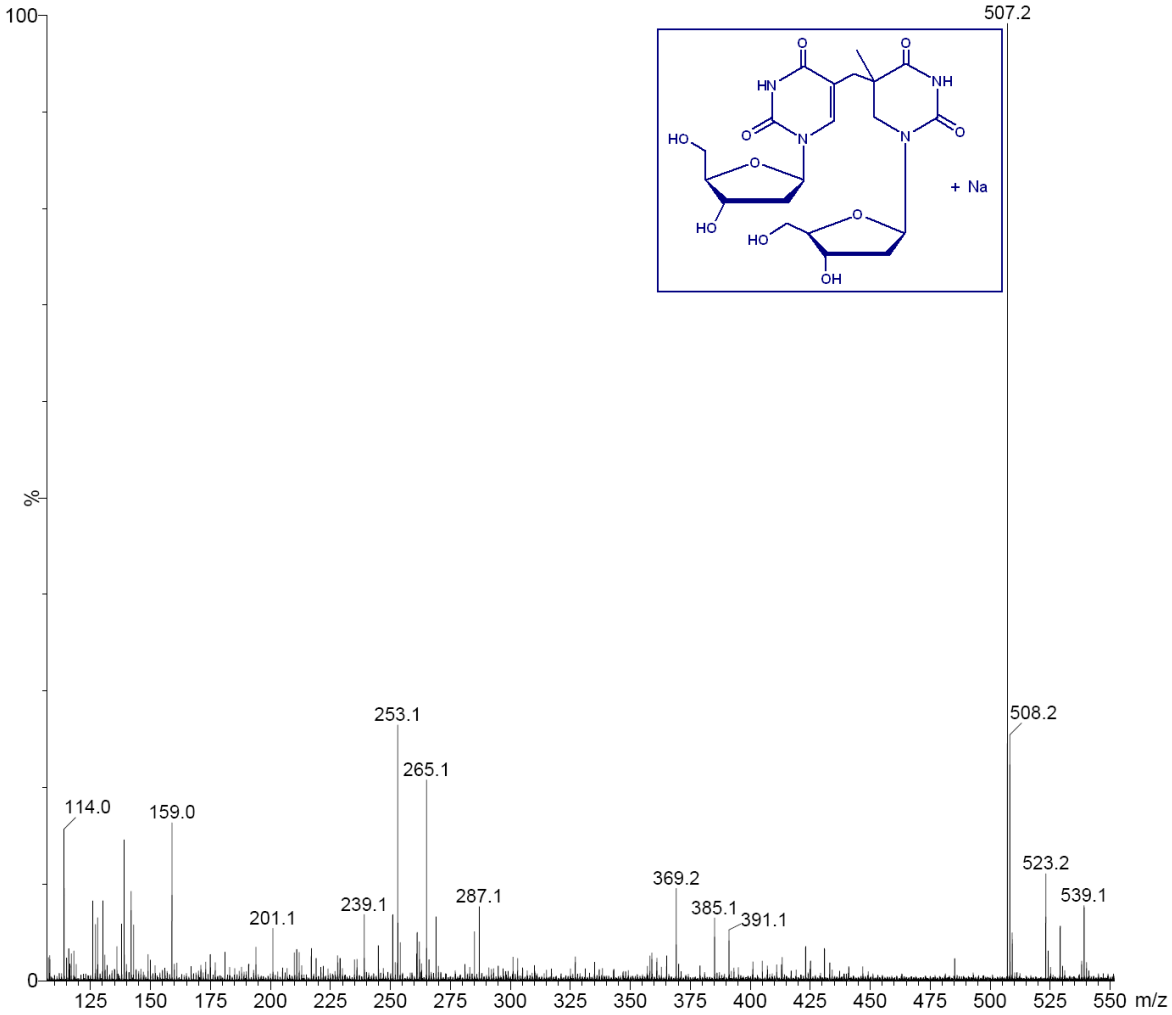

Figure 2.8. The mass spectrum of the fraction that eluted at 18.5 minutes in the 5*R*-SP repair assay. The molecular ion peak at 507.2 m/z matches 5*R*-SP + Na.

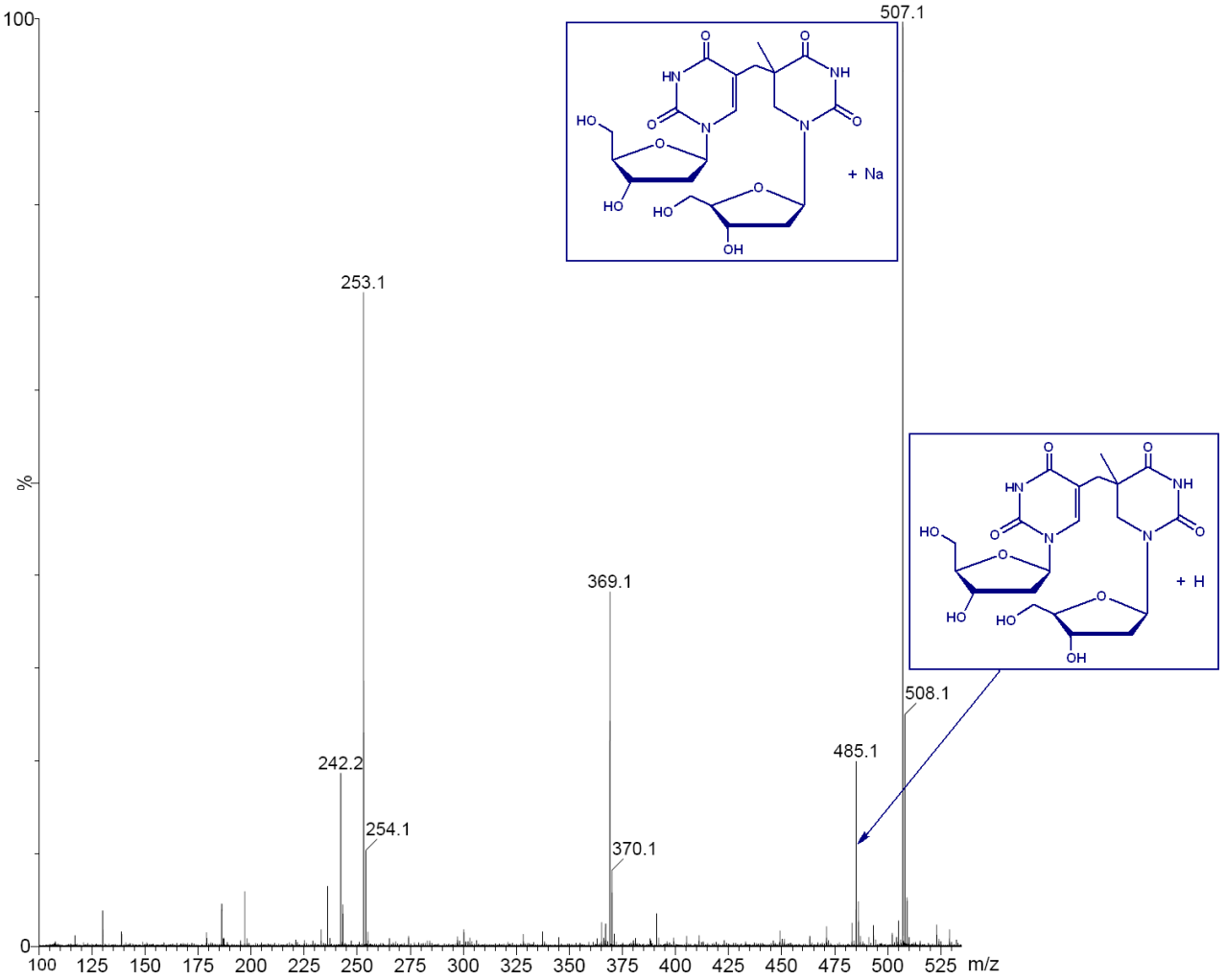

Figure 2.9. The mass spectrum of 5*R*-SP standard. The molecular ion peak at 507.1 m/z matches 5*R*-SP + Na and peak at 485.1 m/z – 5*R*-SP + H.

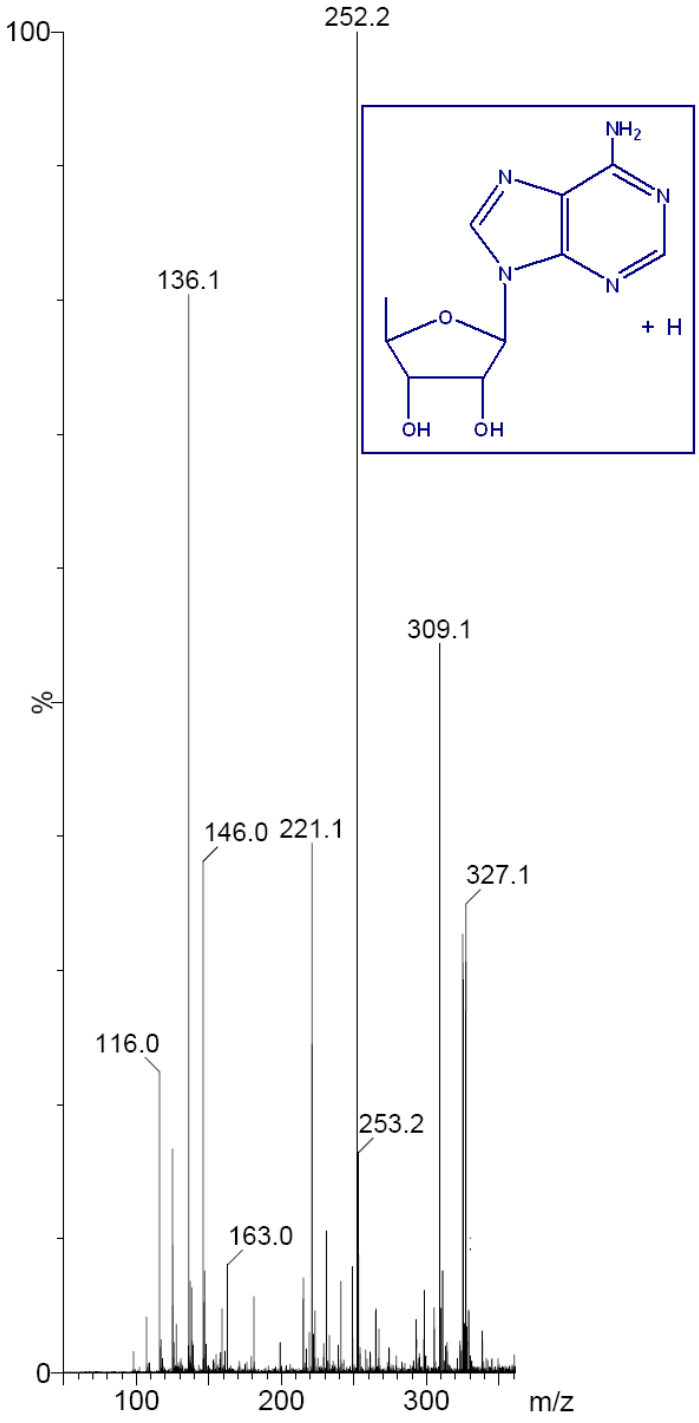

Figure 2.10. The mass spectrum of the fraction that eluted from HPLC at 24 minutes. The molecular ion peak at 252.2 m/z matches 5’-deoxyadenosine + H.

The Repair Rates of 5*R*-SP and 5*S*-SP

The repair assays that were carried out showed that SPL repairs 5*R*-SP, but not 5*S*-SP (Figures 2.1 and 2.2). These experiments were repeated several times with the protein from different growth and purifications to further confirm the results. Repair assays of 5*R*- and 5*S*-SP were also carried out in phosphate buffer as described in Material and Methods. The results from these assays were in agreement with the previous assays done in HEPES buffer.

Integration of the peaks from HPLC chromatograms allowed quantification of the amounts of thymidine produced (Figure 2.11). The repair rates were determined to be ~0.4 nmol/min/mg of SPL for the 5*R*-SP, with no repair observed for 5*S*-SP. The repair rate of 5*R*-SP was significantly slower than that observed for natural substrate generated by UV-irradiation (0.33 μmol/min/mg) (42). Also, our results contradicted with previous results from Carell and co-workers, which stated that 5*S*-SP, but not 5*R*-SP is repaired (49,148).

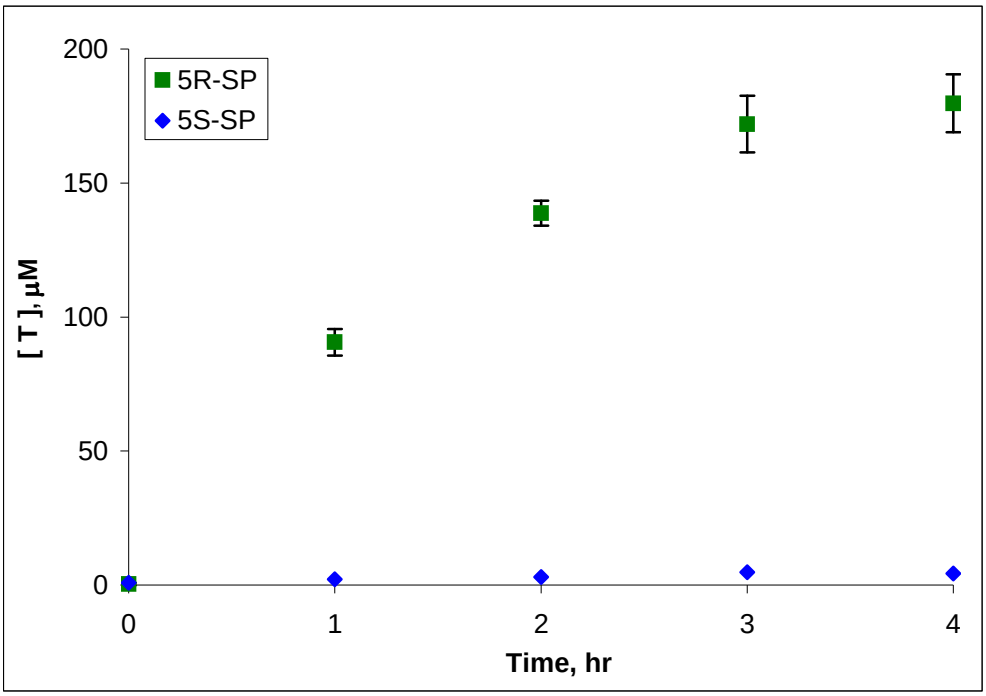

Figure 2.11. The thymidine formation over time from both *R*- and *S*-isomer of spore photoproduct. The experiments were carried out more than three times and were repeated in the presence of two different buffers (HEPES and phosphate) and from two different SPL growths. Error bars represent the standard deviation of product formation.

Interestingly, during our repair assay reaction, 5'-deoxyadenosine peak on HPLC chromatogram was also observed (Figure 2.3). This product can be formed only during SAM cleavage or degradation. This was an unusual observation considering our previous reports that SAM acts as a cofactor for SPL and should not be irreversibly cleaved during repair (39,42). Also, the 5'-deoxyadenosine peak was increasing with the incubation time, suggesting that it could be related to the activity of SPL (data not shown). Previous experiments focusing on the repair of spore photoproduct in DNA clearly showed that SAM was not cleaved during the reaction (42). However, Carell and co-workers observed SAM cleavage and they proposed that SAM was acting as a co-substrate (148).

In their work, SAM cleavage was also observed even in the absence of the substrate (49). We suggest that due to the fact that the spore photoproduct dinucleoside is not a natural substrate for SPL, unlike UV-irradiated DNA, and because strong reducing agent (sodium dithionite) was utilized in these reactions, an uncoupling between substrate turnover and the reductive SAM cleavage occurred. Similar reductive SAM cleavage was observed in other radical SAM enzymes as well (155,156) which occurred in the presence of non-physiological reducing agents, like sodium dithionite or photoreduced deazariboflavin, but not in the presence of flavodoxin-reductase/flavodoxin (79,155). Interestingly, dAdo is produced in both 5*R*-SP and 5*S*-SP repair assays, which was also observed by Carell and co-workers (148). Production of dAdo in the absence of the synthetic substrates further indicates uncoupling between SP repair and the reductive cleavage of SAM.

The Repair of Spore Photoproduct Dinucleotide by Spore Photoproduct Lyase

To further investigate SPL activity towards the spore photoproduct, assays for the repair of 5*R*-SP and 5S-SP dinucleotides (5*R*-SPTpT and 5*S*-SPTpT, Scheme 2.2) were carried out in a similar way to those of the 5*R*-SP and 5*S*-SP dinucleosides. The difference was that SP dinucleotide (Scheme 2.2), which has a bridging phosphate group between two thymines, was used as a substrate instead of SP dinucleoside (Scheme 2.1). Due to the fact that SP dinucleotides resemble the natural substrate (DNA) more closely than the dinucleoside, faster rates of repair were expected. Also, the SP dinucleotide cannot rotate around the methylene group and is more constrained than the SP dinucleoside due to the bridging phosphate. The repair assays of 5*R*-SPTpT demonstrated

its complete conversion to thymidine dinucleotide (TpT) (Scheme 2.5) over the course of one hour (Figure 2.12). The initial repair assays of 5*S*-SPTpT have shown no repair (data not shown) and further confirm that the 5*R*-isomer, rather than the 5*S*-, is the substrate for SPL (Scheme 2.5).

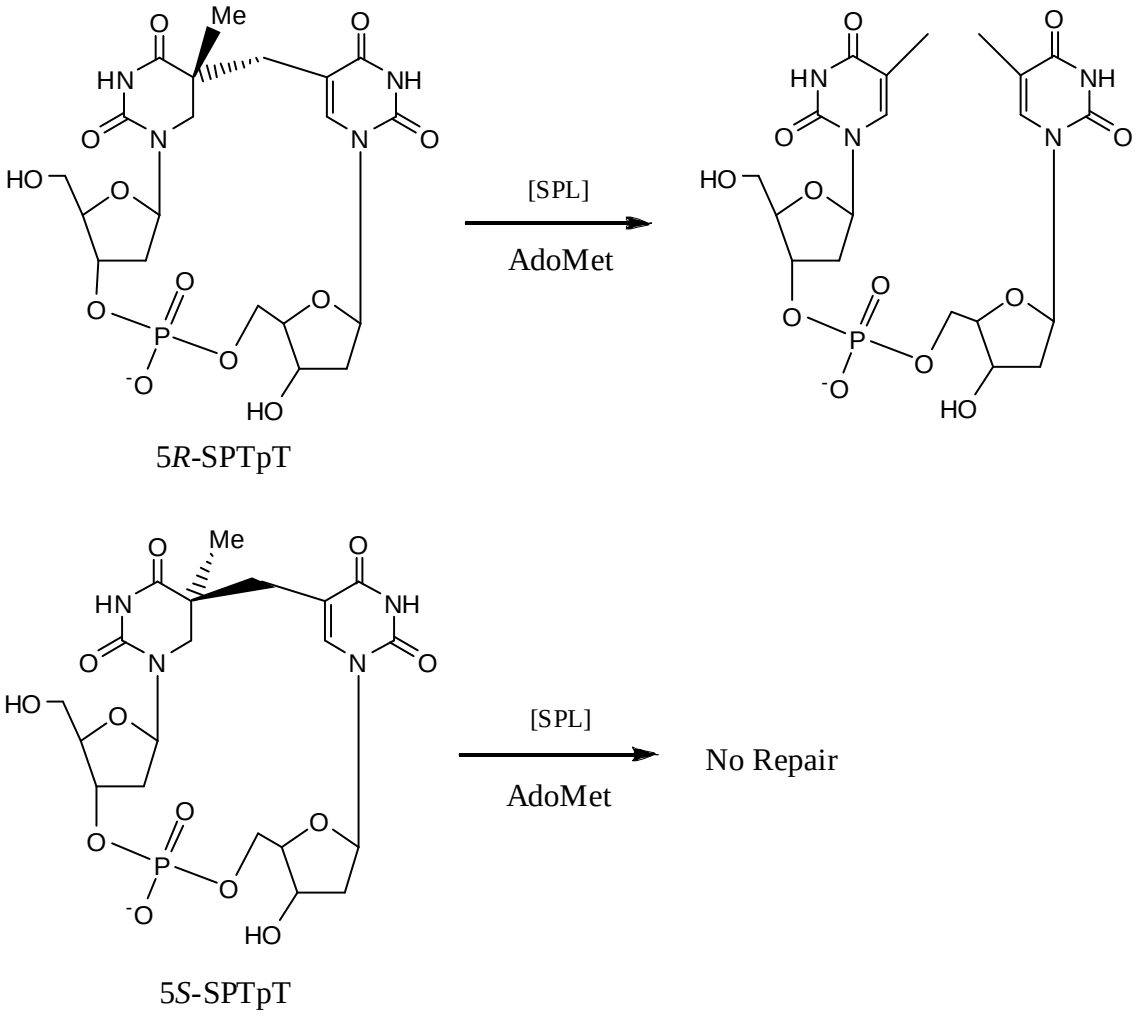

Scheme 2.5. The repair of 5*R*- and 5*S*- spore photoproduct dinucleotides (5*R*-SPTpT and 5*S*-SPTpT) by spore photoproduct lyase

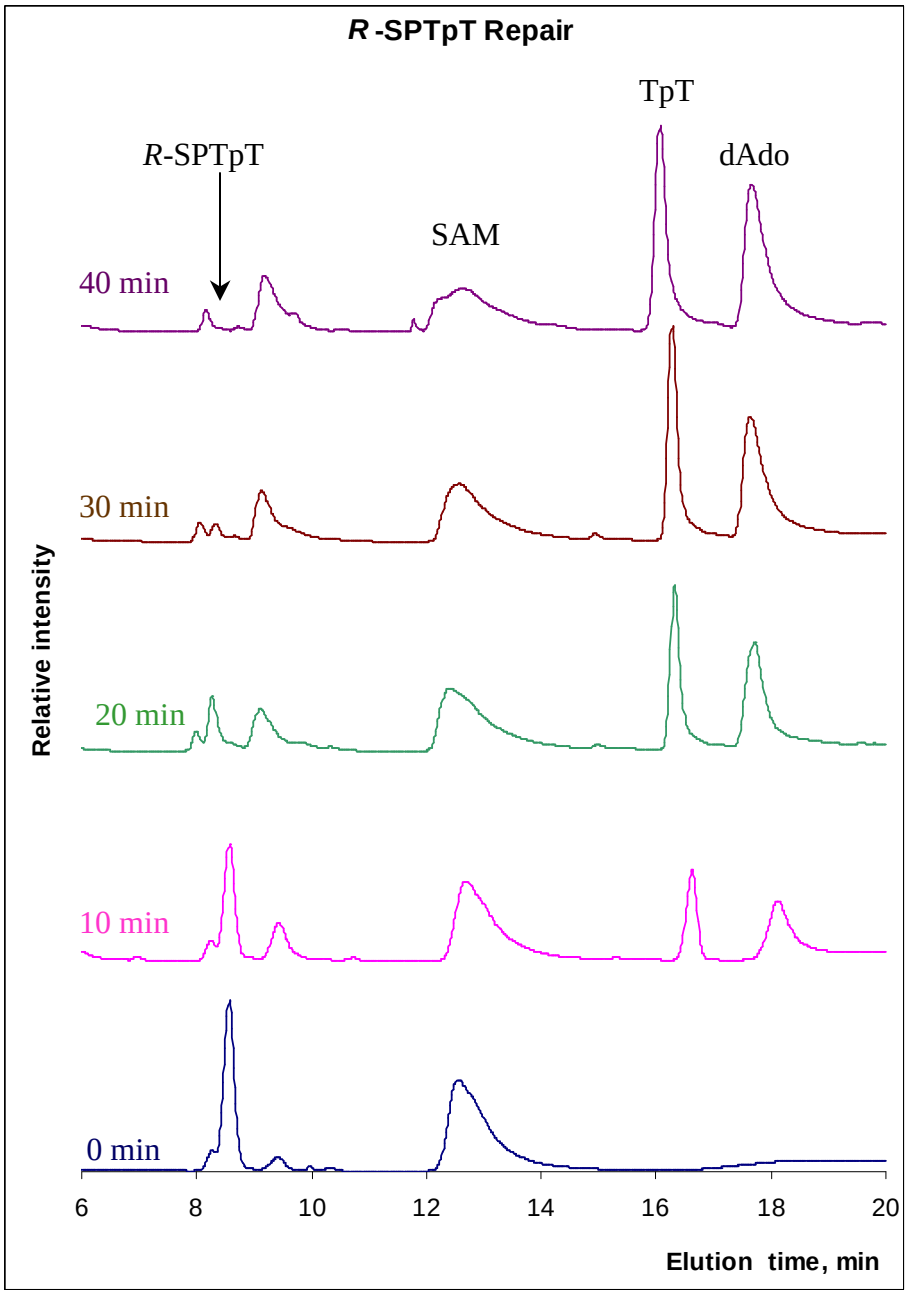

Figure 2.12. HPLC chromatograms of 5*R*-SPTpT repair and TpT formation over time. The diluted reaction mix (20 µl) was injected onto a Spherisorb ODS2 column (4.6 x 150mm, 5 µm, Waters). The samples were eluted using a gradient of acetonitrile in 2 mM TEAA (0% to 10% acetonitrile from 2 min to 25 min). The flow rate was 1 ml/min and column temperature was 28 ^{o}C. 5*R*-SPTpT elutes at 8.5 min, SAM at 12.5 min, TpT at 16.5 min and dAdo at 18 min. The chromatograms of 50 and 60 minute repair assays are not shown.

Characterization of the Peaks from HPLC (5*R*-SPTpT Dinucleotide)

The products of the 5*R*-SPTpT repair assay were identified the same way as for 5*R*-SP repair assay, by both co-injection of authentic compounds on HPLC and by ESI-MS of isolated fractions. For the co-injections, one of the repair assay samples (*R*-SPTpT repair assay after 30 minutes) was spiked with each of the following standard compounds in separate experiments – TpT, 5*R*-SPTpT, *S*-adenosylmethionine (SAM), methylthioadenosine (MTA), *S*-adenosylhomocysteine (SAH) and 5'-deoxyadenosine (dAdo). Then HPLC was run under standard conditions and the increase in one peak was used to identify the HPLC peaks. From these results we were able to identify that peak eluting at 8 minutes as 5*R*-SPTpT, the peak at 12 minutes as *S*-adenosylmethionine, the peak at 16 minutes as TpT, and the peak at 18 minutes as 5'-deoxyadenosine (Table 2.2).

Table 2.2. HPLC elution times of standard compounds. For HPLC, a reverse-phase Waters Spherisorb ODS2 column (4.6 x 150mm, 5 μm) was used. The samples were eluted using a gradient of acetonitrile in 2 mM TEAA (0% to 10% acetonitrile from 2 min to 25 min). The flow rate was 1 ml/min and column temperature was 28 ^{o}C. The buffers were filtered through 0.22 μm membrane and de-gassed before using.

Compound	**Elution time, min**
Thymidylyl (3'-5') thymidine (TpT)	16.5
Spore photoproduct dinucleotide (5*R*-SPTpT)	8.5
Spore photoproduct dinucleotide (5*S*-SPTpT)	11.0
S-adenosylmethionine (SAM)	12.5
5'-deoxyadenosine (dAdo)	18.0
Methylthioadenosine (MTA)	15.5
S-adenosylhomocycteine (SAH)	13.0

To further confirm this data, the fractions collected after from HPLC of the *R*-SPTpT repair assays were concentrated and identified by ESI-MS (Figures 2.13 - 2.15). The fraction at 8.5 minutes was identified as 5R-SPTpT (Figure 2.13), at 16.5 minutes as TpT (Figure 2.14) and at 18 minutes as 5'-deoxyadenosine (Figure 2.15). The MS of the standard compounds (TpT and *R*-SPTpT) were also run for comparison (data not shown). The mass spectrometry further confirmed the information suggested by HPLC spiking. ESI-MS also showed that the peak at 26 minutes possibly contained some amino acids and peptide fragments of several amino acids (MS data not shown), resulting from protein degradation during the sample preparation.

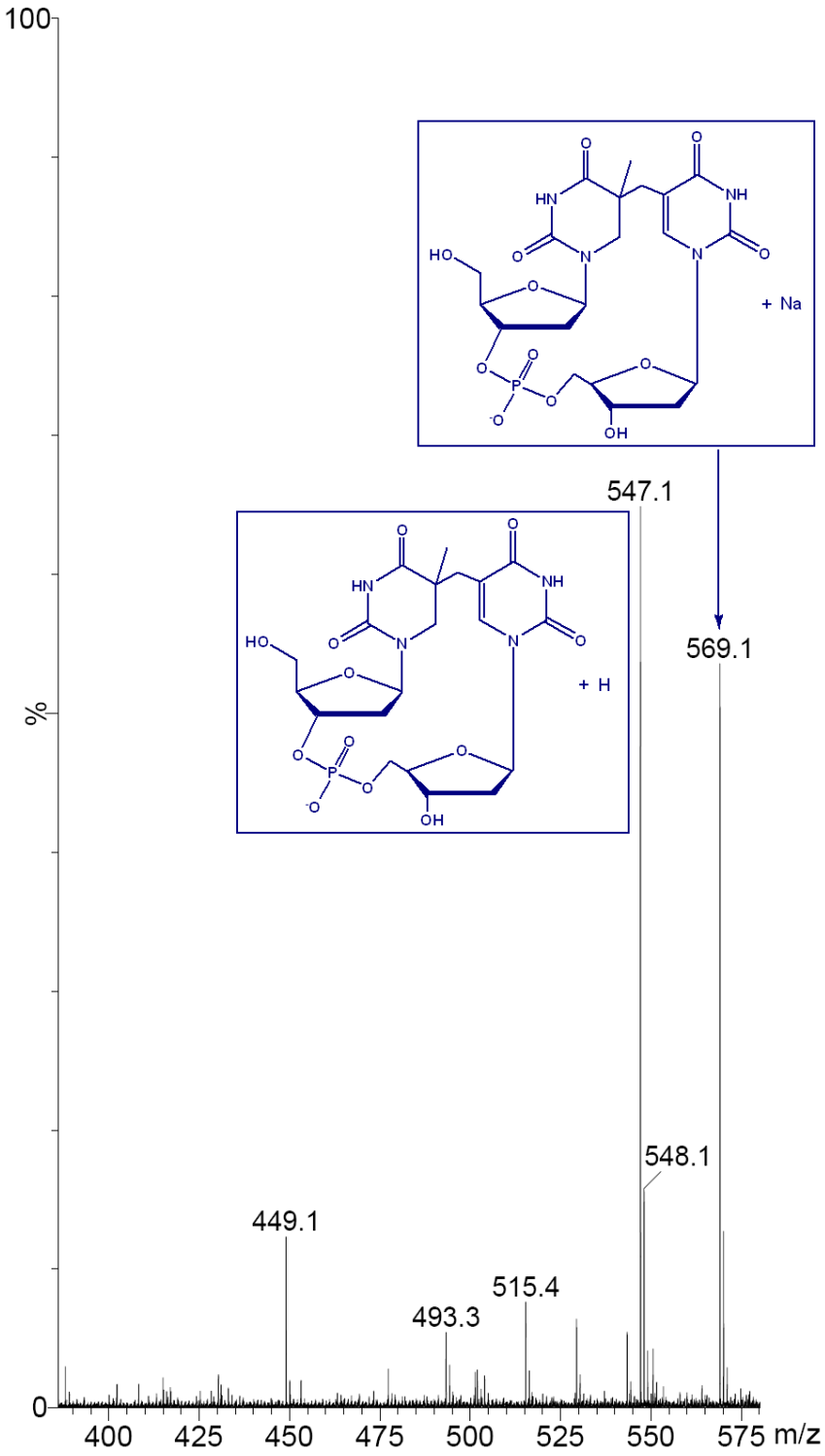

Figure 2.13. The mass spectrum of the fraction that eluted at 8.5 minutes in the 5*R*-SPTpT repair assay. The molecular ion peak at 547.1 m/z matches SPTpT + H and peak at 569 m/z – SPTpT + Na.

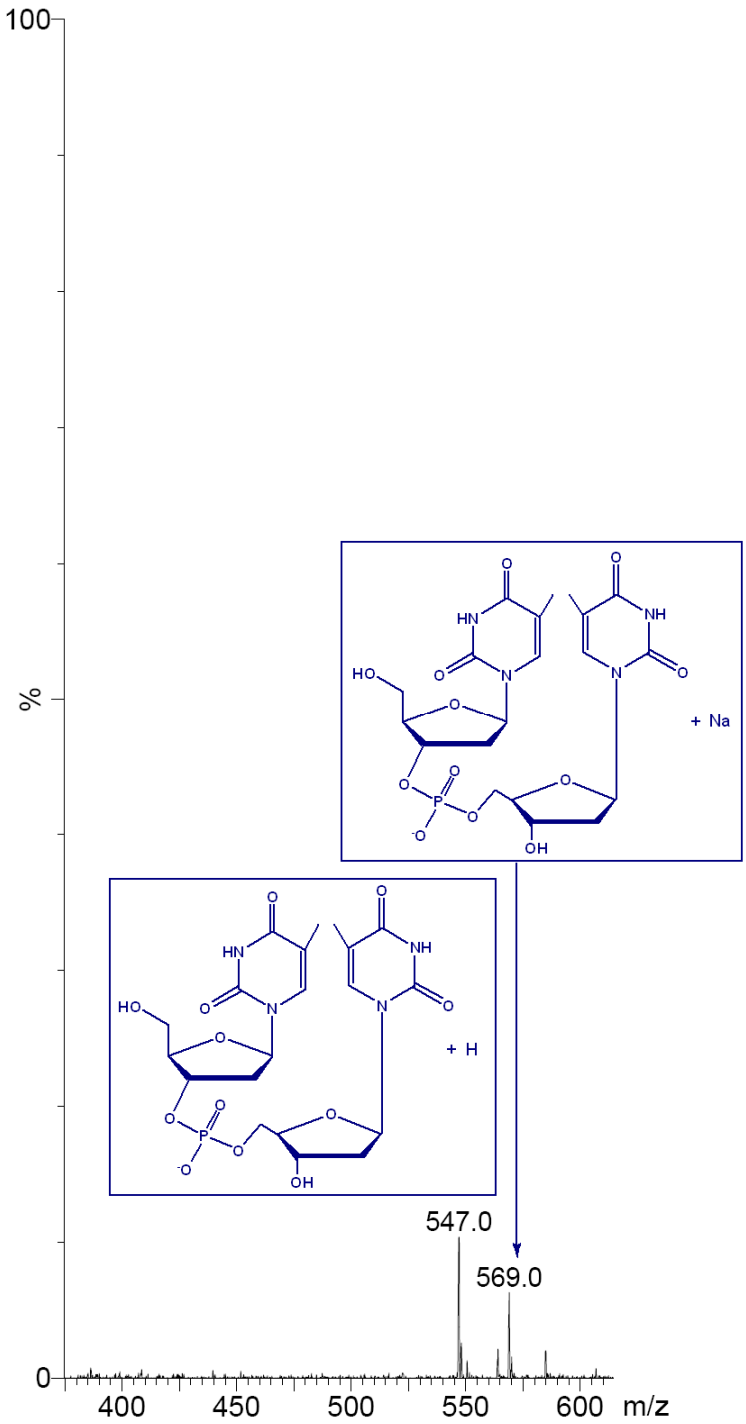

Figure 2.14. The mass spectrum of the fraction that eluted at 16.5 minutes. The molecular ion peak at 547 m/z matches TpT + H and at 569 m/z – TpT + Na.

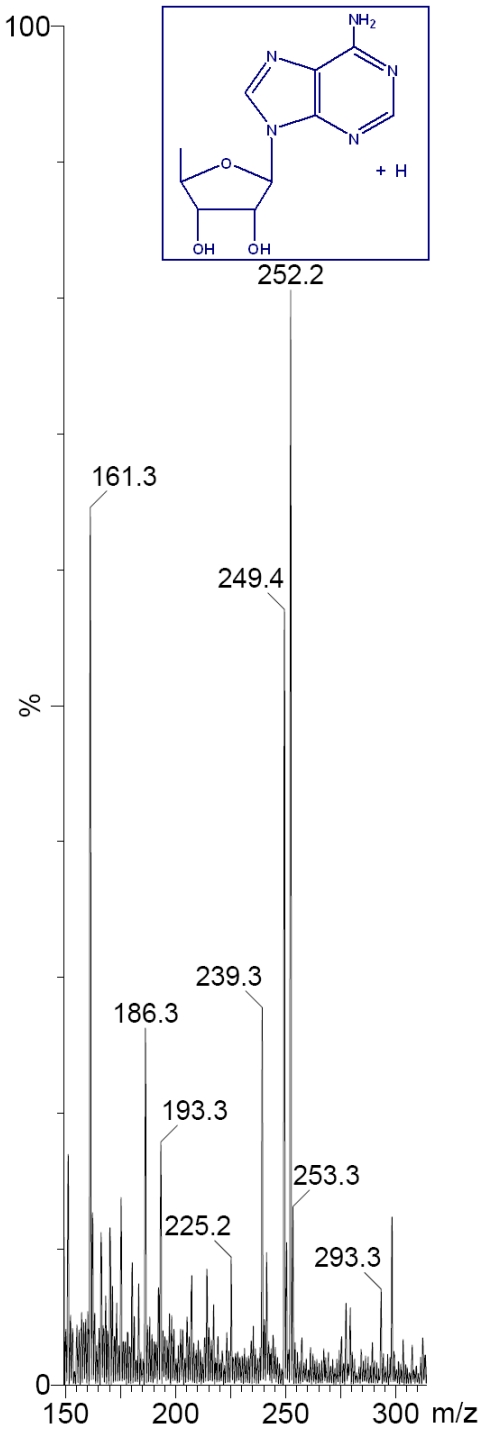

Figure 2.15. The mass spectrum of the fraction that eluted at 18 minutes. The molecular ion peak at 252.2 m/z matches the mass of 5’-deoxyadenosine + H.

The Repair Rates of 5*R*-SPTpT and 5*S*-SPTpT

Unlike the repair assays in which SP dinucleoside was used, complete repair was observed with 5*R*-SPTpT (Figure 2.12). These results indicate that 5*R*-SPTpT dinucleotide with the bridging phosphate group is a better substrate than 5*R*-SP dinucleotide. The reaction was completed after 40 min with 100% of 5*R*-SPTpT converted to TpT. The peaks from HPLC chromatograms were integrated and quantified in order to determine the rate of TpT production (Figure 2.16). The repair rates were found to be ~4 nmol/min/mg of SPL for 5*R*-SPTpT. These rates were 10 times higher than *R*-SP dinucleoside (~0.4 nmol/min/mg of SPL) but significantly slower than those observed for natural substrate generated by UV-irradiation of (0.33 μmol/min/mg) (42).

During this reaction, 5'-deoxyadenosine formation from *S*-adenosylmethionine was also observed (Figure 2.12). The SAM cleavage was dependent on reaction time and SPL activity, similar to the 5*R*-SP repair assays (Figure 2.11). For 5*R*-SPTpT control samples, just like in the 5*R*-SP dinucleoside assays, there was no dAdo production in the absence of SPL. These results confirmed that in order to cleave SAM, both SPL and the substrate have to be present. Again, SAM cleavage could be due to the fact the 5*R*-SPTpT is not as good substrate as natural substrate, UV-irradiated DNA, and due to the presence of reducing agent sodium dithionite.

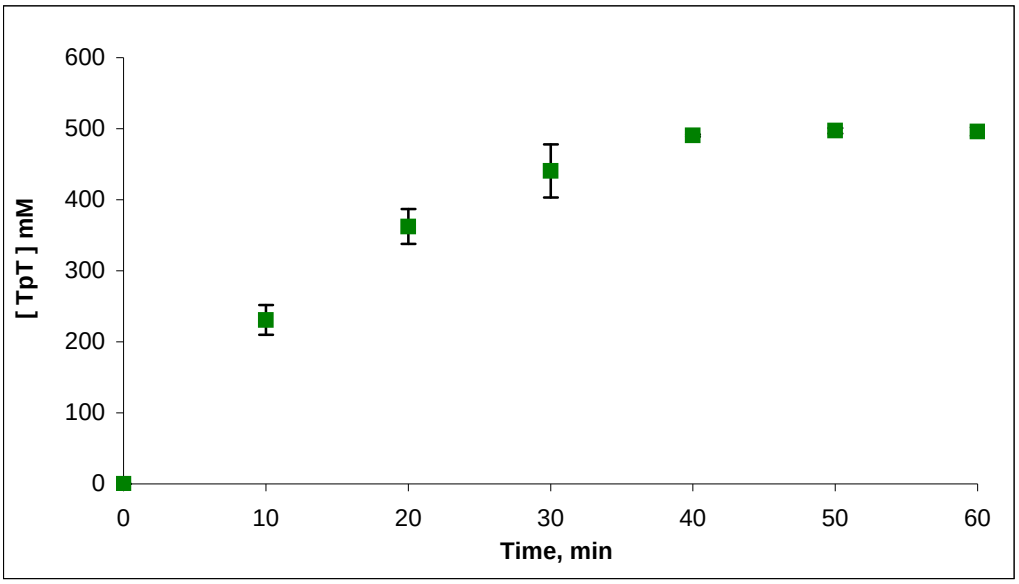

Figure 2.16. The TpT production in the 5*R*-SPTpT dinucleotide repair assays over time. The experiments were carried out in duplicate. Error bars represent the standard deviation of product formation.

Conclusions

SPL was successfully overexpressed and purified from both *Bacillus subtilis* and *Clostridium acetobutylicum*. *C.a.* SPL was purified with ~3 Fe/SPL, indicating a significantly higher cluster content than previously reported by Fontecave and co-workers (1.6 iron/protein) (147) and was not subjected to artificial reconstitution.

Due to the higher stability and solubility of *C.a.* SPL, it was used for both spore photoproduct dinucleoside and dinucleotide repair assays. Interestingly, when *C.a.* SPL was used for the spore photoproduct repair assays, it was found that it repaired the 5*R*-isomer rather than the 5*S*-isomer (146), which differs from what was reported previously (49,148). The repair rates for this assay were found to be 0.4 nmol/mg/min of SPL for 5*R*-SP and 0 nmol/mg/min of SPL for 5*S*-SP. These rates are lower than the ones

observed from DNA repair assays using the UV irradiated DNA (42) and could be due to the fact that the synthetic substrate was used without incorporation into DNA. The repair of 5*R*-SPTpT dinucleotide further confirmed that SPL repairs the 5*R*-isomer with the repair rate of 4 nmol/mg/min of SPL. These findings agree with the results showing that 5*R*- is the isomer produced during the UV-irradiation of a thymidine dinucleotide (TpT) (150). Also it showed that 5*R*-SPTpT is a better substrate than 5*R*-SP. For the longer-term goals, the repair assays of oligonucleotide containing 5*R*- and 5*S*- spore photoproduct, have to be carried out.

CHAPTER 3

SPORE PHOTOPRODUCT LYASE BINDING TO UNDAMAGED DNA

Introduction

Many proteins bind DNA to perform a variety of functions, including transcription, regulation, DNA protection and repair (157,158). Before binding to its target site, a DNA-binding protein is thought to scan along the DNA by 2-dimensional diffusion to find the specific sequence or, in case of repair proteins, the damaged site (159). Therefore nonspecific binding is thought to precede binding to the specific/target site. Nonspecific binding, therefore, should be an important intermediate step in the process of recognizing and binding the target/damaged site. Binding affinities, specific and non-specific, can help provide insights into the interactions between the proteins and DNA. It can provide information as to how strong these interactions are, and, if non-specific binding precedes the specific binding, how much binding of the protein is stronger to specific DNA than to non-specific DNA (the 'selectivity' ratio), and how protein repairs the DNA.

Previous studies have shown that specific binding can induce conformational changes in the DNA or both the protein and DNA (121,160-163). However, little is known about how proteins bind to nonspecific or undamaged DNA. Also, it is not clear if nonspecific binding changes the structural and dynamic properties of the DNA (164) like they do in case of specific binding. There is very little known about how the proteins switch from nonspecific binding to specific during the 'scanning' process (164).

The *lac* repressor is a DNA-binding protein that is involved in lactose metabolism in bacteria and binds to the major groove of the operator region of the *lac* operon. It was found that the *lac* repressor protein can form a nonspecific complex with DNA by making electrostatic interactions, which can be further stabilized by protein side-chain and backbone interactions with the phosphates (164). Interestingly, most of these interactions are preserved when the protein binds to DNA specifically (Figure 3.1, (164)). Kaptein and co-workers suggested that this kind of transition between the nonspecific and specific complexes may be more energetically favored when a target site is found during the 'scanning' process (164). Therefore the DNA-binding protein should have a scaffold for DNA binding that can be adjusted for either nonspecific or specific binding (164).

Although the *lac* repressor has a completely different function than spore photoproduct lyase, it also has a helix-turn-helix motif and there might be some binding similarities/analogies. For example, SPL might bind to non-specific DNA with relatively appreciable affinity and most of the bonding could be made up from electrostatic and/or hydrogen bonding with the phosphate backbone.

DNA photolyase, a DNA repair protein that converts the *cis,syn* cyclobutane photodimer (CPD) to two thymines, shares some sequence similarities with SPL (see Chapter I). DNA photolyase was also found to bind DNA nonspecifically (165,166). However, it efficiently discriminates between target and non-target structures as do sequence-specific DNA binding proteins (165). DNA photolyase dissociation constant for undamaged DNA was determined using electrophoretic mobility shift assay (EMSA) by binding competition (165). It was found that the addition of a large amount of undamaged

oligonucleotide decreased some of the specific complexes formed between the enzyme and damaged oligonucleotide, suggesting weak interaction with undamaged DNA (167).

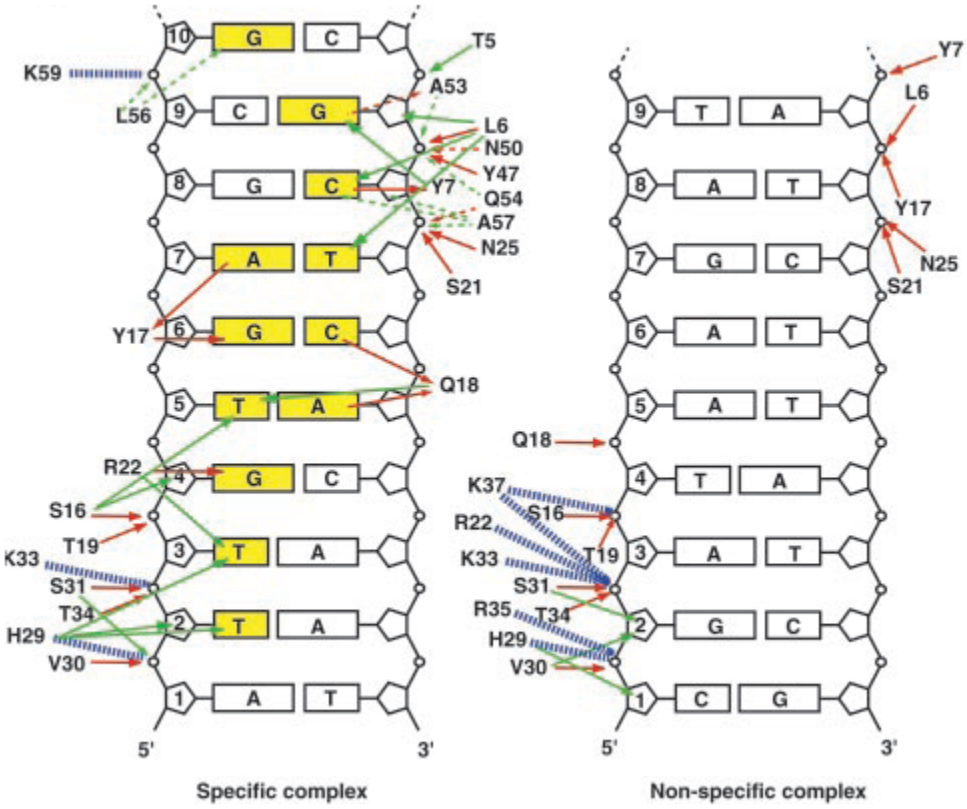

Figure 3.1. Schematic summary of specific and nonspecific binding interactions between *lac* repressor and DNA. The bases that are specifically recognized by lac repressor are colored in yellow. The solid lines indicate interactions in the major groove, and dashed lines - in the minor groove. Red lines indicate hydrogen binding, green – hydrophobic interactions, and dashed lines indicate electrostatic contacts (164).

Husain and Sancar proposed that the complexes between photolyase and undamaged DNA were too weak and did not survive electrophoresis (167)). In their 1987 *Nucleic Acid Research* paper they determined the nonspecific dissociation constant for *E. coli* DNA photolyase to be $K_d = 3.45 \times 10^{-5}$ M in comparison to $K_d = 2.6 \times 10^{-8}$ M for the specific binding, with a stoichiometry of 1.0 molecule of enzyme per thymine dimer

(167) (Table 3.1). In 1993, Baer and Sancar found that *E. coli* DNA photolyase had K_d = 2.6 x 10^{-5} M for non-specific DNA and K_d = 3.7 x 10^{-9} M for specific DNA (165) (Table 3.1). For both of these assays a 43-bp long oligonucleotide with or without cyclobutane dimer damage in the center was used. It seems that K_d for non-specific binding from these two papers were consistent, but for specific binding K_d was 7 times smaller in the latter paper (Table 3.1). That could be due to several modifications in the photolyase purification procedure, since other conditions were the same. The results from nitrocellulose filter binding assays utilized long plasmid DNA, with 5.5 damaged sites per molecule, gave a K_d value of 6.0 ± 2.1 x 10^{-7} M (168) (Table 3.1). It is not clear at this point whether the difference in binding between this and previous assays is due to a different type of DNA used or that filter binding assays were done instead of electrophoretic mobility shift assays, although the earlier work of Husain and Sancar suggested that there is no significant difference between these two types of assay (167). There is no data available on what nonspecific binding between long plasmid DNA and DNA photolyase could potentially be (Table 3.1).

Despite similarities between the DNA photolyase/(6-4) photolyase and SPL, such as repair of thymine dimers, and some sequence similarities, these enzymes are likely very different in structure and binding/damage recognition. SPL has a predicted helix-turn-helix motif, while DNA photolyase has not. Also, photolyase's DNA binding regions have very little match with SPL sequence. That could mean that despite some sequence similarities these two enzymes might have different binding sites. Also, many DNA binding enzymes, which share the same function, can have similar protein folds

(169), as do radical SAM superfamily enzymes, despite low sequence conservation within each family (51,116,119).

Table 3.1. DNA photolyase dissociation constants from different experiments.

DNA	Type of binding	K_d, M	Type of assay	Reference
43-bp oligo	non-specific	3.5×10^{-5}	EMSA	(167)
43-bp oligo with CPD*	specific	2.6×10^{-8}	EMSA	(167)
43-bp oligo	non-specific	2.6×10^{-5}	EMSA	(165)
43-bp oligo with CPD*	specific	3.7×10^{-9}	EMSA	(165)
plasmid DNA**	specific	4.7×10^{-7}	nitrocellulose filter	(168)
plasmid DNA	non-specific	N/A	N/A	N/A

* Oligonucleotide that contains *cis,syn* cyclobutane dimer (CPD) at the center position
** pBR322 plasmid DNA that contains ~5.5 damaged sites (CPD's) per molecule

Beyond the repair of spore photoproduct (39,42,43,49,142), there is very little knowledge on how SPL recognizes and binds DNA with or without a damaged site. Nicholson and co-workers found that SPL binds to SP containing oligonucleotide and bends the DNA, presumably to flip out the damaged site (142). They also found that SPL protects a 9 base-pair region around the damaged site (142). Because SPL binds to SP but not the *cis,syn* cyclobutane dimer, it presumably recognizes an SP-specific helical distortion in DNA which differs in its geometry from the distortion caused by a *cis,syn* cyclobutane pyrimidine dimer (142) that is recognized by DNA photolyase. Also, since UV irradiation can create a damaged site at any two adjacent thymines in the DNA, presumably SPL has to be able to find the damage and repair it in any sequence context. We also assume that non-specific binding occurs within the predicted helix-turn-helix

region of SPL, with the most conserved amino acids likely making bonds with the phosphate groups on the DNA backbone (see Figure 1.7 –Chapter I).

There are several methods, such as electrophoretic mobility assays (EMSA), filter binding assays, and calorimetric assays that are employed to investigate protein binding to DNA. Although these methods can provide useful information about protein-DNA interactions, they also have some limitations. For example, the observed affinities from these assays could be the sum of all interactions occurring between the protein and the DNA, especially in nonspecific binding. Also, the protein-DNA interactions that are short-lived might not be detected in electrophoretic mobility or filter binding assays. Filter binding assays are not necessarily 100% efficient under different experimental conditions (166).

In order to investigate how SPL binds to undamaged DNA, electrophoretic mobility shift assays were carried out. Here we show for the first time that SPL binds to undamaged/nonspecific DNA with rather high affinity. Also, we show that the absence of [4Fe-4S] cluster in SPL and the presence of *S*-adenosylmethionine (SAM) or small-acid soluble proteins (SASPs) had little effect on binding. The binding of SPL from two different bacteria, *Bacillus subtilis* and *Clostridium acetobutylicum*, to undamaged DNA was also compared.

Experimental Methods

Materials

All chemicals used in this work were purchased commercially and were of the highest purity available. The synthetic oligonucleotides were purchased from Integrated DNA Technologies. [γ-^{32}P] ATP was purchased from MP Biomedicals. T4 polynucleotide kinase, required for radioactive labeling, was commercially obtained from Invitrogen.

Purification and Dialysis of SPL

Spore photoproduct lyase enzymes from *Bacillus subtilis* and *Clostridium acetobutylicum* were purified as described previously (42,146). After purification the protein was concentrated and kept frozen at –80 ^{o}C until use. For electrophoretic mobility shift assays (EMSA) protein was first dialyzed to remove imidazole (which could be up to 250 mM) and also substitute 50mM sodium phosphate with 50mM HEPES. Dialysis was always done anaerobically at +4 ^{o}C against 2 L of Buffer A (50mM HEPES, 0.5 M NaCl, 5% glycerol, pH 8) for 2 hr and then repeated. The concentration of SPL from *B. subtilis* was 0.183 mM and it had 2.3 irons per protein. The concentration of *C.a.* SPL was 0.104 mM and had the 2.9 irons per protein. For DNA binding assays this protein was later diluted with Buffer A in order to maintain constant salt concentration in the DNA binding reaction mix.

Preparation of *apo*-SPL

Purified SPL from *B. subtilis* was dialyzed against 2 L of EDTA buffer (10 mM EDTA, 50 mM HEPES, 0.5 M NaCl, 5% glycerol, pH 8) for 2 hr at +4 ^{0}C and then this cycle was repeated. The EDTA was then removed by dialyzing against Buffer A for 2 hours. The protein concentration after the dialysis was 0.049 mM and it had 0.43 irons per protein. The protein was then diluted with the buffer A and used for the binding assay. SPL concentration after dialysis was 0.086 μM and it had 0.5 irons per protein. An analogous dialysis procedure was carried out for SPL from *C. acetobutylicum*.

5'-End Labeling of 94-bp Oligonucleotide

Two complementary oligonucleotides were synthesized (Integrated DNA Technologies) based on the *B. subtilis* sequence (from 322456 to 322550). Oligonucleotides had 94 nucleobases (the adjacent thymidines are shown in bold):

TK4-72a (MW = 28,902 Da) 5'- CGGGATCAACCAGAGCATCATGC**TT**GC G**TT**ATCAATGG**TT**G**TT**ATCGCCGCAATGGTCGGTGCACCGGGAC**TT**GG**TT**CT GAAGTATACAGTGC C –3' and

TK4-72b (MW = 29,057 Da) 5'- GGCACTGTATAC**TT**CAGAACCAAGTCC CGGTGCACCGACCA**TT**GCGGCGATAACAACCA**TT**GATAACGCAAGCATGAT GCTCTGG**TT**GATCCC G -3'.

TK4-72a oligomer (1 μL, 5.8 pmoles or 0.17 μg) was added to 5 μL 5X Forward Reaction Buffer (Invitrogen), 2.5 μL [γ-^{32}P] ATP (10 μCi/μL, 3000 Ci/mmol)(MP Biomedicals), 1 μL T4 polynucleotide kinase (Invitrogen) and 13.5 μL of autoclaved MQ

water to the total volume of 25 μL. The mixture was incubated for 10 minutes at 37 ^{o}C followed by heat inactivation at 65 ^{o}C for 10 min. Ethanol precipitation was carried out as follows: to the Eppendorf tube containing labeled oligomer was added 250 μL 4.67 M NH_4OAc and 750 μL 100 % ethanol (ice cold). Then, the sample was kept on ice for 30 minutes and centrifuged at 12,000 rpm for 20 minutes. The supernatant was removed and 500 μL of 80 % ethanol (ice cold) was added. The sample was centrifuged at 12,000 rpm for another 20 minutes and the supernatant was discarded. The oligomer was dried under a N_2 stream and resuspended in 50 μL TE Buffer (pH 8). The labeled strand was then hybridized to the complementary strand TK4-72b by heating at 90 ^{o}C for 2 minutes and cooling down slowly to room temperature. The double-stranded oligomer was purified using mini Quick Spin Oligo Column (Roche Applied Science), and stored at –80 ^{o}C.

Electrophoretic Mobility Shift Assay
of the Double-Stranded 94-bp Oligonucleotide

The electrophoretic mobility shift assay (EMSA) reactions were prepared in a total volume of 20 μL containing 10 mM HEPES, 50 mM NaCl, 10% glycerol, 0.05% NP-40, 0.5 mM DTT, 2.9 nM labeled double-stranded oligonucleotide, and different concentrations of either *B.s.* or *C.a.* spore photoproduct lyase (pH 8). The assay reactions were prepared anaerobically in an MBraun glove box and incubated for 1 hour at room temperature. The samples were loaded on an 8% non-denaturing polyacrylamide gel and electrophoresed at 200 V (20 V/cm^2) for 2 hours. Next, the gel was dried overnight and the electrophoresis products were visualized by autoradiography (X-Omat AR-5 film

(Kodak)). The bands on the film were quantified using GS-900 gel scanner (Bio-Rad) and QuantityOne 4.0.2. software.

Electrophoretic Mobility Shift Assay at Different pH

The reaction conditions were identical to those described above, except the pH of Buffer A (50 mM HEPES, 0.5 M NaCl, 5% glycerol) was adjusted to pH 8, pH 7.5, pH 7.0 or pH 6.5. Analogous experiments were done with *C.a.* SPL.

Electrophoretic Mobility Shift Assay at Different Conditions

For the assay under aerobic conditions, the reaction conditions were the same as above, except the samples were prepared aerobically. For the assay with *apo*-SPL, the only difference was that *B.s.* SPL lacking iron-sulfur cluster was used. For the reaction with *S*-adenosylmethionine (SAM), in addition to the reaction mix, SAM was added to each sample to the final concentration of 1 mM. For the assay with the small acid-soluble proteins (SASPs), SspC was added to the ratio of [DNA]/[SspC] = 1:5. SspC was purified as described previously (42).

Electrophoretic Mobility Shift Assay
of the Single-Stranded 94-bp Oligonucleotide

For the labeling of single-stranded TK4-72a oligonucleotide, the procedure was the same as for the double-stranded oligonucleotide, except the annealing step was omitted. The EMSA conditions were identical to the ones for double-stranded oligonucleotide under anaerobic conditions.

Electrophoretic Mobility Shift Assay
of the Double-Stranded Long DNA

In order to investigate how DNA binding depends on its length, the EMSA with long DNA was carried out. For that purpose linear pUC18 DNA was used. The advantage of this method is that it does not require radioactive labeling and it is faster. The major disadvantage, however, is a lower accuracy. First, plasmid pUC18 DNA was transformed into NovaBlue (Novagen) cells and overnight cultures were grown. Then DNA was purified using the QIAprep® Spin Miniprep DNA purification kit (Qiagen). In order to obtain linear DNA, pUC18 DNA was cut with the restriction enzyme EcoRI (Promega) and purified from 1% agarose gel using the QIAquick® Gel Extraction kit (Qiagen). The binding assays were carried out the same way as for 94-bp oligonucleotides. Agarose gels (1 %) were run at 110 V (20 V/cm^2) for 1 hr. The bands on the gel were scanned and quantified using UVP scanner (Doc-It LS software).

Calculation of SPL-DNA Dissociation Constant

The dissociation constant, K_d was determined from the point at which 50 % of DNA is bound to protein by determination using Origin 8.0 software with the Hill equation for cooperative binding:

$$I = \frac{I_{max}[L]^n}{(K_d + [L]^n)},$$

Where: I is band intensity at a specific concentration of the ligand; I_{max} is the intensity at which ligand binding reached saturation; n is Hill coefficient, describing cooperativity;

K_d is the dissociation constant (at which half of the ligand molecules are bound); L is the ligand concentration

This equation was chosen because the binding curves were sigmoidal, indicating cooperative binding.

Results and Discussion

Rationale and General Approach

The electrophoretic mobility shift assays (EMSA) provides a method for detecting DNA-protein complexes. The assay is based on the observation that the complexes between the protein and DNA migrate through a gel more slowly than free DNA fragments or double-stranded oligonucleotides. Unfortunately, there is no general procedure or optimal conditions that would be applicable to all protein-DNA complexes. Therefore for each protein-DNA system the optimum conditions have to be determined empirically. For the complex between SPL and undamaged DNA we found that the conditions described in Experimental Methods were optimal for our purposes.

The binding reactions were performed by incubating protein with either a long piece linearized plasmid of undamaged DNA or ^{32}P end-labeled non-SP containing oligonucleotide under anaerobic conditions. After incubation the reaction mix was applied to agarose or polyacrylamide gel, respectively, and electrophoresed in order separate protein-bound and unbound DNA. Two bands, one for free DNA and the other for bound DNA (in the presence of protein) were observed. Unlike the results for DNA photolyase (166), we were able to detect both free undamaged DNA and DNA-protein

complexes on the gel. Therefore our binding assays were performed to observe the binding between undamaged DNA and spore photoproduct lyase directly rather than indirectly.

Binding of *B.s.* SPL to Plasmid DNA

First, the preliminary binding assays between *Bacillus subtilis* SPL and plasmid pUC18 DNA were carried out. From these experiments we found that SPL could bind to plasmid DNA, which consisted of both circular and nicked DNA (Figure 3.2), with full binding being reached at ~10 x 10^{-8} M. We also observed that protein-DNA complexes were stuck in the gel wells at higher protein concentrations. This could be due to the fact that the protein has a positive charge at the pH of the binding assay (pH = 8.0) as the predicted pI for SPL is 8.48 and 8.58 for the *Bacillus subtilis* and *C. acetobutylicum* enzymes, respectively. The theoretical pI was calculated using the online calculator from Scripps Research Institute (170). The pI estimate assumes all residues have pKa values that are equivalent to the isolated residues which might not be valid for a folded protein (170). To make SPL-DNA complexes enter the gel it would be necessary to adjust the pH of the gel and running buffer to the one above the pI (pH 9-10). However, it is not clear how this high pH might affect the SPL-DNA complex or the protein itself, which can precipitate very easily. Therefore the pH = 8.0, which is closer to the physiological value of spores (which is 6.5 in a dormant stage and goes up to 7.5 during germination) but still below the calculated pI, was used. The dissociation constant for these binding assays could not be calculated due to the fact that at lower SPL concentrations the DNA-SPL complex appears as a very faint broad band and it was difficult to estimate where the free

DNA band ends and bound DNA band starts. Due to that issue the quantification of free DNA versus bound DNA was impossible and the dissociation constant K_d could not be calculated. From analogous assays with linearized pUC18 DNA, we were able to obtain full binding of DNA at SPL concentration of ~10 x 10^{-8} M (Figure 3.3). The dissociation constant, due to the same reasons could not be determined. These results indicate that the affinity to circular and linear DNA is either very similar or the same.

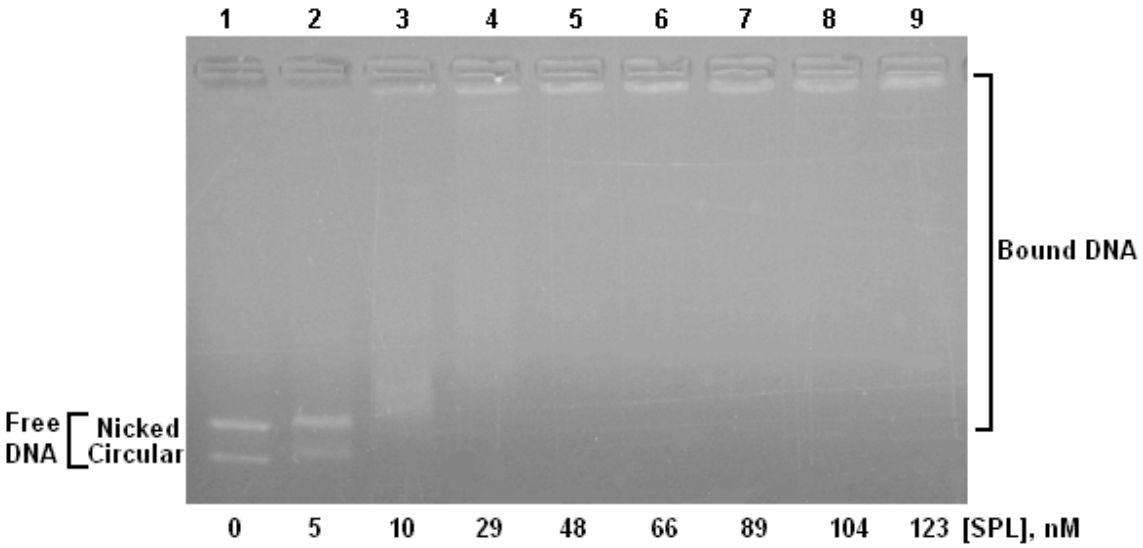

Figure 3.2. *B.s.* SPL binding to undamaged plasmid pUC18 DNA (nicked and circular). The EMSA reactions had a total volume of 20 μL containing 10 mM HEPES, 50 mM NaCl, 10% glycerol, 0.05% NP-40, 0.5 mM DTT, 3 nM pUC18 DNA, and increasing concentrations of *B.s.* SPL (pH 8). The assays were performed anaerobically and incubated for 30 min at room temperature. Agarose gels (1%) were run at 110 V (20 V/cm^2) for 1 hr.

In order to gain more accurate results and also to investigate how nonspecific binding might depend on the length of the DNA or other conditions, like pH, agarose gels

were replaced by polyacrylamide gels and 94-base pair double-stranded oligonucleotide was used instead of plasmid DNA.

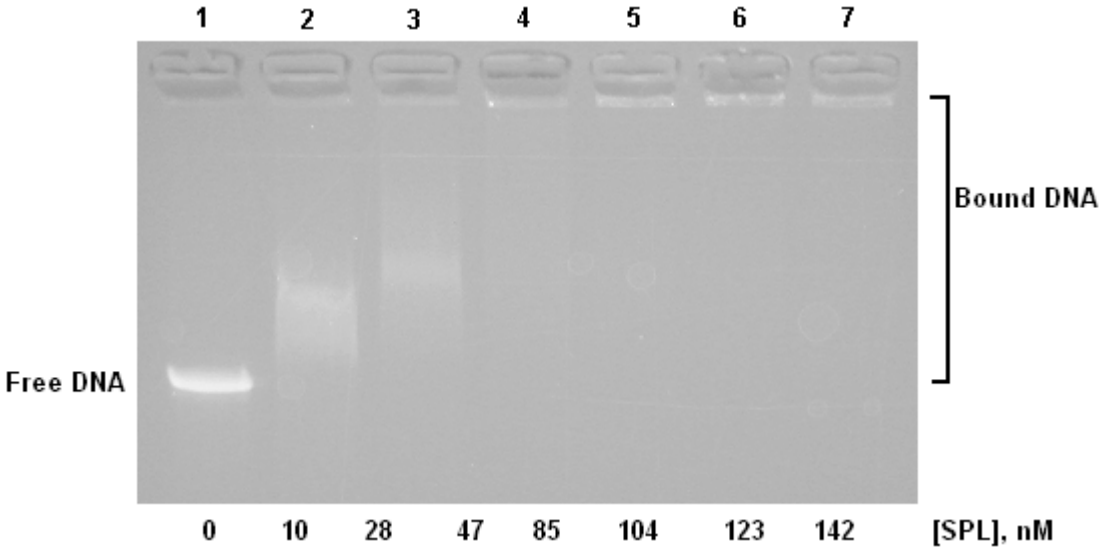

Figure 3.3. *B.s.* SPL binding to undamaged linearized pUC18 DNA. The EMSA reactions had a total volume of 20 μL containing 10 mM HEPES, 50 mM NaCl, 10% glycerol, 0.05% NP-40, 0.5 mM DTT, 3.09 nM linearized pUC18 DNA, and increasing concentrations of *B.s.* SPL (pH 8). The assays were performed anaerobically and incubated for 30 min at room temperature. Agarose gels (1%) were run at 110 V (20 V/cm^2) for 1 hr.

Binding of *B.s.* SPL to 94-bp Oligonucleotide

The sequence for TK-4 oligonucleotide was taken from *Bacillus subtilis.* The principle of these binding assays was the same as for pUC18 DNA. The only differences were that P^{32}-labeled oligonucleotide was used instead of plasmid DNA and polyacrylamide gels instead of agarose. All the other binding assay conditions were left unchanged. Due to this more sensitive method, clear bands for free and bound DNA were observed (Figure 3.4). These bands could later be quantified and dissociation constants in

each case could be calculated. Full binding of *B. subtilis* SPL to TK-4 oligonucleotide under anaerobic conditions could be reached at ~ 8 x 10^{-9} M, with K_d = 4.7 ± 0.44 x 10^{-9} M (Figure 3.4). These finding suggest that SPL binding to undamaged DNA is very tight and much stronger than that of DNA photolyase, which has K_d of ~10^{-5} M (165-167). This kind of strong binding suggests that there might more than one molecule of SPL binding to the oligonucleotide/DNA. The cooperativity factor (or Hill coefficient), n, calculated from Hill equation, suggests that there are 7.1 ± 3.2 molecules of SPL binding to one molecule of DNA in a cooperative fashion. The dissociation constants also suggest that there is very little difference in the binding of SPL to long DNA (pUC18) and short DNA (94-bp oligonucleotide) and therefore SPL binding affinity to undamaged DNA has only moderate dependence on the length of the DNA strand.

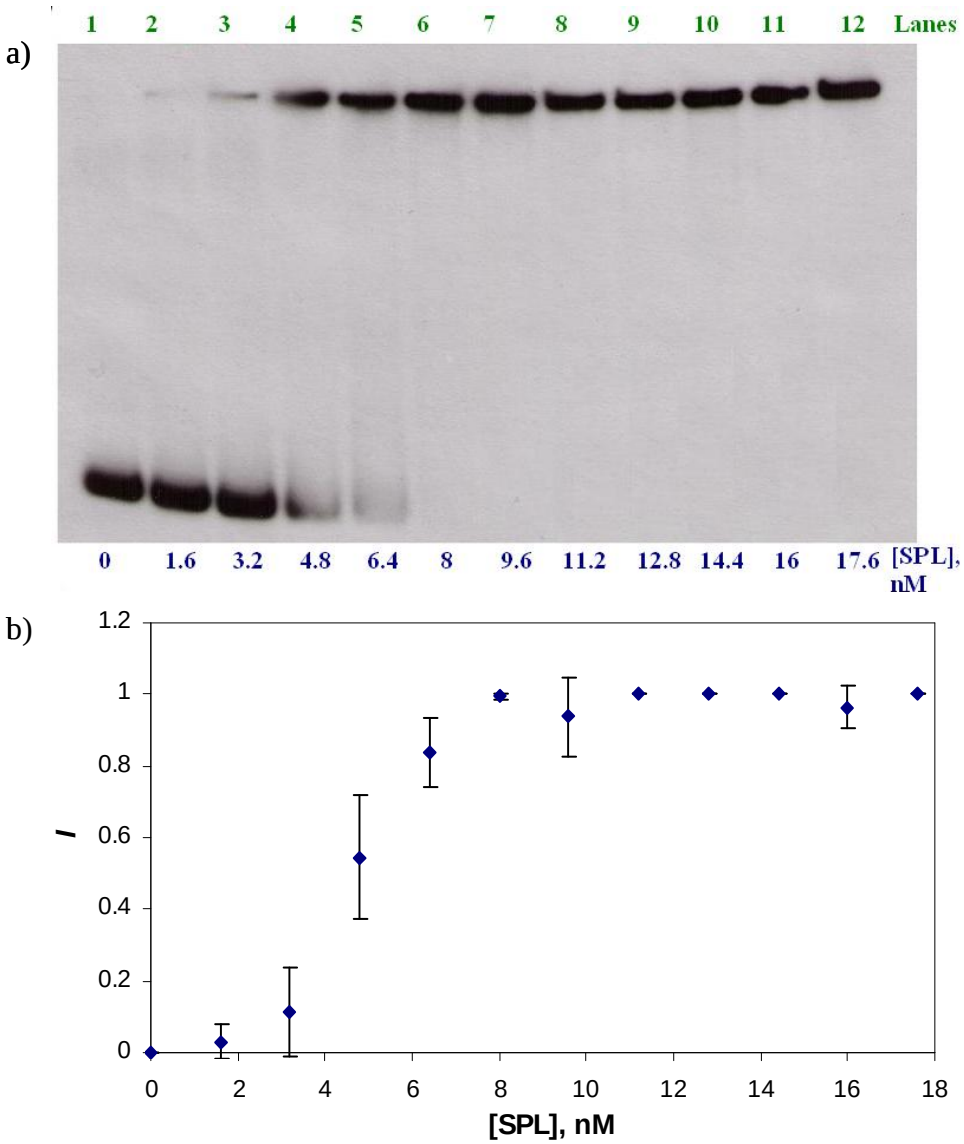

Figure 3.4. *B.s.* SPL binding to 94-bp oligonucleotide under anaerobic conditions. a) X-Ray film of SPL-oligonucleotide binding. The EMSA reactions were prepared in 20 μL containing 10 mM HEPES, 50 mM NaCl, 10% glycerol, 0.05% NP-40, 0.5 mM DTT (pH 8), 2.9 nM P^{32}-labeled 94-bp oligo, and different concentrations of *B.s.* SPL. The assays were prepared anaerobically and incubated for 1 hr at room temperature. The samples were loaded onto an 8% non-denaturing polyacrylamide gel and electrophoresed at 200 V (20 V/cm^2) for 2 hours. The electrophoresis products were visualized by autoradiography. b) The bands on the film were quantified using GS-900 gel scanner (Bio-Rad) and QuantityOne 4.0.2. software. All free oligo was bound at SPL concentration of ~ 8 nM with the dissociation constant $K_d = 4.7 \pm 0.44$ nM. The assays were done in triplicate. The error bars represent the standard deviation of band intensities.

Effect of Oxygen, SAM, SASP and Iron-Sulfur Cluster on SPL Binding to DNA

SPL binding properties were further investigated under different conditions, including in the presence of oxygen, AdoMet and small, acid-soluble proteins (SASPs). Since SPL repairs DNA damage under anaerobic conditions, it was unclear if this protein can still bind to DNA in the presence of oxygen. The repair of SP cannot proceed under aerobic conditions due to the degradation of SPL's [4Fe-4S] cluster. Interestingly, when binding assays were done in the presence of oxygen, SPL still bound undamaged DNA. Full binding could reached at ~ 8 x 10^{-9} M, with K_d = 5.3 ± 0.21 x 10^{-9} M (Figures 3.5). The binding curve also suggests that there is high degree of cooperativity, with roughly 11.6 ± 7.9 molecules of SPL binding to one DNA. Therefore, although SPL cannot repair the SP under aerobic conditions, it could still bind to DNA with high affinity.

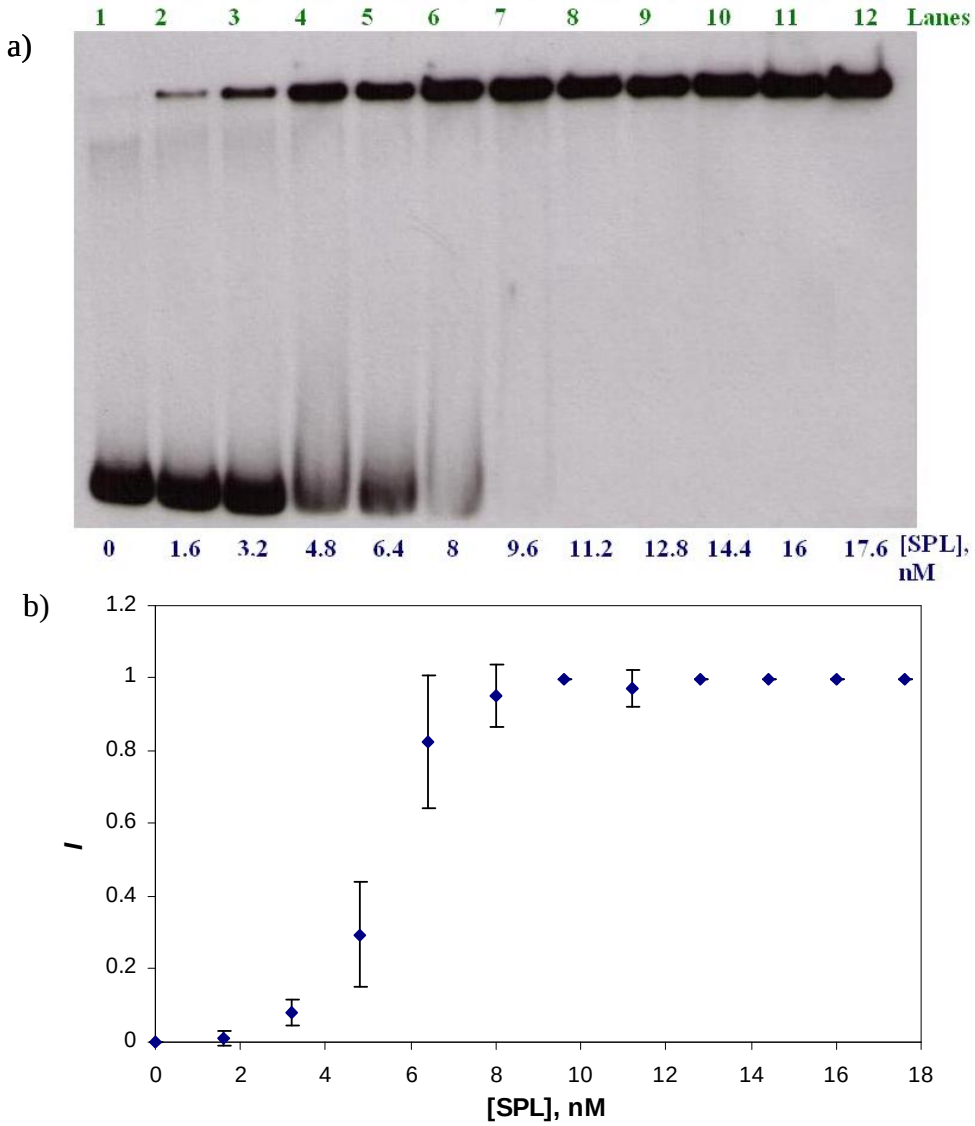

Figure 3.5. *B.s.* SPL binding to 94-bp oligonucleotide under aerobic conditions. a) X-Ray film of SPL-oligonucleotide The EMSA reactions were prepared in 20 μL containing 10 mM HEPES, 50 mM NaCl, 10% glycerol, 0.05% NP-40, 0.5 mM DTT (pH 8), 2.9 nM P^{32}-labeled ds- oligo, and different concentrations of *B.s.* SPL. The assays were done aerobically and incubated for 1 hr at room temperature. The samples were loaded onto an 8% non-denaturing polyacrylamide gel and electrophoresed at 200 V (20 V/cm^2) for 2 hours. The electrophoresis products were visualized by autoradiography. b) The bands on the film were quantified using GS-900 gel scanner (Bio-Rad) and QuantityOne 4.0.2. software. Full binding is reached at [SPL] ~ 8 nM; K_d = 5.3 ± 0.21 nM. The assays were done in triplicate. The error bars represent the standard deviation of band intensities.

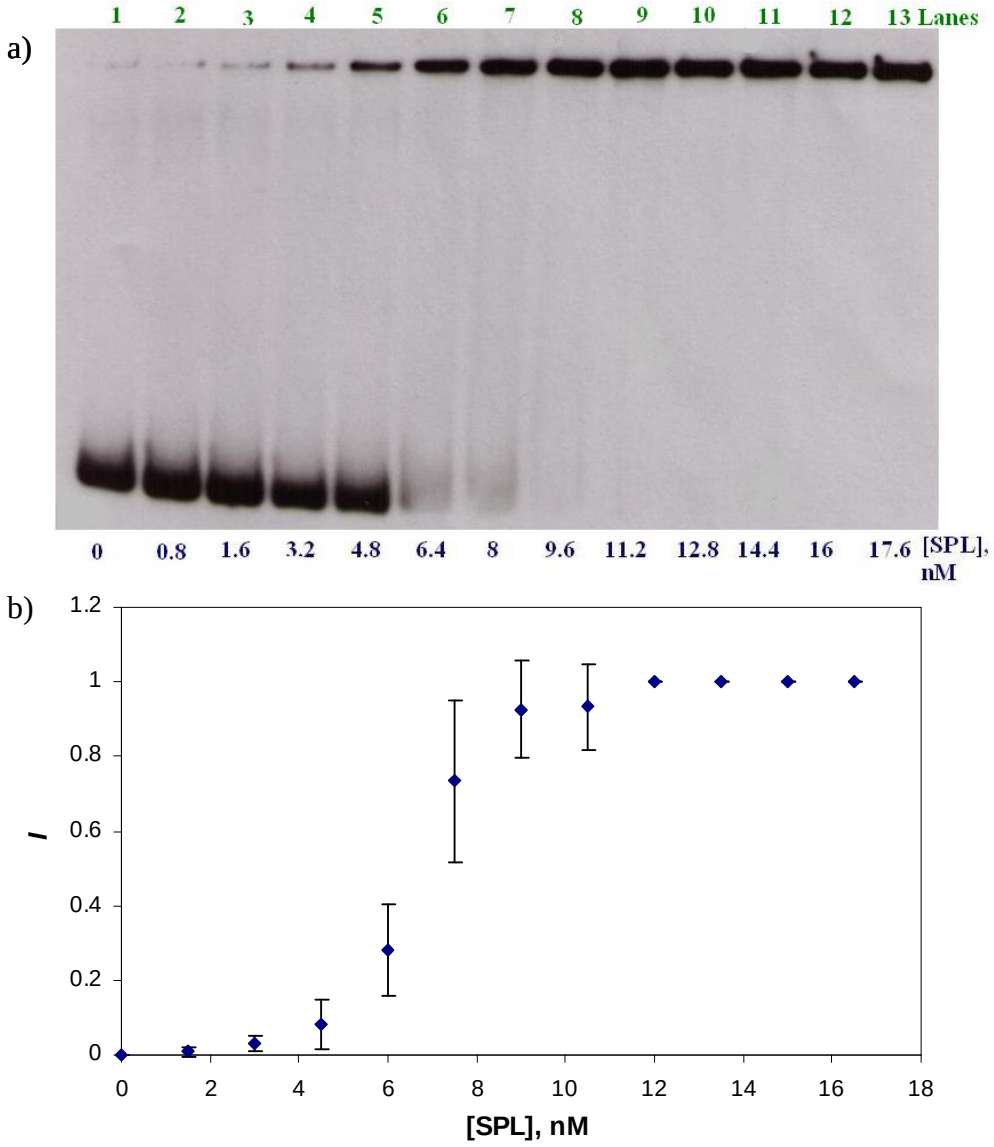

Figure 3.6. *Apo*-SPL binding to 94-bp oligonucleotide. a) X-Ray film of *apo*-SPL-oligonucleotide EMSA. The EMSA reactions were prepared in 20 μL containing 10 mM HEPES, 50 mM NaCl, 10% glycerol, 0.05% NP-40, 0.5 mM DTT (pH 8), 2.9 nM P^{32}-labeled ds-oligo, and different concentrations of *B.s. apo*-SPL. The assays were done anaerobically and incubated for 1 hr at room temperature. The samples were loaded onto an 8% non-denaturing polyacrylamide gel and electrophoresed at 200 V (20 V/cm^2) for 2 hours. The electrophoresis products were visualized by autoradiography. b) The bands on the film were quantified using GS-900 gel scanner (Bio-Rad) and QuantityOne 4.0.2. software. Full binding is reached at [SPL] ~ 12 nM; K_d = 6.7 ± 0.39 nM. The assays were done in triplicate. The error bars represent the standard deviation of band intensities.

The role of the iron-sulfur cluster in non-specific binding of SPL to DNA was further investigated. There are proteins, like MutY and Endonuclease III, which contain [4Fe-4S] clusters that have a structural role (171,172). The experiments with *apo*-SPL were carried out to determine if non-specific binding could be affected by the absence of SPL's [4Fe-4S] cluster. The full binding of *apo*-SPL was reached at ~12 x 10^{-9} M and K_d = 6.7 ± 0.39 x 10^{-9} M (Figures 3.6). Cooperative binding is also observed, with n = 11.6 ± 6.7. These results indicated that the absence of iron-sulfur cluster had no affect on binding to undamaged DNA. However, it is still not clear if the binding to specific DNA would be equally unaffected, since more contacts between the protein and DNA might need to be established.

Further experiments involved the SPL cofactor *S*-adenosylmethionine (AdoMet or SAM). *S*-adenosylmethionine is required for SPL to repair the spore photoproduct and it is known that radical SAM superfamily enzymes bind SAM. Therefore it was of interest to investigate whether SAM plays a role in DNA binding. However, we found that the presence of 5 mM SAM had very little effect on SPL binding to undamaged oligonucleotide. Full binding in the presence of AdoMet could be reached at ~12 x 10^{-9} M with K_d = 5.5 ± 1.21 x 10^{-9} M (Figures 3.7). As in previous cases, non-specific SPL binding is cooperative and there are 5.4 ± 1.4 molecules of protein per DNA. Table 3.2 summarizes the dissociation constants of SPL to 94-base pair double-stranded oligonucleotide at different experimental conditions.

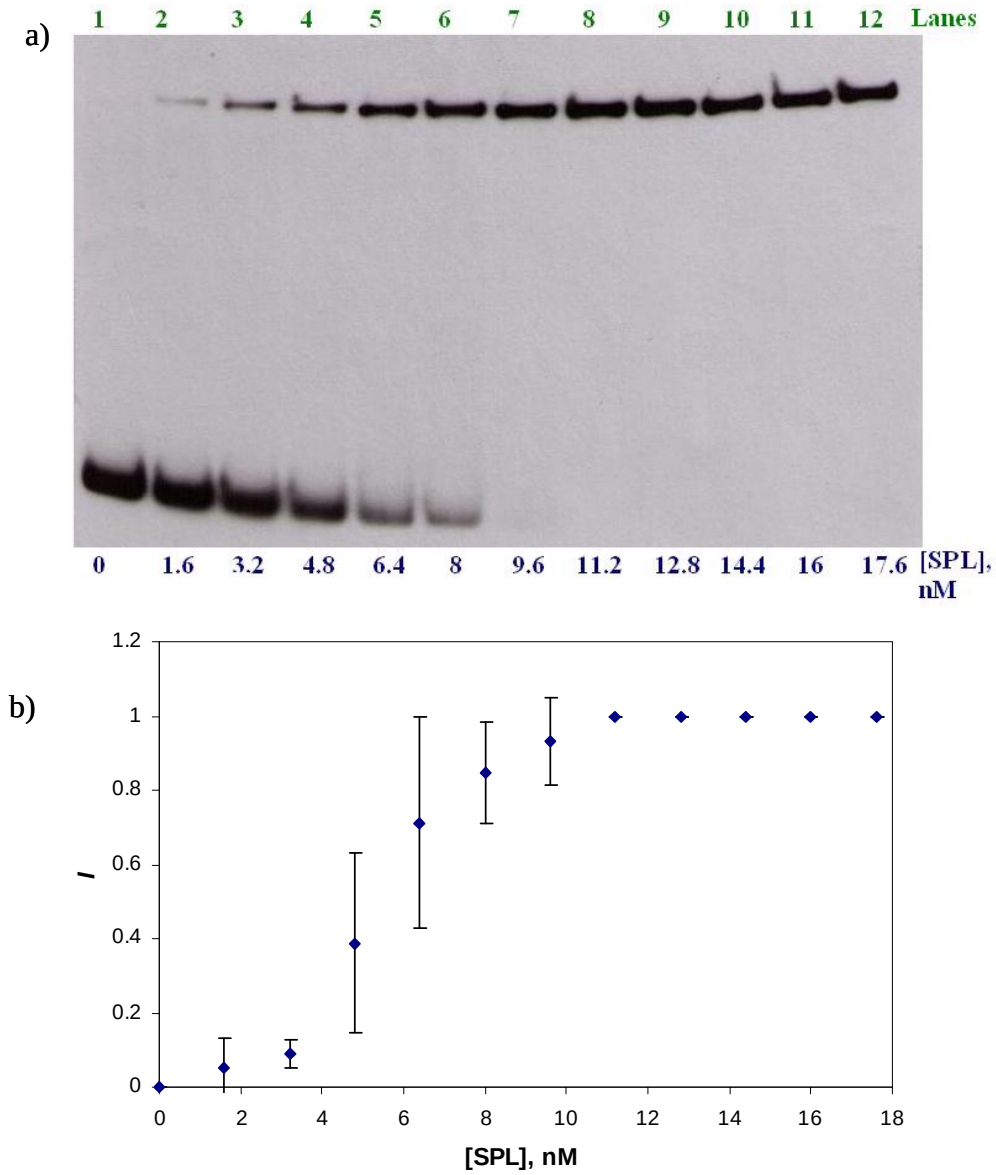

Figure 3.7. Binding of *B.s.* SPL to 94-bp oligonucleotide in the presence of SAM. a) X-Ray film of SPL-oligonucleotide EMSA. The reactions were prepared in 20 μL containing 10 mM HEPES, 50 mM NaCl, 10% glycerol, 0.05% NP-40, 0.5 mM DTT (pH 8), 2.9 nM P^{32}-labeled ds-oligo, 1 mM SAM, and different concentrations of *B.s.* SPL. The assays were done anaerobically and incubated for 1 hr at room temperature. The samples were loaded onto an 8% non-denaturing polyacrylamide gel and electrophoresed at 200 V (20 V/cm^2) for 2 hours. The electrophoresis products were visualized by autoradiography. b) The bands on the film were quantified using GS-900 gel scanner (Bio-Rad) and QuantityOne 4.0.2. software. Full binding is reached at [SPL] = 12 nM; K_d = 5.5 ± 1.21 nM. The assays were done in triplicate. The error bars represent the standard deviation of band intensities.

Table 3.2. Spore photoproduct lyase binding to undamaged DNA (94-bp oligonucleotide) at various conditions.

Bacteria	**Conditions***	**Dissociation constant K_d, nM**
Bacillus subtilis	Anaerobic:	
	pH = 8.0	4.7 ± 0.4
	pH = 7.5	17.2 ± 1.5
	pH = 7.0	60.3 ± 3.8
	pH = 6.5	27.0 ± 6.5
	Aerobic	5.3 ± 0.2
	apo-SPL	6.7 ± 0.4
	With *S*-adenosylmethionine	5.5 ± 1.2
	With SspC	6.0 ± 0.7
Clostridium acetobutylicum	Anaerobic:	
	pH = 8.0	169.0 ± 4.9
	pH = 7.0	44.6 ± 2.3

* The experiments were carried out at pH = 8.0 unless stated otherwise

Small, acid soluble proteins play an important role in spore resistance and they are in high abundance inside of the spore (17,28,173). It is known that these proteins bind and protect DNA (29,30), but is not clear if they can affect SPL binding to the DNA. In order to investigate the influence of small-acid soluble proteins to SPL binding, SspC was added to the binding reaction mix with the ratio 5:1 (SspC:DNA). However, the presence of the small-acid soluble protein SspC has no influence on SPL binding. Full binding of SPL can be reached at ~ 8 x 10^{-9} M and K_d is 6.0 ± 0.73 x 10^{-9} M (Figures 3.8), which is similar to that without SspC (Table 3.2).

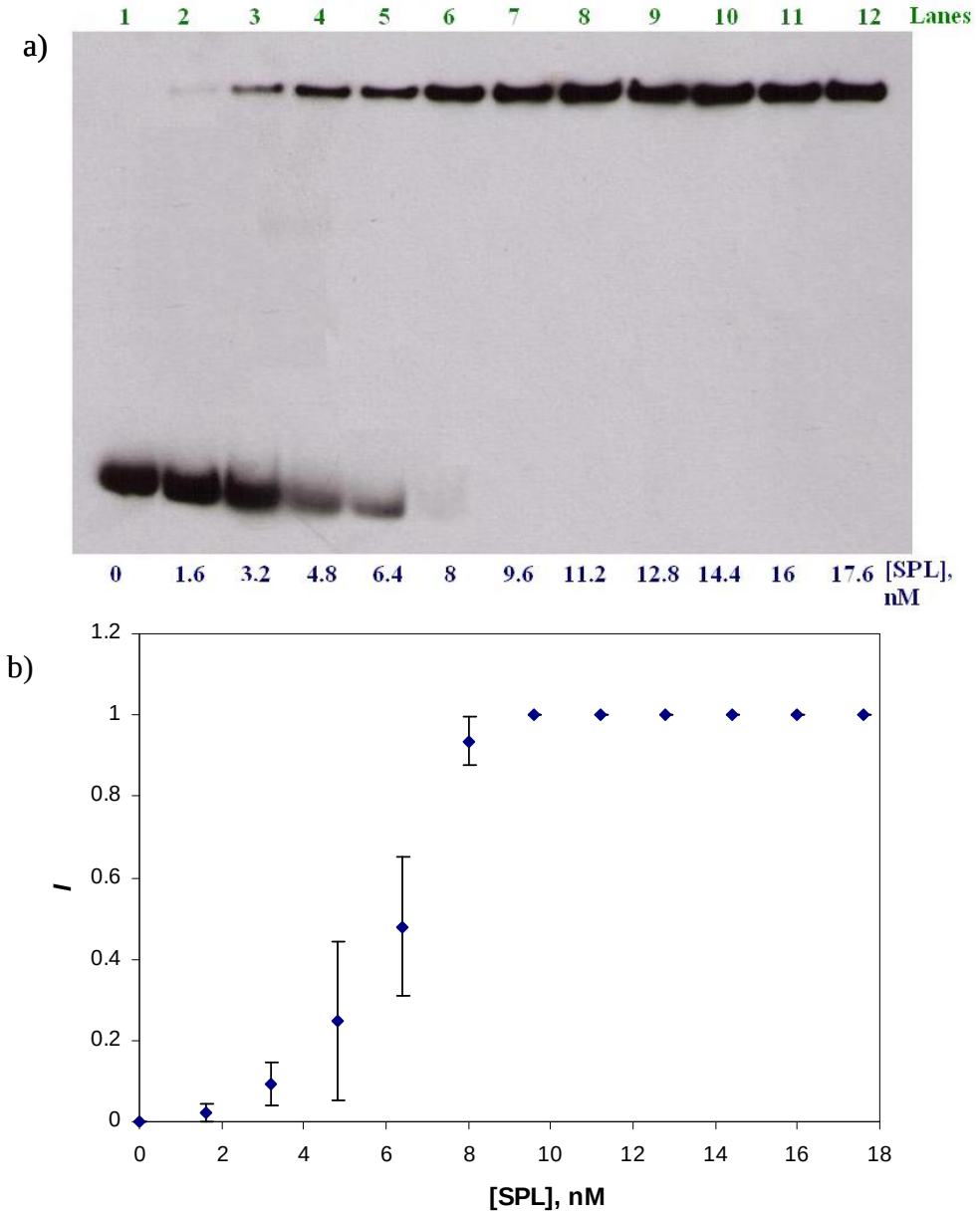

Figure 3.8. Binding of *B.s.* SPL to 94-bp oligonucleotide in the presence of SspC. a) X-Ray film of SPL-oligonucleotide EMSA. The reactions were prepared in 20 μL containing 10 mM HEPES, 50 mM NaCl, 10% glycerol, 0.05% NP-40, 0.5 mM DTT (pH 8), 2.9 nM P^{32}-labeled ds-oligo, SspC (SspC:DNA ratio 5:1) and different concentrations of *B.s.* SPL. The assays were done anaerobically and incubated for 1 hr at room temperature. The samples were loaded onto an 8% non-denaturing polyacrylamide gel and electrophoresed at 200 V (20 V/cm^2) for 2 hours. The electrophoresis products were visualized by autoradiography. b) The bands on the film were quantified using GS-900 gel scanner (Bio-Rad) and QuantityOne 4.0.2. software. Full binding is reached at [SPL] = 8 nM; K_d = 6.0 ± 0.73 nM. The assays were done in triplicate. The error bars represent the standard deviation of band intensities.

Also, the SspC has no effect on cooperativity – the Hill coefficient is n = 8.2 ± 5.8. SspC might not have much influence on SPL binding to DNA due of its' own affinity to DNA (15 ÷ 100 x 10^{-3} M (26)), which is low in comparison to that of SPL. Therefore small, acid-soluble proteins appear not to compete with the non-specific binding of SPL to DNA and most likely do not interfere with recognition and repair spore photoproduct by SPL.

While bacterial spores have pH ~ 6.5, once they start germinating, the pH changes to 7.0 – 7.5. During that germination process SPL must find and repair UV-damaged DNA. Therefore the SPL DNA binding properties at different pH levels were investigated. For this set of the experiments the pH of all the buffers was adjusted depending on the assay conditions, including the pH of oligonucleotide and the protein. The rest of the conditions were the same as for the anaerobic binding assays. The assays were carried out at pH 8.0 (K_d = 4.7 ± 0.44 x 10^{-9} M), pH 7.5 (K_d = 17.2 ± 1.45 x 10^{-9} M), pH 7.0 (K_d = 60.3 ± 3.82 x 10^{-9} M) and pH 6.5 (K_d = 27 ± 6.53 x 10^{-9} M) (Figure 3.9 and Table 3.2).

<u>*B.s.* SPL Binding at Different pH</u>

From these experiments we can draw the conclusion that the strongest binding of SPL to non-specific DNA is at pH 8.0 and the weakest is at pH 7.0 (Figure 3.9), with the binding at pH 8.0 being ~13 times stronger than at pH 7.0. For all these assays SPL showed significant cooperativity. The Hill coefficients for these binding assays were n = 7.1 ± 3.2 at pH 8.0, n = 11.1 ± 3.6 at pH 7.5, n = 6.4 ± 1.4 at pH 7.0 and n = 9.1 ± 2.0 at pH 6.5. The summary of all the dissociation constants is shown in Table 3.2. Weaker

non-specific binding at pH 7.0 could contribute to more selective binding due to lower energy that would be required when protein has to switch from non-specific binding to specific.

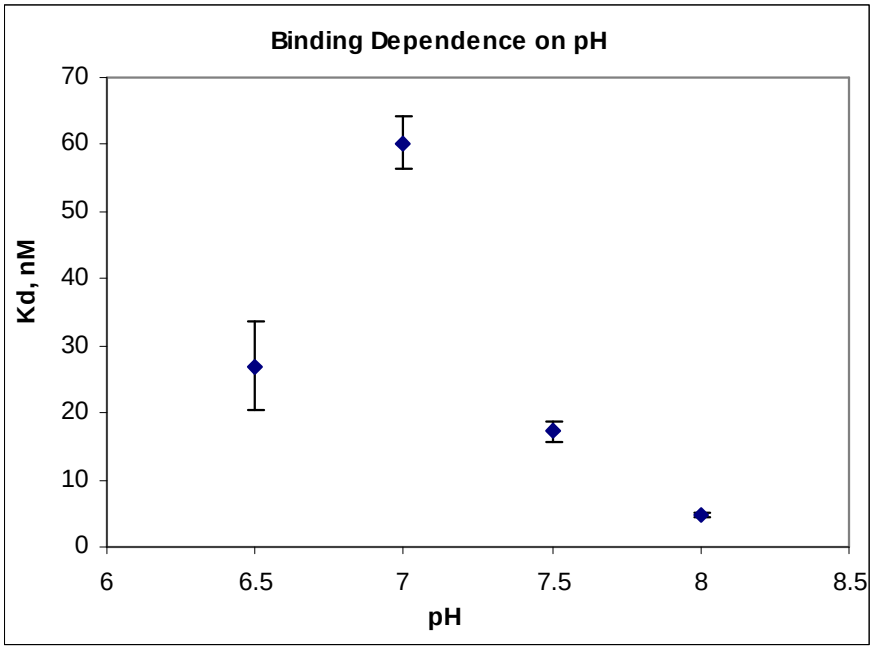

Figure 3.9. SPL nonspecific dissociation constant (K_d) dependence on pH. The error bars represent the standard deviation of dissociation constant.

SPL binding to single-stranded ^{32}P-labeled oligonucleotide was also investigated. The results demonstrate that *B.s.* SPL can bind single-stranded DNA. Full binding is achieved at ~16 x 10^{-9} M, although it is impossible to determine the dissociation constant, because it is not clear where free DNA bands end and where complexed DNA/SPL begins. There is some shifting of free DNA band starting at concentrations ~3.2 nM, which becomes wider and more spread out at higher concentrations. Repeating this experiment under the identical conditions yielded the same results. Although it indicates

binding, it is different from type of binding we saw with double-stranded oligonucleotide (Figure 3.10). Therefore the unusual binding is caused not by experimental conditions, but due to the fact that single-stranded DNA is used, which would have different structure. However, based on SPL concentration at which full binding is reached, we suggest that the affinity towards single-stranded DNA is similar to that for double-stranded DNA.

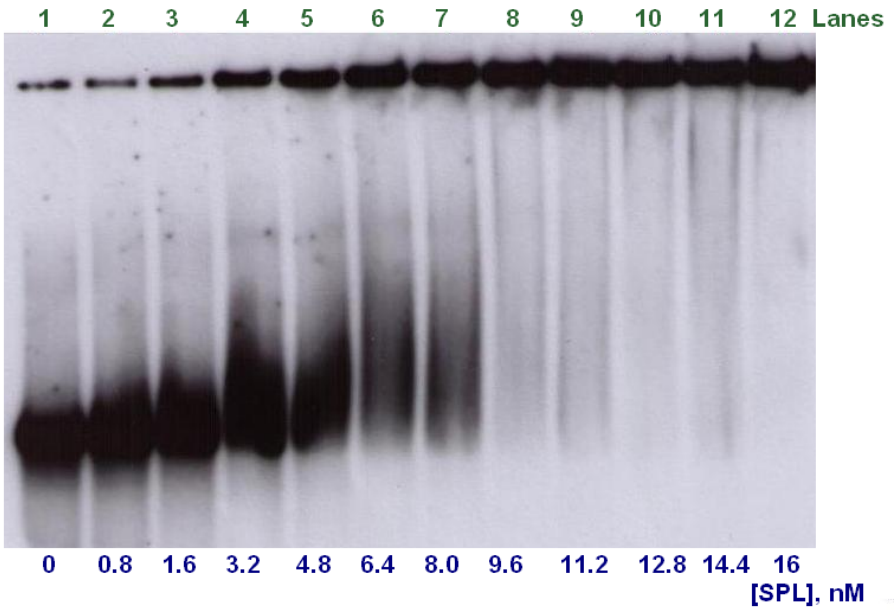

Figure 3.10. Binding of *B.s.* SPL to 94-bp single-stranded oligonucleotide. Shown an X-ray film of SPL-oligonucleotide EMSA. The reactions were prepared in 20 μL containing 10 mM HEPES, 50 mM NaCl, 10% glycerol, 0.05% NP-40, 0.5 mM DTT (pH 8), 2.9 nM P^{32}-labeled single-stranded oligo and different concentrations of *B.s.* SPL. The assays were carried out anaerobically and incubated for 1 hr at room temperature. The samples were loaded on an 8% non-denaturing polyacrylamide gel and electrophoresed at 200 V (20 V/cm^2) for 2 hours. The electrophoresis products were visualized by autoradiography. Full binding is reached at [SPL] = 16 nM. The assays were performed in triplicate.

Binding of *C.a.* SPL to DNA

DNA photolyase from different bacteria, *E. coli* and *M. thermoautotrophicum*, were shown to have very different binding, which could vary as much as 100 times (129). To investigate how binding might differ for SPL from *Bacillus* and *Clostridium*, the EMSA of pUC18 DNA were carried out with SPL from *Clostridium acetobutylicum*. Since *B.s.* SPL showed no difference in binding to circular and linear DNA, for these assays only linear pUC18 DNA was used. We found that *Clostridium acetobutylicum* SPL fully binds to DNA at concentration of ~10 x 10^{-9} M (Figure 3.11) and the binding pattern/shifting is similar to the one observed for *B.s.* SPL (Figure 3.3).

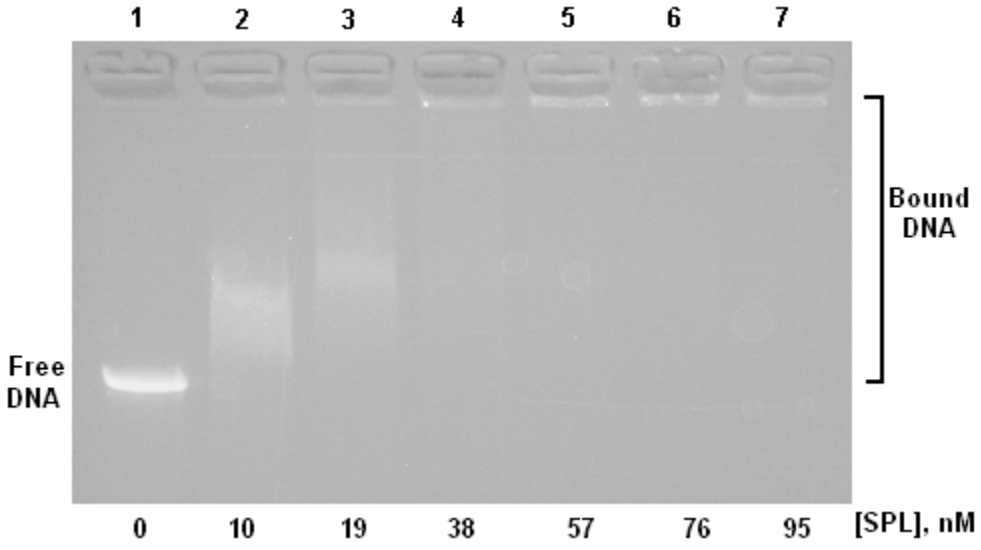

Figure 3.11. *C.a.* SPL binding to undamaged linearized pUC18 DNA. The EMSA reactions had a total volume of 20 μL containing 10 mM HEPES, 50 mM NaCl, 10% glycerol, 0.05% NP-40, 0.5 mM DTT, 3.09 nM linearized pUC18 DNA, and increasing concentrations of *C.a.* SPL (pH 8). The assays were performed anaerobically and incubated for 30 min at room temperature. An agarose (1 %) gels were run at 110 V (20 V/cm^2) for 1 hr.

The next step was to further investigate *C.a.* SPL binding to ^{32}P-labeled double-stranded oligonucleotide in order to determine the dissociation constant. These assays were done as for *B.s.* SPL with 94-base pair oligonucleotide at two different pH conditions, pH 8.0 and 7.0. From these assays we found that *C.a.* SPL binding to non-specific DNA is actually weaker than that of *B.s.* SPL. *C.a.* SPL binds to DNA at pH 7.0 with $K_d = 44.6 \pm 2.34 \times 10^{-9}$ M, better than at pH 8.0, which has $K_d = 169 \pm 4.91 \times 10^{-9}$ M. Interestingly, the binding at different pH values was in reverse order for *C.a.* SPL compared to *B.s.* SPL. This might be due to the fact that even though the calculated pI for both proteins is similar, the pI of the predicted DNA binding region of each protein is different. The pI of the helix-turn-helix motif in *B.s.* SPL is 8.69, while that of *C.a.* SPL is 6.25. Therefore DNA binding regions for these two proteins should be charged differently at both pH 7.0 and 8.0. If the predicted helix-turn-helix motif is indeed involved in DNA binding, these different isoelectric point values could explain the significant differences in protein affinities. Interestingly, *C.a.* SPL had higher affinity to long DNA (pUC18) than to a shorter oligonucleotide. The only explanation could be that longer DNA might resemble a more natural and structured substrate than shorter DNA. This hypothesis could be confirmed by using different length oligonucleotides/DNA.

Conclusions

The data from EMSA showed that SPL could bind to undamaged DNA. This non-specific binding could precede binding to specific DNA and/or is the way for SPL to 'scan' DNA looking for damage (the spore photoproduct). SPL could bind to circular,

nicked or linear DNA, as well as single-stranded or double-stranded oligonucleotides that contained no spore photoproduct. SPL binding to long DNA (linear pUC18 DNA, 2686 bp) suggests that full binding could be reached at ~10 x 10^{-9} M. The binding results for 94-oligonucleotide suggested that there was little difference in binding between short oligonucleotide and long DNA for *Bacillus subtilis* SPL. Similar results were observed for DNA photolyase, which bound different conformations of UV-irradiated DNA, as well as double-stranded DNA and single-stranded DNA with similar affinities (166).

When non-specific binding assays were carried out under anaerobic or aerobic conditions, the differences in K_d values were insignificant. The addition of *S*-adenosylmethionine had no effect on non-specific binding. However, there was slightly less binding when *apo*-protein was used. Therefore the iron-sulfur cluster might have little or no effect on SPL binding to undamaged DNA. The presence of small, acid-soluble protein had no effect on SPL binding as well, most likely due to differences in binding affinities between SPL and SspC. The pH of the reaction mixture had a more pronounced effect on non-specific binding; the highest affinity of SPL to undamaged DNA is observed at pH 8.0 and the lowest at pH 7.0. This suggests that SPL affinity could be affected during spore germination, when the pH of the spore core changes from 6.5 to ~7.5. Lower SPL affinity for undamaged DNA at pH 7.0 could also indicate that transition from non-specific binding to specific binding at this pH could be more favored energetically.

The binding of *Clostridium acetobutylicum* SPL to undamaged 94-bp oligonucleotide revealed that nonspecific binding is weaker than that for *B.s.* SPL but still

very tight. It also showed that binding is stronger at pH 7.0 rather than pH 8.0, the opposite of *Bacillus subtilis* SPL. This potentially could be due to different pI value of DNA-binding region in *C.a.* SPL. However, more experiments have to be carried out to confirm this hypothesis.

Future work may include side-directed mutagenesis to create SPL mutants in order to determine which amino acids are involved in binding. Some of these mutations could include amino acids from the predicted helix-turn-helix motif, which would clarify the role of this motif in SPL-DNA binding. Also, spore photoproduct lyase without a H-T-H region could be designed and its binding properties could be investigated. Another set of experiments may involve SPL binding to DNA with GC- or AT-rich regions in order to determine if SPL has higher affinity to certain DNA bases.

CHAPTER 4

SPORE PHOTOPRODUCT LYASE BINDING TO DAMAGED DNA

Introduction

Many proteins bind to DNA both specifically and non-specifically (164). DNA photolyase, as discussed in Chapter III, has affinity towards both damaged and undamaged DNA (167,174). This enzyme has a relatively high affinity toward the DNA containing *cis,syn* cyclobutane thymine dimers with a dissociation constant K_d ~10^{-9} M. DNA photolyase from *Methanobacterium thermoautotrophicum* has different affinity to *E. coli* photolyase. This enzyme has a dissociation constant K_d = 1.4 x 10^{-11} M and 1.1 molecules of enzyme binds per thymine dimer (129). DNA footprinting assays showed that both enzymes from *E. coli* and *M. thermoautotrophicum* protected the same 11-16 base pair region around the thymine dimer (174,175). The authors, based on these results and those of Sancar (167), suggested that photolyase from these two sources have very different dissociation constants, but no conclusion was drawn as to the probable cause of their different affinities (175). From this data, however it is possible to infer how DNA photolyase interacts with DNA. DNA photolyase binds to both damaged and undamaged DNA with the specific binding being several orders of magnitude tighter than non-specific. Also, the enzyme makes many contacts to the DNA backbone in order to flip out the damaged site for repair (121).

The (6-4) photoproduct photolyase is another DNA repair enzyme that converts (6-4) photoproduct (see Scheme 1.1) to two thymines (176). These enzymes also share

sequence homology with cyclobutane pyrimidine dimer (CPD) photolyases and have a similar repair mechanism (141). (6-4) Photolyases bind to DNA relatively tightly and with high specificity (141). The dissociation constants for this protein with damaged DNA were determined using EMSA to vary from ~10^{-9} to 10^{-10} M (177). DNase I footprinting assays also demonstrated that (6-4) photolyases can protect 11 to 20 bases around the damaged site (141).

In contrast to CPD and (6-4) photolyases, there is very little knowledge on how SPL recognizes and binds SP-containing DNA. In previous studies, Nicholson and co-workers showed that SPL bound specifically to and repaired spore photoproduct, not cyclobutane dimer (142). However, these studies did not provide information about the affinity of SPL towards UV-damaged DNA. Therefore after determining the affinity of SPL for undamaged DNA (Chapter 3) we further investigated SPL binding to specific/damaged DNA as described in this Chapter.

The electrophoretic mobility shift assays (EMSA) that were employed to investigate SPL binding to undamaged DNA could, in principle, be utilized to investigate SPL binding to UV-damaged/SP-containing DNA as well. However, previous attempts to do EMSA binding assays between *B.s.* SPL and UV-irradiated DNA were unsuccessful (142). DNase I footprinting assays showed that SPL bound to the SP-containing DNA and protected 9-bp region surrounding SP from DNase I digestion (142). Nicholson and co-workers suggested that SPL binds to SP containing oligonucleotide and bends the DNA, presumably to flip out the damaged site (142). Because SPL binds to SP but not the *cis,syn* cyclobutane dimer, it presumably recognizes an SP-specific helical distortion

in DNA which differs in its geometry from the distortion caused by a *cis,syn* cyclobutane pyrimidine dimer (142).

Our attempts to do binding assays by EMSA showed that while *B.s.* SPL could bind UV-irradiated DNA, the dissociation constant could not be determined. In order to determine the affinity of SPL to spore photoproduct dinucleoside and dinucleotide, time-resolved fluorescence decay assays were developed. It has previously been shown that time-resolved fluorescence assays could be utilized to investigate protein-DNA interactions (178). Jones and co-workers utilized time-resolved fluorescence to investigate base flipping from DNA by DNA methyltransferase HhaI (178). For that purpose, DNA was labeled with the fluorescent analog of adenine, 2-aminopurine (2-AP), and then fluorescence lifetime change of 2-AP due to interaction of the DNA with protein was measured (178). A similar approach was applied to investigate base flipping by DNA photolyase, except steady-state fluorescence was utilized, where quenching of fluorescence emissions was observed due to the photolyase flipping out the cyclobutane pyrimidine dimer (179). For DNA photolyase binding experiments fluorescence assays can also be utilized because of the presence of its $FADH_2$ cofactor (180,181). When the substrate, cyclobutane pyrimidine dimer, bound to DNA photolyase, the change in $FADH_2$ fluorescence due to its proximity to the substrate binding site was observed (180,181). Since SPL does not contain $FADH_2$ and its substrate does not contain a fluoropore, for our DNA binding assays we applied the novel approach of measuring protein intrinsic fluorescence in a time-domain format. This method measures the change in fluorescence lifetime waveform rather than the change in fluorescence lifetime or

amplitude, which was previously shown to be useful for studying protein aggregation over time in the presence of dendrimers (182). The results from our time-resolved fluorescence assays suggest this method can be successfully applied to SPL-DNA binding studies. It also suggests that SPL binds to the SP dinucleotide more strongly than to the dinucleoside. This data is in good agreement with the SPL repair assays, which show that the SPL repair rate for SP dinucleotide is significantly higher than for the dinucleoside (44,146). These results are also in good agreement with those of DNA photolyase, which was found to have different affinities to the cyclobutane pyrimidine photodimer dinucleoside (CPD) and dinucleotide (CPDTpT) (180,183). The fluorescence lifetime decay assays also show that SPL binds more tightly to spore photoproduct, both dinucleoside and dinucleotide, than its repair products, thymidine and thymidylyl (3'-5') thymidine (TpT), respectively. While two distinct diastereomers of SP (5*R*- and 5*S*-SP) could in principle be formed upon UV irradiation in bacterial spores, only the 5*R*-isomer is possible for SP formed from adjacent thymines in double helical DNA, due to the constraints imposed by the DNA structure (48,144). Recent results showed that SPL repairs 5*R*-, but not 5*S*-spore photoproduct (44,146,150). Interestingly, we found that SPL bound not only 5*R*-isomer of SP, but also 5*S*-isomer. SPL binding affinities from two different bacteria, *B. subtilis* and *C. acetobutylicum*, towards spore photoproduct were also investigated.

Experimental Methods

Materials

All chemicals used in this work were purchased commercially unless otherwise indicated and were of the highest purity available. The synthetic oligonucleotides were purchased from Integrated DNA Technologies. [γ-^{32}P] ATP was purchased from MP Biomedicals. T4 polynucleotide kinase, required for the radioactive labeling, was commercially obtained from Invitrogen. Thymidine (T) and thymidine dinucleotide (TpT) were purchased from Sigma-Aldrich. Spore photoproduct dinucleoside and dinucleotide, both *5R*- and *5S*- isomers, were synthesized and characterized by Dr. T. Chandra in our lab (44,146).

Purification and Dialysis of SPL

Spore photoproduct lyase from *Bacillus subtilis* and *Clostridium acetobutylicum* was purified as described in Chapter 2. For binding assays this protein was later diluted with Buffer A (50 mM HEPES, 50 mM NaCl, 5% glycerol, pH 8.0) in order to maintain constant salt concentration in the binding reaction mix.

5'-End Labeling of 94-bp Oligonucleotide

Two complementary oligonucleotides were synthesized (Integrated DNA Technologies) based on the *Bacillus subtilis* sequence (from 322456 to 322550). Oligonucleotides had 94 nucleobases (the adjacent thymidines are shown in bold):

TK4-72a (MW = 28,902 Da) 5'- CGGGATCAACCAGAGCATCATGC**TT**GC G**TT**ATCAATGG**TT**G**TT**ATCGCCGCAATGGTCGGTGCACCGGGAC**TT**GG**TT**CT GAAGTATACAGTGC C –3' and

TK4-72b (MW = 29,057 Da) 5'- GGCACTGTATAC**TT**CAGAACCAAGTCC CGGTGCACCGACCA**TT**GCGGCGATAACAACCA**TT**GATAACGCAAGCATGAT GCTCTGG**TT**GATCCC G -3'.

These oligonucleotides were labeled as described in Chapter 3 and were UV-irradiated as described below.

Generation of Spore Photoproduct
on 94-bp Oligonucleotide by UV-irradiation

The ^{32}P-labeled 94-bp oligonucleotide was prepared for UV irradiation under three different conditions, involving 1) lyophilizing the oligonucleotide in water, 2) lyophilizing the solution of oligonucleotide and small, acid soluble protein (SspC, ratio [DNA]/[SspC] = 1:5), and 3) lyophilizing the oligonucleotide in a Buffer A (50 mM Hepes, 0.5 M NaCl, 5% glycerol, pH 8.0), which also contained dipicolinic acid sodium salt (10 mM, pH 8.0). SspC was purified as described previously (42) and sodium dipicolinate salt was prepared by titrating NaOH to dipicolinic acid until the pH = 8.0 (184-186). After the lyophilization the films of dried oligonucleotide were irradiated under UV light (254 nm) by using Stratalinker UV Crosslinker (Model 2400, 15 W, Strategene), which has the intensity of 4 mW/cm^2, for 30 minutes (total dosage of 7.2 J/cm^2). After the irradiation the oligonucleotide was re-suspended in de-oxygenated water under anaerobic conditions and used for electrophoretic mobility shift assays.

Electrophoretic Mobility Shift Assay of the UV-Irradiated Double-Stranded 94-bp Oligonucleotide

The EMSA reactions were prepared in a total volume of 20 μL containing 10 mM HEPES, 5 mM NaCl, 10% glycerol, 0.05% NP-40, 0.5 mM DTT, 2.9 nM labeled, UV-irradiated, double-stranded oligonucleotide, and different concentrations of *B.s.* spore photoproduct lyase (pH 8.0). The assay reactions were prepared anaerobically in an MBraun glove box and incubated for 30 minutes at room temperature. The samples were loaded on an 8% non-denaturing polyacrylamide gel and electrophoresed at 200 V (20 V/cm^2) for 2 hours. After that, the gel was placed between two gel drying films and dried overnight. The electrophoresis products were visualized by autoradiography (X-Omat AR-5 film (Kodak)). The bands on the film were quantified using GS-900 gel scanner (Bio-Rad) and QuantityOne 4.0.2. software. The data were analyzed with ORIGIN 8.0 software.

SPL Binding Assays Using Time-Resolved Fluorescence Decay

The assays were performed as follows. The binding reactions were prepared in total volume of 1 mL containing 50 mM HEPES, 500 mM NaCl, 5% glycerol, 5 mM DTT, and 5 μM of *B.s.* or *C.a.* spore photoproduct lyase. The assay reactions were prepared anaerobically (O_2 < 1 ppm) in an MBraun glove box and transferred to anaerobic Spectrosil quartz 3.5 mL cuvettes (Starna Cells, Inc., Atascadero, CA). The substrate was added with a gas-tight syringe under N_2 and the fluorescence lifetime decay was measured at different substrate concentrations. For these assays, different substrates were used – thymidine, TpT, *5R*-SP, *5S*-SP, *5R*-SPTpT, *5S*-SPTpT and a 94-base pair

double-stranded oligonucleotide. Fluorescence data were collected at Fluorescence Innovations, Inc. The fluorescence measurements were taken on a Varian Cary Eclipse spectrometer that was modified for fluorescence lifetime experiments by replacing the standard photomultiplier tube (PMT) to R7400 PMT (Hamamatsu), and introducing a transient digitizer. It was also equipped with a cuvette holder (Quantum Northwest, WA) for temperature control and magnetic stirring capabilities. The tunable UV light around 295 nm was generated by pumping a frequency-doubling compact dye (Rhodamine 6G) laser with a pulsed Nd:YAG laser (Teem Photonics, France). Other parameters include 200 μJ energy per pulse, 1000 Hz pulse repetition frequency, and 0.5 ns pulse duration. Time-domain fluorescence data were recorded with a proprietary transient digitizer that generates a complete fluorescence decay curve on every laser shot. The digitizer employs an analog memory to sample at 1 gigasample/sec (i.e., 1 ns spacing in the time domain). The effective sampling rate is increased to a time point every 200 ps via 5X interleaving. Each fluorescence decay waveform is averaged over 1000 laser shots, corresponding to 1 second acquisition time per waveform. Fluorescence data were recorded every 2 nm from 300 nm to 400 nm; the emission bandpass was set at 5 nm. The PMT was biased at 500 V for these experiments. All the experiments were carried out at 20 ^{o}C.

The data were collected in the form of wavelength-time matrices, i.e. fluorescence decay curves at a series of emission wavelength. The data were analyzed in intensity format at a single emission wavelength of 350 nm. This wavelength was chosen due to its proximity to the emission wavelength of maximum intensity (ca. 334) and situation to sufficiently long wavelength to avoid interference by solvent Raman scattering. The area

under the fluorescence decay curves is proportional to the fluorescence intensity that would be measured in a state-state fluorescence experiment.

The dissociation constant was calculated from fluorescence waveform change due to ligand addition to SPL using a method developed by Gillispie and co-workers (187). By considering the fluorescence decay spectra as vectors, all data points were utilized instead of condensing them to a single value, as done in iterative reconvolution. The free vector was obtained from the baseline taken preceding ligand addition and the bound vector after adding ligand. A linear combination of these two vectors was used to fit each decay curve:

$$W_i = c_{if} W_f + c_{ib} W_b$$

A waveform at time *i*, (W_i) can be represented by mixing the basis waveforms of the free and bound SPL (W_f and W_b, respectively). The relative amount of each basis waveform is determined by preceding coefficients. Therefore for any given time *i*, c_{if} and c_{ib} identify how much of the free and bound waveform, respectively, is present.

Each waveform W_i can be area-normalized using the following formula:

$$W_i^N = \frac{W_i}{A(L)} A_f ,$$

where: W_i^N is normalized fluorescence intensity/waveform at a given concentration at time *I*; *A(L)* is the area under the fluorescence decay curve for the corresponding ligand concentration c_i; and A_f is the area under the fluorescence decay curve of SPL tryptophan(s) in the absence of ligand.

The area under any fluorescence decay curve can be calculated as:

$$A = \sum W_i \ \Delta t \ .$$

Then, the change in fluorescence waveform ($W_{\Delta}{}^{N}$) due to SPL-ligand formation at a given ligand concentration can be calculated from the following formula:

$$\Delta W^{N} = W_{i}^{N} - W_{f}^{N} ,$$

where: $W_{f}{}^{N}$ is SPL fluorescence waveform in the absence of ligand.

Finally, the sum of fluorescence intensities (fluorescence waveform change) at a given ligand concentration can be calculated as:

$$\Delta I \ = \sum \left| \Delta W_{i}^{N} \right| .$$

The data obtained from the fluorescence experiments were further analyzed with ORIGIN 8.0 software. Although the binding mechanism between SPL and the ligand could be more complicated, the dissociation constant K_{d}, at which half of the ligand molecules are bound to SPL, was determined using the Michaelis-Menten equation by nonlinear fit:

$$\Delta I \ = \ \frac{\Delta I_{\max} \ [L]}{K_{\mathrm{d}} \ + [L]} ,$$

where: ΔI is fluorescence waveform change at a specific concentration of the ligand; ΔI_{max} is fluorescence waveform change at which ligand binding reached saturation; K_{d} is dissociation constant; and $[L]$ is ligand concentration.

Free energy of SPL binding to various substrates were calculated using following formula:

$$\Delta G^{o} = - RT \ln K_a$$

where: ΔG^{o} – change in Gibbs free energy, R – gas constant (R = 8.314 J/mol K), T – temperature, K_a – association constant ($K_a = 1 / K_d$).

Results and Discussion

Binding of *B.s.* SPL to 94-bp UV-damaged Oligonucleotide

The electrophoretic mobility shift assays (EMSA) proved to be a good method for detecting undamaged DNA-protein complexes and determining the K_d, as described in Chapter 3. Therefore this method was chosen to investigate the interaction between SPL and damaged DNA. First, the spore photoproduct had to be generated on 94-bp double-stranded oligonucleotide that was previously used for nonspecific binding assays (Chapter 3) and which contained several adjacent thymine pairs. For that purpose this oligonucleotide was irradiated under several different conditions that were published by different groups. It involved making oligonucleotide dry films by lyophilization of the oligonucleotide either from water (43,142), or from a DNA/SspC mix (42), or from DNA mix with sodium dipicolinate (43,49). All three conditions were utilized in order to determine the best method for generating spore photoproduct. After UV irradiation at 254 nm, the UV-damaged oligonucleotide was applied onto a polyacrylamide gel to analyze the damage (Figure 4.1). The results suggest that the UV irradiation of oligonucleotides under all three different conditions resulted DNA damage since the major DNA band that

was present before UV irradiation was altered upon exposure to UV light (Figure 4.1). However, from this preliminary data it is impossible to conclude whether the damage is spore photoproduct and how much of it was formed. Also, it was impossible to tell how many base pairs were damaged on one oligonucleotide, or if this type of damage was uniform in all oligonucleotides. The streaking in all of the "+ UV" lanes suggested that more than one type of damage might have occurred, with other possible photodimers (*cis,syn* cyclobutane pyrimidine dimer, (6-4)-photoproduct etc.) formed as well (Figure 4.1).

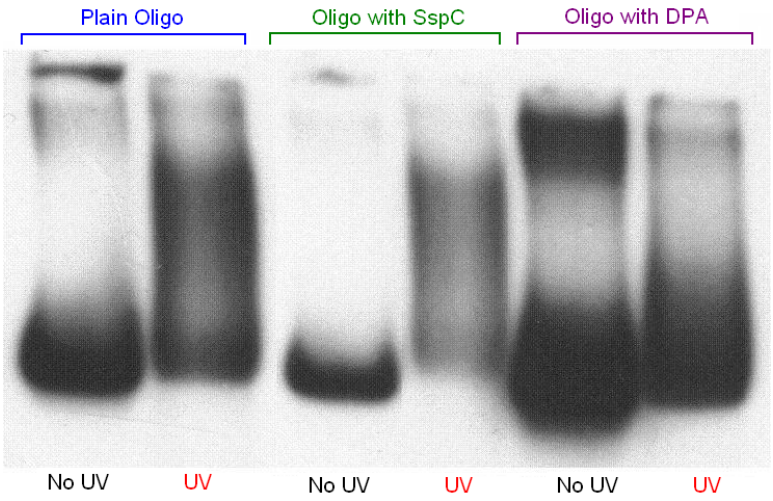

Figure 4.1. UV-irradiation of 94-bp oligonucleotide under different conditions. Lanes 1-2, oligonucleotide with no SspC or dipicolinic acid (DPA); lanes 3-4, oligonucleotide in the presence of SspC (1:5 ratio); lanes 5-6, oligonucleotide in the presence of 10 mM DPA. The samples for EMSA were prepared in 20 µL containing 10 mM HEPES, 50 mM NaCl, 10% glycerol, 0.05% NP-40, 0.5 mM DTT, 2.9 nM ^{32}P-labeled 94-bp oligo (pH 8) and loaded onto an 8% non-denaturing polyacrylamide gel and electrophoresed at 200 V (20 V/cm^2) for 2 hours. The electrophoresis products were visualized by autoradiography. Under all three conditions UV irradiation resulted in certain kind of damage (lanes 2, 4 and 6) in comparison to non-irradiated DNA (lanes 1, 3 and 5).

To investigate whether SPL binds to this UV-damaged DNA, EMSAs were carried out. For these experiments UV-irradiated DNA:SspC complex was chosen, because this kind of damaged DNA was previously used for DNA repair assays (42). When binding assays were carried out between the UV-irradiated DNA and *B.s.* SPL, the SPL bound to UV-damaged DNA with higher affinity than to undamaged DNA (Figure 4.2). Full binding between *B.s.* SPL and UV-irradiated oligonucleotide was reached at ~ 2 x 10^{-9} M, while for non-irradiated DNA full binding was reached at ~ 8 x 10^{-9} M. Unfortunately, UV-irradiated DNA bands on the gel could not be quantified accurately due to the streaking of DNA bands and therefore K_d could not be determined.

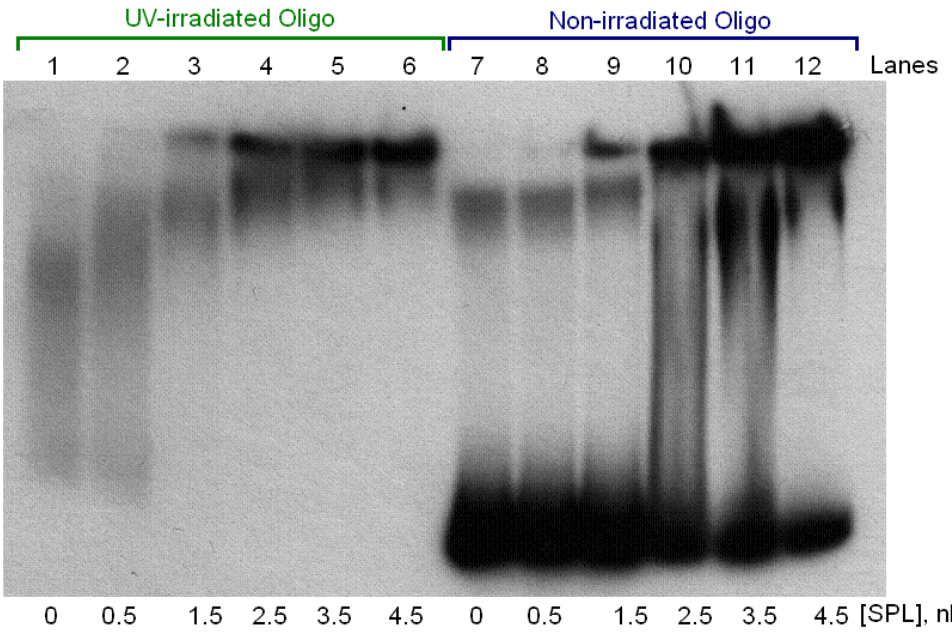

Figure 4.2. *B.s.* SPL binding to both UV-damaged (lanes 1-6) and undamaged 94-bp oligonucleotide (lanes 7-12). For the UV-irradiated oligo, the one irradiated in the presence of SspC was utilized. The EMSA reactions were prepared in 20 μL containing 10 mM HEPES, 50 mM NaCl, 10% glycerol, 0.05% NP-40, 0.5 mM DTT, 2.9 nM ^{32}P-labeled 94-bp oligo, and different concentrations of *B.s.* SPL (pH 8). All UV-irradiated oligo was bound at SPL concentration of ~ 2 nM, while at the same SPL concentration less than half of non-irradiated oligo was bound.

Determination of Dissociation Constant K_d
of SPL to Spore Photoproduct

Since irradiation of DNA proved to be an unreliable method for generating clean spore photoproduct in oligos, synthetic SP was utilized to gain insights into SPL binding to damaged DNA. For that purpose a novel technique involving measuring SPL intrinsic fluorescence waveform change due to substrate binding was developed. One advantage of this method is that it does not require labeling of DNA or protein. A protein's intrinsic fluorescence is due to the amino acids tyrosine, phenylalanine and tryptophan. Most of the emissions are due to excitation of tryptophan residues with a few emissions due to tyrosine and phenylalanine. Therefore protein fluorescence is generally excited at 295 nm, which is λ_{max} of tryptophan. Also, tryptophan fluorescence in proteins is usually very sensitive to its local conformation and can be utilized to gain useful information, like interactions with solvent, protein conformational changes or binding interactions (188). When substrate molecules were added to SPL, change in fluorescence waveforms could be observed. Another advantage of this method is that while light scattering and inner filter effects due to the addition of a substrate can interfere in steady-state experiments, fluorescence lifetime experiments are not effected since the desired information is extracted from the shape of the fluorescence lifetime curve rather than from intensity (182,188). In order to calculate the dissociation constant, the changes in SPL fluorescence decay waveforms (rather than the change in fluorescence lifetime) were calculated at different concentrations of a ligand.

For the fluorescence lifetime decay experiments, the synthetic spore photoproduct dinucleosides and dinucleotides, both *R*- and *S*-, were utilized (Scheme 4.1). In order to

compare SPL binding to nonspecific substrates, binding assays with thymidine (T) and thymidine dinucleotide (TpT) were also performed (Scheme 4.1).

The first set of assays was carried out with *C.a.* SPL, which contains one tryptophan (W240), and *5R*-SPTpT dinucleotide. Fluorescence lifetime quenching due to SPL-SP complex formation was observed (Figure 4.3). When increasing concentrations of *5R*-SPTpT were added to SPL, the fluorescence waveform peak at ~42 ns increased, while the shoulder at 45 ns decreased, until binding reached saturation (Figure 4.3.a). The presence of an isosbestic point suggests the presence of two different fluorescent species, bound and unbound SPL, in the reaction mix. The difference in fluorescence waveforms was also plotted (Figure 4.3.b). The SPL fluorescence quenching was quantified and the dissociation constant K_d was calculated using ORIGIN software as described in Experimental Methods (Figure 4.4). The dissociation constant for binding of 5*R*-SPTpT to SPL was determined to be 6.8 x 10^{-5} M, which is lower that the K_d for to non-specific DNA (See Chapter 3). The lower K_d for SPL binding to 5*R*-SPTpT is likely lower due to the fact that the substrate was only a dinucleotide, rather than full-length DNA.

Similar fluorescence lifetime decays were observed for *C.a.* SPL in the presence of *5S*-SPTpT dinucleotide (Figure 4.5) and thymidylyl (3'-5') thymidine (TpT) (Figure 4.6). The change in fluorescence waveform suggests that SPL can bind to both *5S*-SPTpT and TpT. Interestingly, SPL was found to bind 5*S*-isomer of SP, although only 5*R*-SPTpT and not 5*S*-SPTpT is a substrate (44). However, the changes that were induced in fluorescence waveform due to addition of 5*S*-SPTpT were very small in comparison with 5*R*-SPTpT (Figures 4.3 and 4.5). This could mean that SPL can bind to 5*S*-SPTpT, but

binding somehow is different that of 5*R*-SPTpT and it effects the tryptophan environment in a different fashion. The dissociation constant of *C.a.* SPL to 5*S*-SPTpT was determined to be K_d = 2.8 x 10^{-4} M (Figure 4.7), which suggests that the binding was rather tight, however not as tight as for the *R*-isomer of SP. The *C.a.* SPL was found to bind to TpT as well. The K_d for TpT was determined to be 1.8 x 10^{-3} M (Figure 4.8), suggesting that SPL binding was stronger to spore photoproduct than to its repair product TpT.

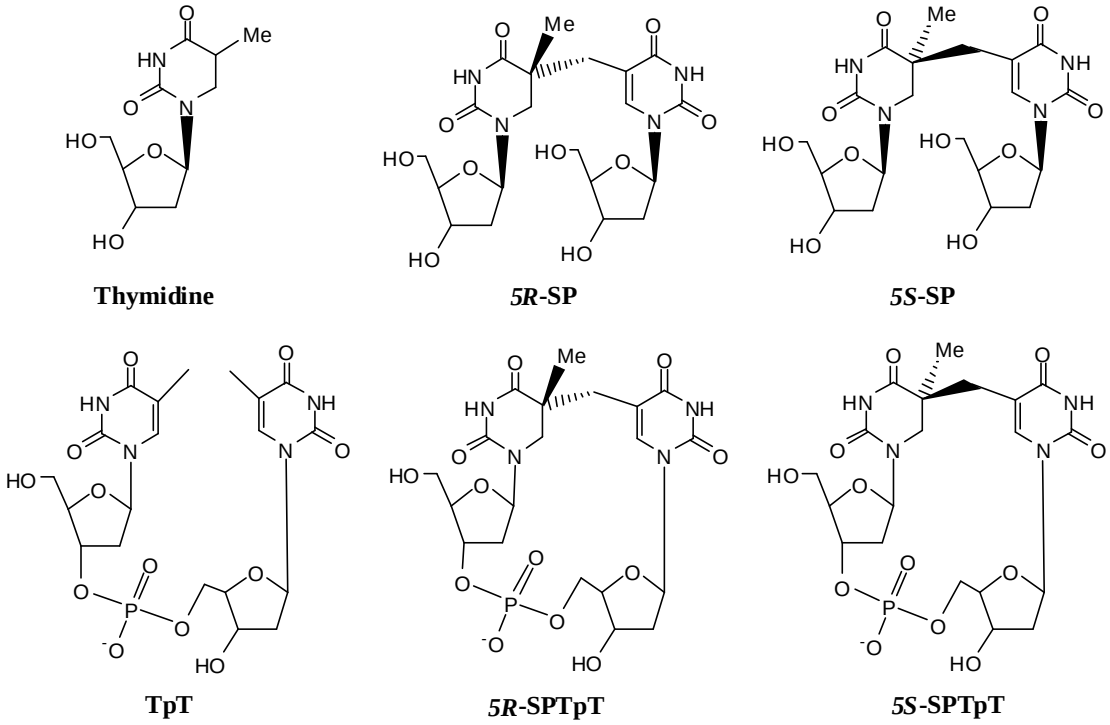

Scheme 4.1. The substrate molecules used for SPL binding assays.

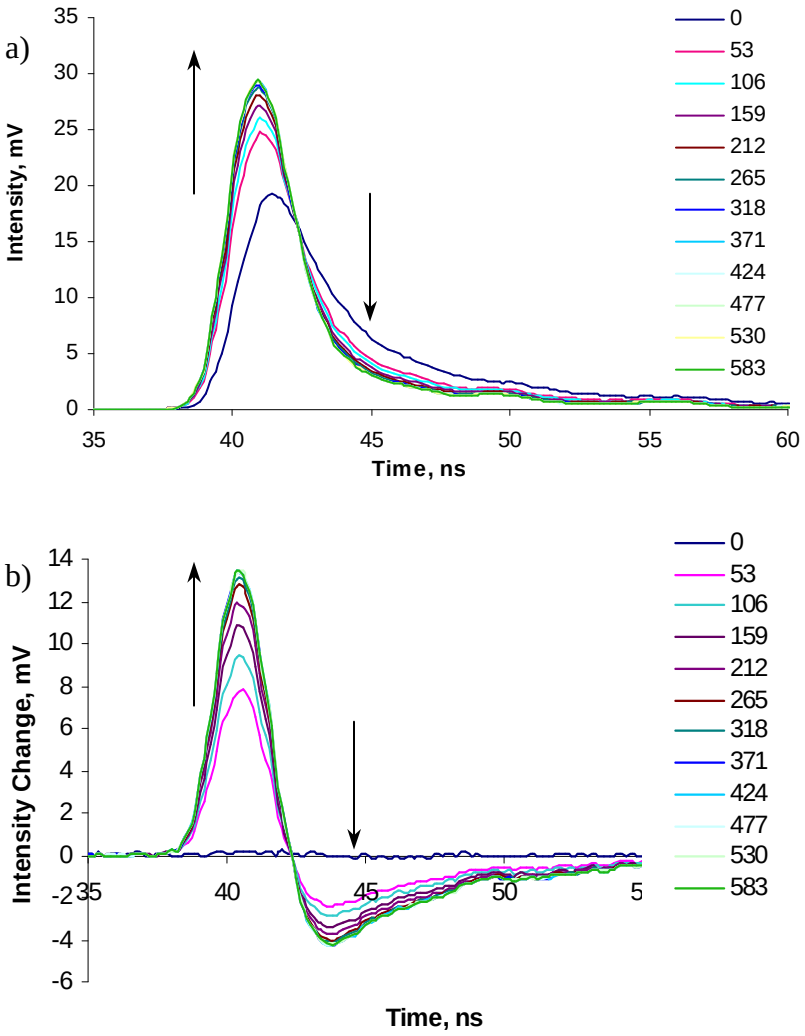

Figure 4.3. Binding assay between *C.a.* SPL and 5*R*-SPTpT carried out by fluorescence lifetime decay. a) Area-normalized *C.a.* SPL fluorescence lifetime decay upon addition of 5*R*-SPTpT at concentrations from 0 to 583 μM. The binding reaction was prepared in a total volume of 1 mL containing 50 mM HEPES, 50 mM NaCl, 5% glycerol, 5 mM DTT, and 5 μM of *C.a.* spore photoproduct lyase (pH 8.0). The reaction mix was prepared anaerobically in an MBraun glove box and transferred to anaerobic Spectrosil quartz 3.5 mL cuvettes (Starna Cells, Inc.). The substrate was added with a gas-tight syringe under N_2 and the fluorescence lifetime decay was measured at different concentrations of *5R*-SPTpT. All the experiments were carried out at 20 ^{o}C. The arbitrary shift in fluorescence signal on time scale was observed due to the delay between excitation and signal collection at transient digitizer. b) SPL fluorescence lifetime waveform changes due to addition of 5*R*-SPTpT at concentrations from 0 to 583 μM.

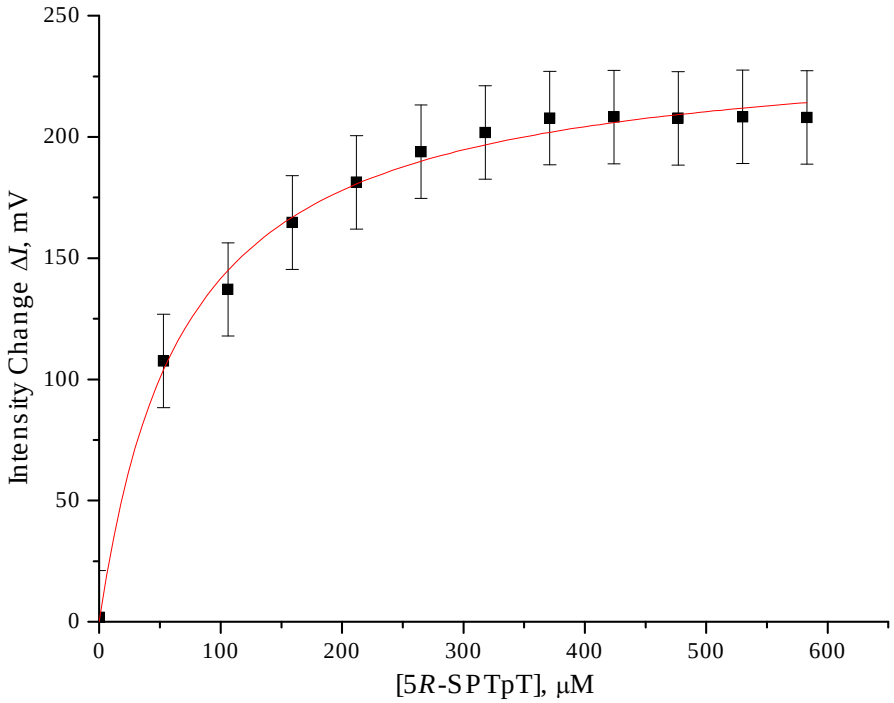

Figure 4.4. Binding assay between *C.a.* SPL and 5*R*-SPTpT carried out by fluorescence lifetime decay. The fluorescence waveform changes at different concentrations of 5*R*-SPTpT were quantified and the data were analyzed with ORIGIN 8.0 software. The saturation of binding was reached ~ 400 μM with the K_d = 68 ± 17 μM. The assay was done in duplicate. The error bars represent the largest standard deviation of fluorescence intensity change. The red line is the nonlinear fitting curve.

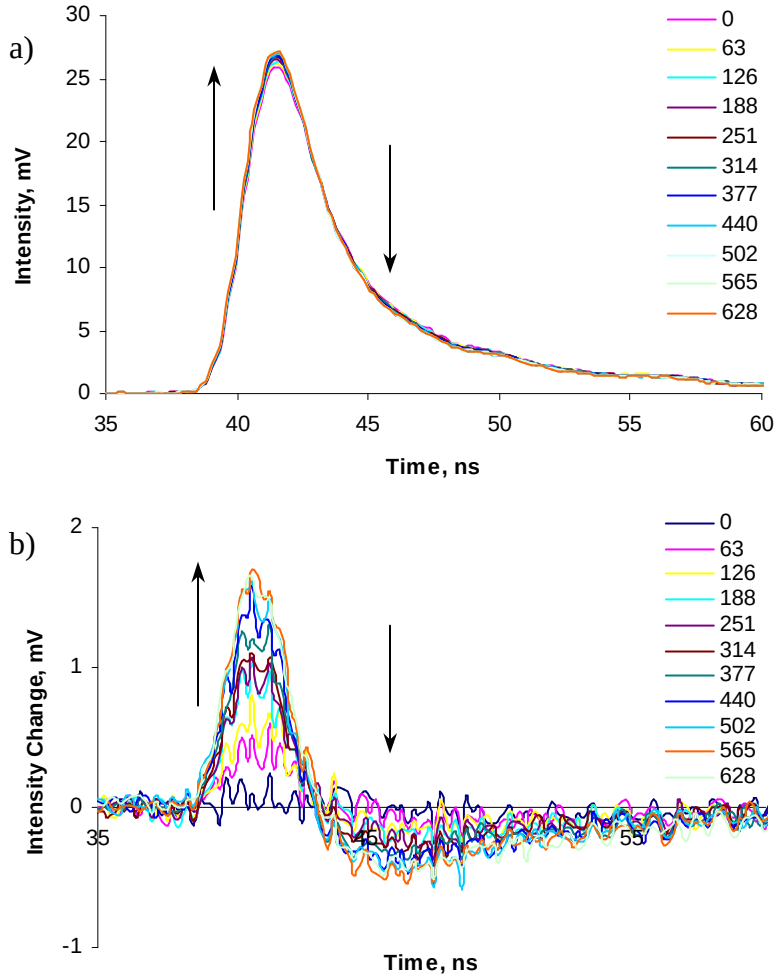

Figure 4.5. Binding assay between *C.a.* SPL and 5*S*-SPTpT carried out by fluorescence lifetime decay. a) Area-normalized *C.a.* SPL fluorescence lifetime decay upon addition of 5*S*-SPTpT at concentrations from 0 to 628 μM. The binding reaction was prepared in a total volume of 1 mL containing 50 mM HEPES, 50 mM NaCl, 5% glycerol, 5 mM DTT, and 5 μM of *C.a.* spore photoproduct lyase (pH 8.0). The reaction mix was prepared anaerobically in an MBraun glove box and transferred to anaerobic Spectrosil quartz 3.5 mL cuvettes (Starna Cells, Inc.). The substrate was added with a gas-tight syringe under N_2 and the fluorescence lifetime decay was measured at different *5S*-SPTpT concentrations. All the experiments were carried out at 20 ^{o}C. The arbitrary shift in fluorescence signal on time scale was observed due to the delay between excitation and signal collection at transient digitizer. b) SPL fluorescence lifetime waveform changes due to addition of 5*S*-SPTpT at concentrations from 0 to 628 μM.

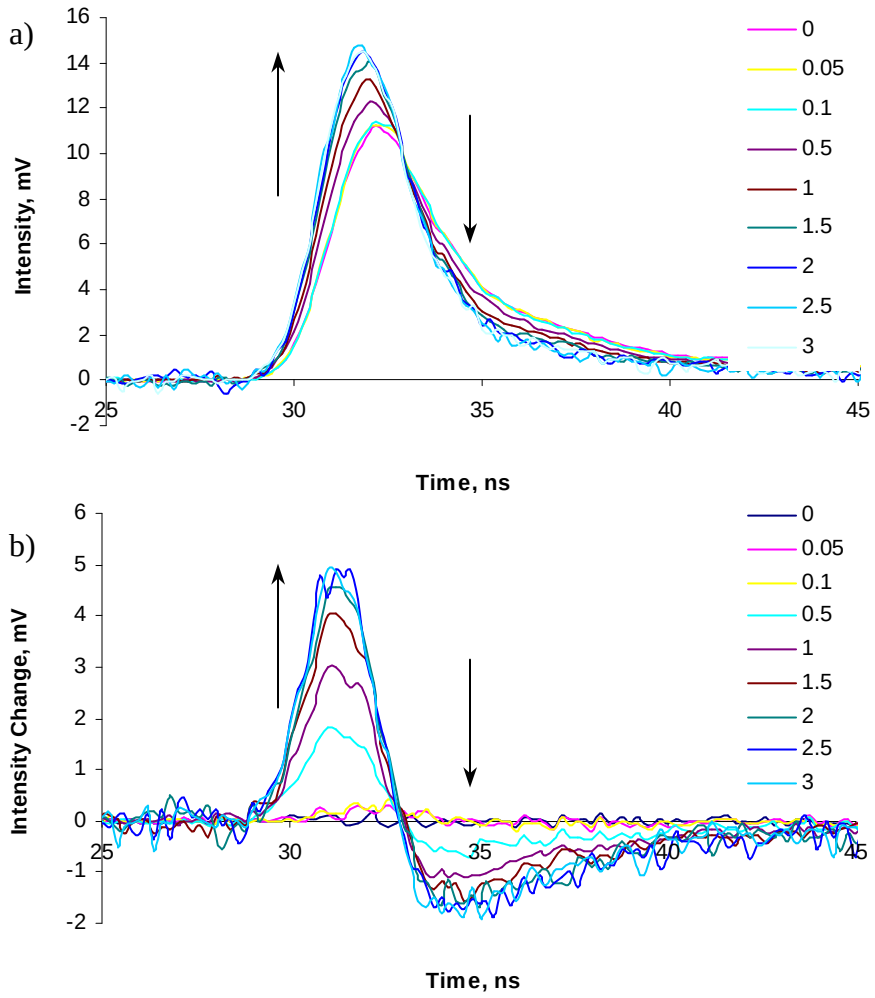

Figure 4.6. Binding assay between *C.a.* SPL and TpT carried out by fluorescence lifetime decay. a) Area-normalized *C.a.* SPL fluorescence lifetime decay upon addition of TpT at concentrations from 0 to 3 mM. The binding reaction was prepared in a total volume of 1 mL containing 50 mM HEPES, 50 mM NaCl, 5% glycerol, 5 mM DTT, and 5 μM of *C.a.* spore photoproduct lyase (pH 8.0). The reaction mix was prepared anaerobically in an MBraun glove box and transferred to anaerobic Spectrosil quartz 3.5 mL cuvettes (Starna Cells, Inc.). The substrate was added with a gas-tight syringe under N_2 and the fluorescence lifetime decay was measured at different TpT concentrations. All the experiments carried out at 20 ^{o}C. The arbitrary shift in fluorescence signal on time scale was observed due to the delay between excitation and signal collection at transient digitizer. b) SPL fluorescence lifetime waveform changes due to addition of TpT at concentrations from 0 to 3 mM.

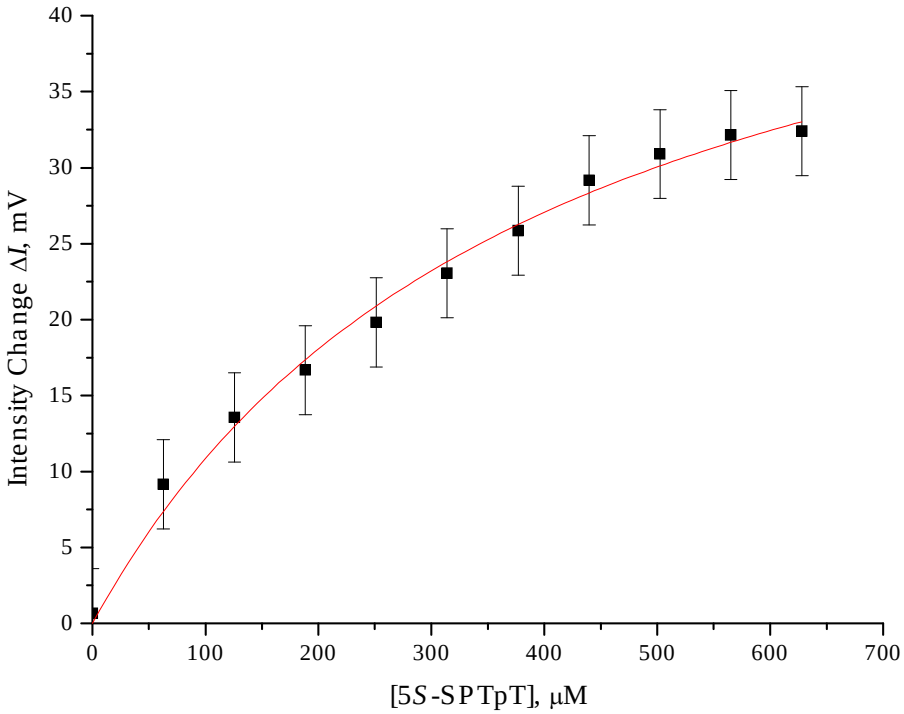

Figure 4.7. Binding assay between *C.a.* SPL and 5*S*-SPTpT carried out by fluorescence lifetime decay. The fluorescence waveform changes at different concentrations of 5*S*-SPTpT were quantified and the data were analyzed with ORIGIN 8.0 software. Saturation of binding was reached at ~ 600 μM with the K_d = 189 ± 71 μM. The assay was done in duplicate. The error bars represent the largest standard deviation of fluorescence intensity change. The red line is the nonlinear fitting curve.

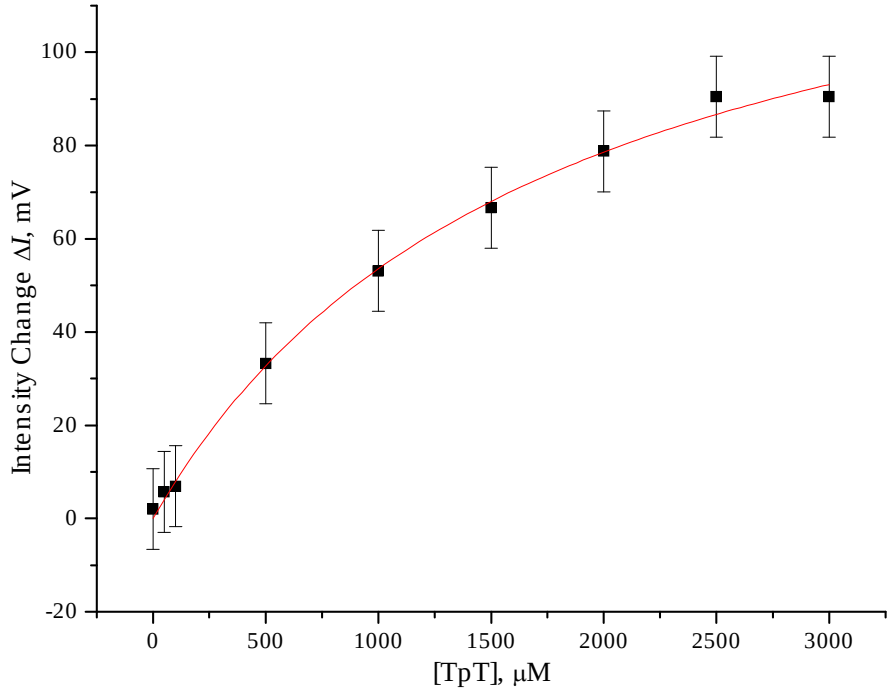

Figure 4.8. Binding assay between *C.a.* SPL and TpT carried out by fluorescence lifetime decay. The fluorescence waveform changes at different concentrations of TpT were quantified and the data were analyzed with ORIGIN 8.0 software. Saturation of binding was reached at ~ 2.5 mM with the K_d = 1.8 ± 0.3 mM. The assay was done in duplicate. The error bars represent the largest standard deviation of fluorescence intensity change. The red line is the nonlinear fitting curve.

In order to investigate the effect of the phosphodiester bridge on SPL binding to SP, the following fluorescence lifetime decay experiments tested *5R*-SP, *5S*-SP dinucleosides and thymidine. Previously we reported (see Chapter 2) that the *C.a.* SPL repair rate increased ~17 times when synthetic SP dinucleotide was used instead of synthetic dinucleoside (44,146). When the binding assays between *C.a.* SPL and synthetic SP dinucleosides were carried out, we found that SPL bound to these substrates as well (data not shown). The dissociation constants were K_d = 3.7 x 10^{-3} M for 5*R*-SP, K_d = 7.4 x 10^{-4} M for 5*S*-SP and K_d = 4.7 x 10^{-3} M for thymidine (Table 4.1). As in the assays with dinucleotide, SPL bound to SP with higher affinity than to its repair product

(thymidine). These dissociation constants suggest that SPL affinity for dinucleoside was weaker than to dinucleotides, consistent with the observation that the phosphodiester bridge-containing spore photoproduct is a better substrate, as previously shown by SP repair assays (44).

When free energy ΔG^o for *C.a.* SPL binding for each synthetic molecule was calculated (Table 4.1), it was found that ΔG^o was lower for SP dinucleotide than nucleoside, indicating that binding is thermodynamically more favorable for SP dinucleotide. ΔG^o was –13.56 kJ/mol for 5*R*-SP and –17.68 kJ/mol for 5*S*-SP while for 5*R*-SPTpT it was –23.46 kJ/mol and -20.89 kJ/mol for 5*S*-SPTpT. SPL binding to TpT had slightly lower ΔG^o (-13.15 kJ/mol) than binding to thymidine (-15.51 kJ/mol) as well.

The analogous fluorescence lifetime decay experiments (for both dinucleosides and dinucleotides, Scheme 4.1) were performed for *B.s.* SPL, which contains two tryptophans (W243 and W303). We found that addition of these substrates to *B.s.* SPL induces changes in the intrinsic fluorescence as well. The dissociation constants were determined similarly to the ones for *C.a.* SPL as described above. The dissociation constants were comparable to the ones from *C.a.* SPL and were determined to be for nucleotides: K_d = 2.7 x 10^{-4} M (5*R*-SPTpT), K_d = 1.6 x 10^{-4} M (5*S*-SPTpT) and K_d = 1.9 x 10^{-3} M (TpT) (Table 4.1). *B.s.* SPL dissociation constants for nucleosides were K_d = 4.8 x 10^{-3} M for 5*R*-SP, K_d = 9.6 x 10^{-4} M for 5*S*-SP and K_d = 1.6 x 10^{-2} M for thymidine (Table 4.1). Free energy ΔG^o for *B.s.* SPL binding was determined similarly to the one for *C.a.* SPL as described above. Binding energies were comparable to the ones from *C.a.* SPL and for nucleotides were determined to be -20.15 kJ/mol (5*R*-SPTpT), -21.44 kJ/mol

(5*S*-SPTpT) and -15.33 kJ/mol (TpT) (Table 4.1). *B.s.* SPL free binding energies for nucleosides were -13.07 kJ/mol for 5*R*-SP, -17.04 kJ/mol for 5*S*-SP and -10.13 kJ/mol for thymidine (Table 4.1). The results from time-resolved fluorescence experiments are summarized in Table 4.1.

Table 4.1. Dissociation constants (K_d) of SPL to various substrates and correlating free energies (ΔG^o).

	B.subtilis SPL		*C.acetobutylicum* SPL	
	K_d, mM	ΔG^o, kJ/mol	K_d, mM	ΔG^o, kJ/mol
Thymidine	16.07 ± 5.15	-10.13	4.70 ± 0.09	-13.15
5*R*-SP	4.85 ± 0.55	-13.07	3.97 ± 0.13	-13.56
5*S*-SP	0.96 ± 0.92	-17.04	0.74 ± 0.10	-17.68
TpT	1.93 ± 0.56	-15.33	1.79 ± 0.30	-15.51
5*R*-SPTpT	0.27 ± 0.03	-20.15	0.07 ± 0.02	-23.46
5*S*-SPTpT	0.16 ± 0.02	-21.44	0.20 ± 0.06	-20.89

Conclusions

To investigate SPL binding to specific/damaged DNA, electrophoretic mobility shift assays involving SPL and UV-irradiated DNA were carried out. The results from these experiments suggested that UV irradiation alters the 94-bp oligonucleotide and that SPL affinity for this type of DNA is higher than for non-irradiated DNA. However, the SPL dissociation constant for UV-damaged DNA could not be determined from these assays. To gain more accurate results of SPL binding for specific DNA, time-resolved fluorescence experiments between SPL and spore photoproduct were carried out. A change in SPL fluorescence lifetime waveform was observed due to the formation of an

enzyme-substrate complex. The presence of only two different fluorescent species, bound and unbound SPL, were also suggested by the presence of isosbestic points in these titrations (Figures 4.2, 4.3 and 4.4).

Fluorometric titrations were utilized to determine dissociation constants (Figures 4.3, 4.5 and 4.6). Previously it was observed that there was a difference in repair rates between spore photoproduct dinucleoside and dinucleotide (44,146). Therefore, to investigate SPL binding to spore photoproduct, two forms of SP, the dinucleoside and dinucleotide, were utilized (Figure 4.1). Our time-resolved fluorescence experiments showed that there was a difference in SPL binding to SP dinucleoside and dinucleotide (Table 4.1), which is likely due to SPTpT having a closer resemblance to the natural substrate and therefore more favorable binding interactions with the enzyme active site. Similarly, DNA photolyase was found to have different affinities to the cyclobutane pyrimidine photodimer dinucleoside (CPD) and dinucleotide (CPDTpT) (180,183). For CPDTpT the dissociation constants of *E. coli* DNA photolyase were found to be ~ 2.4 x 10^{-4} M (180) and ~ 1.8 x 10^{-4} M (183), while for cyclobutane photodimer dinucleoside (CPD) it was ~ 1 x 10^{-3} M (183), ~ 5 times weaker. While SP repair rate for *C.a.* SPL increased 17-fold from 5*R*-SP dinucleoside to 5*R*-SPTpT dinucleotide, the differences in binding were ~ 54-fold for *C.a.* SPL and ~18-fold for *B.s.* SPL. In the case of thymidine and TpT, the difference was only ~3 and ~8-fold for *C.a.* and *B.s.* SPL, respectively. For the *S*-isomer of SP, there was a difference in binding between 5*S*-SP and 5*S*-SPTpT as well, at ~ 4 – 6-fold. Interestingly, these results suggest that the binding changed the most for the *R*-isomer of SP (SP→SPTpT) in comparison with the 5*S*-isomer or

thymidine/TpT. Also, the dissociation constants were comparable between *B.s.* and *C.a.* SPL, which suggest that the SPL binding pocket might consist of highly conserved amino acids despite the low overall identity of 42 % between these two proteins.

Interestingly, SPL was found to bind the 5*S*-isomer of SP, although we have previously reported that only the 5*R*-isomer is repaired (44,146). Despite the apparent different structures of the two diastereomers (Figure 4.9) (146,150), binding could be possible due to partial recognition of only one of the nucleobases. Also, the amino acids that are involved in binding the 5*R*-isomer may quite possibly make some of the same contacts with the 5*S*-isomer as well. However, without having a crystal structure of SPL with substrate bound, it is hard to make any further conclusions.

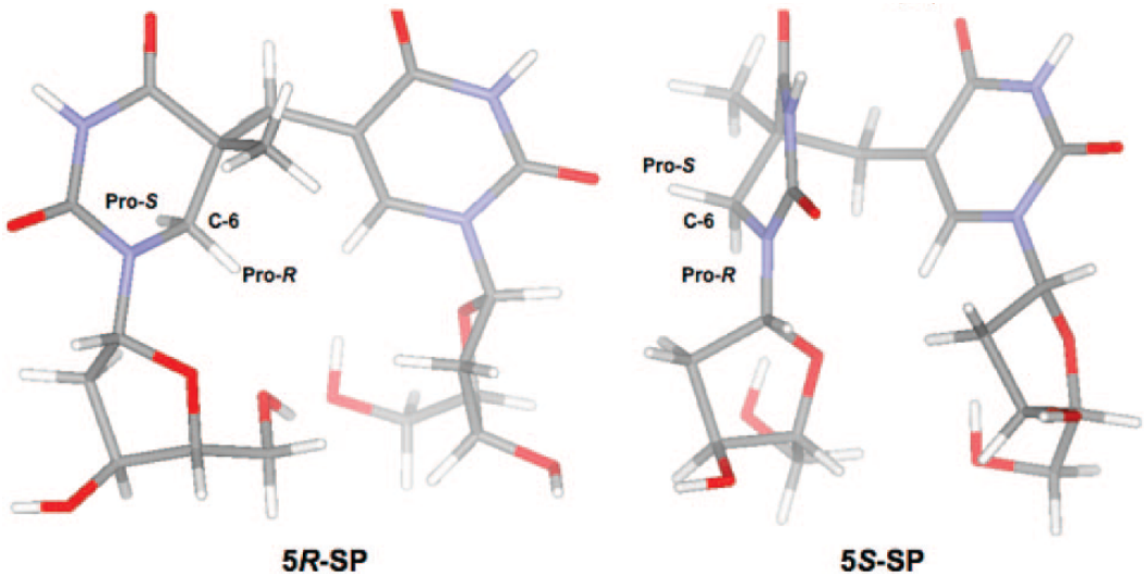

Figure 4.9. Computational models for the 5*R*- and 5*S*-isomers of synthetic spore photoproduct dinucleoside lacking a DNA backbone. Adapted from (146).

The time-resolved fluorescence decay experiments with undamaged DNA (94-base pair double-stranded oligonucleotide) showed no change in fluorescence lifetime (data not shown). This is most likely due to the DNA binding region being too far from tryptophan. Similarly, it was found that fluorescence quenching for DNA photolyase was not observed when undamaged oligonucleotide was used (180). It might also suggest that SPL binds non-specific DNA with different amino acids than at the spore photoproduct binding site. However, more research in order to investigate this hypothesis has to be done.

Future work could also include SPL binding assays to SP-containing double-stranded oligonucleotide, which could be carried out by doing electrophoretic mobility assays (EMSA) or time-resolved fluorescence decay assays. Damage on the DNA strand could to be created by incorporating synthetic spore photoproduct into an oligonucleotide. SP amidite (a precursor that can be used in DNA synthesis) has already been synthesized in our lab and now must be inserted into a 14-bp oligonucleotide (Scheme 4.2).

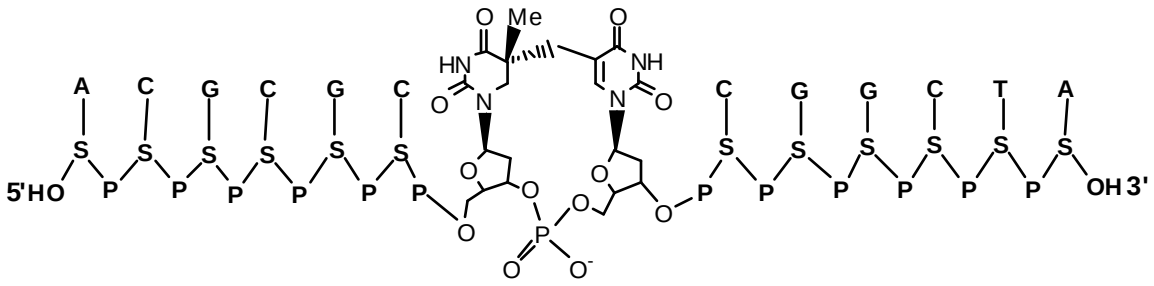

Scheme 4.2. Single-stranded oligonucleotide containing *R*-isomer of spore photoproduct. Letter S represents deoxyribose; P – phosphate; A,T,G and C – adenine, thymine, guanine and cytosine, respectively.

CHAPTER 5

GENERAL CONCLUSIONS AND FUTURE DIRECTIONS

Purification and Characterization of Spore Photoproduct Lyase

Spore photoproduct lyase is an enzyme that catalyzes the specific repair of 5-thyminyl-5,6-dihydrothymine to two thymines. It utilizes *S*-adenosylmethionine as a cofactor and a $[4Fe\text{-}4S]^{2+/1+}$ cluster as an electron donor (35,37,39,142). Most of the research done previously focused on repair by using UV-irradiated DNA as a substrate with little investigation on the formation of the spore photoproduct. There are two different diastereomers of spore photoproduct, *S*- and *R*-, based on the orientation of methyl group on the C5 carbon. The formation of the *R*-isomer of SP should be more favored due to the steric constrains in the *A* form of DNA that is present in bacterial spores (144). The *S*-isomer potentially could be formed on two interstrand thymidines, however, there is no direct evidence of which isomer is formed on DNA due to UV irradiation of spores and is repaired by SPL.

SPL was successfully overexpressed and purified from two different bacteria, *Bacillus subtilis* and *Clostridium acetobutylicum*. The anaerobically purified *C. acetobutylicum* SPL was found to contain 2.9 Fe / SPL and had a concentration of 0.104 mM, while SPL from *B. subtilis* had a concentration of 0.025 mM and contained 2.3 irons per protein. The amount of iron present in the purified SPL is dependent on the precise growth and purification conditions, and the protein was not subjected to artificial reconstitution (47,147).

The Repair of Stereochemically-Defined Spore Photoproduct Dinucleoside And Dinucleotide by Spore Photoproduct Lyase

Repair assays were utilized to investigate SPL activity in repairing the *R*- and *S*-spore photoproduct dinucleosides. The repair assay mix was then injected onto the HPLC and the peaks that eluted were characterized by both co-injection of authentic compounds and by ESI-MS. These assays showed that SPL repairs the *R*-, but not the *S*-isomer of SP. Integration of the peaks from HPLC chromatograms allowed quantification of the amounts of thymidine produced. Repair rates were determined to be ~0.4 nmol/min/mg for the 5*R*-SP and 0 nmol/mg/min of SPL for 5*S*-SP. These results contradicted the ones from Carell and co-workers, which stated that 5*S*-SP, but not 5*R*-SP is repaired (49,148). Interestingly, during the SP repair reaction, 5'-deoxyadenosine and methionine peaks on the HPLC chromatogram were also observed. This was an unusual observation considering the fact that SAM acts as a cofactor for SPL and should not be irreversibly cleaved during repair (39,42). We suggest that due to the fact that the spore photoproduct dinucleoside is not a natural substrate for SPL, unlike SP-containing DNA, and because non-physiological reducing agent sodium dithionite was utilized in our repair reactions, reductive SAM cleavage occurred. Reductive SAM cleavage was uncoupled from substrate turnover and was also observed in the absence of the synthetic substrates.

In order to investigate the effect of the phosphodiester bridge on the repair of SP by SPL, we also assayed repair of *5R*-SPTpT and *5S*-SPTpT dinucleotides. Due to the fact that SP dinucleotides resemble the natural substrate (DNA) more closely than the dinucleosides, the results were expected to be different. Because of the bridging

phosphate the SP dinucleotide cannot rotate around the methylene group and is more constrained than the SP dinucleoside. The repair assays of 5*R*-SPTpT demonstrated its complete conversion to thymidine dinucleotide (TpT) over the course of ~ 40 minutes. The repair assays of 5*S*-SPTpT show no production of TpT and further confirm that the *R*-isomer, rather than the *S*-, is the substrate for SPL. The products of the 5*R*-SPTpT repair assay were identified the same way as for 5*R*-SP repair assay, by both co-injection of authentic compounds on HPLC and by ESI-MS. The peaks from HPLC chromatograms were integrated and quantified in order to determine the rate of TpT production. The repair rates were found to be ~4 nmol/min/mg of SPL for *R*-SPTpT and 0 nmol/mg/min of SPL for 5*S*-SPTpT. During this reaction, 5'-deoxyadenosine formation from *S*-adenosylmethionine was also observed, which was dependent on reaction time. For 5*R*-SPTpT control samples, just like in the 5*R*-SP dinucleoside assays, there was no 5'-dAdo production in the absence of SPL. Again, SAM cleavage could be due to the fact the 5*R*-SPTpT is not a natural substrate for SPL or due to utilization of non-physiological reducing agent. These assays also showed that 5*R*-SPTpT dinucleotide is a better substrate for SPL than 5*R*-SP dinucleoside likely due to its closer resemblance to natural DNA substrate.

Spore Photoproduct Lyase Binding To Undamaged DNA

Many proteins bind DNA to perform a variety of functions, including DNA protection and repair (157,158). Nonspecific binding is thought to precede binding to the target site and therefore should be an important intermediate step in the process of

recognizing and binding the target site. DNA photolyase, another DNA repair protein that shares some sequence similarities with SPL, was found to bind DNA nonspecifically (165,166). The dissociation constant (K_d) of *E. coli* DNA photolyase to undamaged DNA is K_d = 3.45 x 10^{-5} M in comparison to K_d = 2.6 x 10^{-8} M for the specific binding (166,167).

Beyond the repair of spore photoproduct (39,42,43,49,142), there is very little knowledge on how SPL recognizes and binds undamaged or UV-damaged DNA. We assume that SPL has to be able to find the damage and repair it in any sequence context and that non-specific binding occurs within the predicted helix-turn-helix region of SPL, with the most conserved amino acids likely making bonds with the phosphate groups on the DNA backbone.

In order to investigate how SPL binds to undamaged DNA, electrophoretic mobility shift assays (EMSA) were carried out. Here we show for the first time that SPL binds to undamaged pUC18 DNA with rather high affinity. This non-specific binding could precede binding to specific DNA. We found that SPL could bind to circular, nicked and linear DNA. SPL binding to long DNA (linear pUC18 DNA, 2686 bp) suggests that full binding could be reached at ~10 x 10^{-9} M of DNA. The dissociation constant, however, from these assays could not be determined.

In order to determine the K_d of SPL to undamaged DNA, the binding assays between SPL and 94-bp double-stranded oligonucleotide were carried out. Full binding of *B. subtilis* SPL to this oligonucleotide under anaerobic conditions could be reached at ~ 8 x 10^{-9} M, with K_d = 4.7 ± 0.44 x 10^{-9} M. These finding suggest that SPL binding to

undamaged DNA is very tight and much stronger than that of DNA photolyase (129,166). It also suggests that binding is cooperative with more than one molecule of SPL binding to one oligonucleotide. The cooperativity factor (or Hill coefficient) was determined to be 7.1 ± 3.2 molecules of SPL per one molecule of DNA. SPL binding affinity to undamaged DNA does not depend significantly on its the length since there is little difference in the binding of SPL to long DNA (pUC18) vs. short DNA (94-bp oligonucleotide). SPL was found to bind single-stranded DNA with similar affinity as well. The binding of *C. acetobutylicum* SPL to undamaged 94-bp oligonucleotide revealed that nonspecific binding is weaker than that for *B.s.* SPL which could be due to different pI values of the predicted helix-turn-helix.

Spore Photoproduct Lyase Non-Specific Binding Under Different Conditions

SPL binding properties were further investigated under different conditions, including in the presence of oxygen, AdoMet and small, acid-soluble proteins (SASPs). The repair of SP cannot proceed under aerobic conditions due to the degradation of [4Fe-4S] cluster that is present in SPL. Interestingly, when binding assays were done in the presence of oxygen, SPL still bound undamaged DNA with $K_d = 5.3 \pm 0.21 \times 10^{-9}$ M. The binding is cooperative, with ~11.6 ± 7.9 molecules of SPL binding to one molecule of DNA. The role of the iron-sulfur cluster in non-specific binding of SPL to DNA was investigated further by carrying out the experiments with *apo*-SPL, which lacks the [4Fe-4S] cluster. The full binding of *apo*-SPL was reached at ~12 x 10^{-9} M and K_{NS} = 6.7 ±

0.39 x 10^{-9} M. Cooperative binding was also observed, with n = 11.6 ± 6.7. These results indicate that the absence of iron-sulfur cluster has no affect on SPL binding to undamaged DNA. However, it is still not clear if the binding to specific DNA would be equally unaffected, since more contacts between the protein and DNA might need to be established.

S-adenosylmethionine (SAM) is required for SPL to repair the spore photoproduct and it is known that radical SAM superfamily enzymes bind SAM. Therefore it was interesting to investigate if SAM plays a role in DNA binding. The next experiments involved SPL binding to 94-bp oligonucleotide in the presence of SAM. However, we found that the presence of 5 mM SAM had very little effect on SPL binding to undamaged oligonucleotide (K_d = 5.5 ± 1.21 x 10^{-9} M). As in previous cases, non-specific SPL binding is cooperative and there are 5.4 ± 1.4 molecules of protein per DNA.

Small, acid-soluble proteins play an important role in spore resistance and they are in high abundance inside of the spore core (17,28,173). It is known that these proteins bind and protect DNA (29,30), but is not clear if they can affect SPL binding to the DNA. In order to investigate the influence of small-acid soluble proteins on SPL binding, SspC was added to the binding reaction mix. We found that the presence of the small-acid soluble protein SspC has no influence on SPL binding and the K_d is 6 ± 0.73 x 10^{-9} M with the Hill coefficient n = 8.2 ± 5.8. Therefore small, acid-soluble proteins appear not to compete with the non-specific binding of SPL to DNA and most likely do not interfere with recognition and repair of spore photoproduct by SPL.

We also found that SPL bound single-stranded 94-bp oligonucleotide with similar affinity to that of double-stranded oligonucleotide with the maximum binding being reached at 8 x 10^{-9} M. Unfortunately, single-stranded DNA bands on the gel could not be quantified accurately and therefore K_d could not be determined.

While dormant bacterial spores have pH ~ 6.5, it changes to 7.0 – 7.5 once the spores start germinating. During that period SPL finds and repairs SP-containing DNA. Therefore it was interesting to investigate if SPL affinities to DNA vary at different pH levels. For this set of the experiments the pH of all the buffers was adjusted depending on the assay conditions. The assays were carried out at pH 8.0 (K_d = 4.7 ± 0.44 x 10^{-9} M), pH 7.5 (K_d = 17.2 ± 1.45 x 10^{-9} M), pH 7.0 (K_d = 60.3 ± 3.82 x 10^{-9} M) and pH 6.5 (K_d = 27 ± 6.53 x 10^{-9} M). In all these assays SPL showed significant cooperativity with the Hill coefficients ranging between 6 and 11. The pH of the reaction mixture has a pronounced effect on non-specific binding. The highest affinity of SPL to undamaged DNA is observed at pH 8.0 and the lowest at pH 7.0, with the binding at pH 8.0 being ~13 times stronger than at pH 7.0. These results suggest that SPL affinity could be affected during spore germination, when the pH of the spore core changes from 6.5 to ~7.5. Interestingly, for *C. acetobutylicum* SPL binding is stronger at pH 7.0 rather than pH 8.0, the opposite of *B. subtilis* SPL. This potentially could be due to different pI value of DNA-binding helix-turn-helix region in *C.a.* SPL.

Spore Photoproduct Lyase Binding To UV-Damaged DNA

Many proteins bind to DNA both specifically and non-specifically (164). DNA photolyase has affinity towards damaged DNA containing *cis,syn* cyclobutane thymine dimers with a dissociation constant K_d ~10^{-9} M. (167,174). DNA footprinting assays showed that DNA photolyase enzymes from *E. coli* and *M. thermoautotrophicum* protected the 11-16 base pair region around the thymine dimer (174,175). Also, DNA photolyase makes many contacts to the DNA backbone in order to flip out the damaged site for repair (121). The (6-4) photoproduct photolyase is another DNA repair enzyme that converts (6-4) photoproduct to two thymines (176) by binding to DNA relatively tightly and with high specificity (141). The dissociation constants for this protein to damaged DNA that were determined from EMSA vary from ~10^{-9} to 10^{-10} M (177). DNase I footprinting assays also demonstrated that (6-4) photolyases can protect 11 to 20 bases around the damaged site (141).

While it was shown that SPL bound specifically to and repaired spore photoproduct, not cyclobutane dimer (142), the attempts to do binding assays between *B.s.* SPL and UV-irradiated DNA were unsuccessful. DNase I footprinting assays showed that SPL bound to the SP-containing DNA and protected a 9-bp region surrounding SP from DNase I digestion (142). However, these studies did not provide information about the affinity of SPL towards UV-damaged DNA. Therefore after determining the dissociation constant of SPL to undamaged DNA we further investigated SPL binding to specific/damaged DNA by employing electrophoretic mobility shift assays (EMSA). Damage on DNA was created by making oligonucleotide dry films by lyophilization of

the oligonucleotide either from water (43,142), from DNA/SspC mix (42), or from DNA mix with sodium dipicolinate (43,49) and then irradiating at 254 nm. UV irradiation of oligonucleotides under all three different conditions resulted in a certain kind of damage, but it was unclear if the damage was spore photoproduct or how much of it was formed. It is possible that more than one type of damage might have occurred, since other photodimers (*cis,syn* cyclobutane pyrimidine dimer, (6-4)-photoproduct etc.) could form as well. When binding assays were carried out between the UV-irradiated oligonucleotide and *B.s.* SPL, we found that SPL bound to UV-damaged DNA with higher affinity than to undamaged DNA. Full binding between *B.s.* SPL and UV-irradiated oligonucleotide was reached at ~ 4 x 10^{-9} M in comparison with ~ 8 x 10^{-9} M for non-irradiated oligo. Unfortunately, the K_d could not be determined since UV-irradiated DNA bands on the gel could not be quantified accurately.

SPL Binding To Stereochemically-Defined SP Dinucleotides and Dinucleosides

In order to gain insights on SPL binding to damaged DNA, synthetically made *R*- and *S*-isomers of SP were utilized. For that purpose we developed a technique that involves measuring the quenching of SPL intrinsic fluorescence was developed. Due to the formation of an enzyme-substrate complex, a change in SPL intrinsic fluorescence was observed. Two different fluorescent species, bound and unbound SPL, were also suggested by the presence of an isosbestic point. In order to compare SPL binding to nonspecific substrates, binding assays with thymidylyl (3'-5') thymidine (TpT) were also performed. The first set of assays was carried out with *C.a.* SPL, which contains one

tryptophan (W240), and *5R*-SPTpT dinucleotide. Fluorescence lifetime quenching due to SPL-SP complex formation was quantified and the dissociation constant (K_d) for 5*R*-SPTpT was determined to be 6.8 x 10^{-5} M. This K_d was lower in comparison to the one for non-specific DNA, which could be due to the fact that the substrate was a dinucleotide, rather than full-size DNA. Similar fluorescence lifetime decays were observed in the presence of *5S*-SPTpT dinucleotide and thymidylyl (3'-5') thymidine (TpT). The change in fluorescence decay suggests that SPL can bind to both 5*S*-SPTpT and TpT. Interestingly, SPL was found to bind the 5*S*-isomer of SP, although only 5*R*-SPTpT is repaired (44). The dissociation constant of *C.a.* SPL for 5*S*-SPTpT was determined to be K_d = 2.8 x 10^{-4} M, which suggests that the binding is rather strong, but not as strong as for the *R*-isomer of SP. Despite the apparent different structures of the two diastereomers (146,150), binding could be possible due to partial recognition of only one of the nucleobases. Also, the amino acids that are involved in binding the 5*R*-isomer may quite possibly make some of the same contacts with the 5*S*-isomer as well. The K_d for TpT was determined to be 1.8 x 10^{-3} M, suggesting that SPL binding was stronger to spore photoproduct than to its repair product TpT.

To better define the structural requirements of SPL binding to SP, the effect on binding by the phosphodiester bridge between two thymines was also investigated. Since SP dinucleoside lacks phosphodiester bridge and therefore is less resembling DNA, SPL binding to SP is expected to be different than that of SPTpT. Also, previously it was reported that the *C.a.* SPL repair rate increased ~17 times when SP dinucleotide was used instead of dinucleoside (44,146,150). Therefore the following fluorescence lifetime decay

experiments tested *5R*-SP and *5S*-SP dinucleosides, as well as thymidine. When the binding assays between *C.a.* SPL and SP dinucleosides were carried out, we found that SPL bound to these substrates as well. The dissociation constants were K_d = 3.7 x 10^{-3} M for 5*R*-SP, K_d = 7.4 x 10^{-4} M for 5*S*-SP and K_d = 4.7 x 10^{-3} M for thymidine. As in the assays with dinucleotide, SPL binds to SP with higher affinity than to its repair product (thymidine). These dissociation constants suggest that SPL affinity towards dinucleoside is weaker than to dinucleotides, further supporting the hypothesis that the phosphodiester bridge-containing spore photoproduct is a better substrate, which is likely due to SPTpT having a closer resemblance to the natural substrate.

Other Binding Experiments Involving Spore Photoproduct Lyase

The analogous fluorescence lifetime decay experiments (for both dinucleosides and dinucleotides) were performed for *B.s.* SP lyase, which contains two tryptophans (W243 and W303). We found that addition of these substrates to *B.s.* SPL quench the intrinsic fluorescence as well. The dissociation constants were determined similarly to the ones for *C.a.* SPL by reaching saturation of binding. The dissociation constants were comparable to the ones from *C.a.* SPL, which suggest that the SP lyase binding pocket might consist of highly conserved amino acids despite the low overall identity of 42 % between these two proteins. The SPL dissociation constants for dinucleotides were determined to be K_d = 2.7 x 10^{-4} M for 5*R*-SPTpT, K_d = 1.6 x 10^{-4} M for 5*S*-SPTpT and K_d = 1.9 x 10^{-3} M for the repair product TpT. The dissociation constants for dinucleosides

were K_d = 4.8 x 10^{-3} M for 5*R*-SP, K_d = 9.6 x 10^{-4} M for 5*S*-SP and K_d = 1.6 x 10^{-2} M for the repair product thymidine.

The fluorescence lifetime decay experiments with undamaged 94-base pair double-stranded oligonucleotide showed no change in fluorescence lifetime. This is most likely due to the SPL's DNA binding region being too far from the tryptophan. It might also suggest that SPL binds non-specific DNA with different amino acids than at the spore photoproduct binding site.

Further Experiments: Repair of SP-Containing Oligonucleotide by SPL

Since we determined the repair rates for spore photoproduct dinucleoside and dinucleotide, the next step will involve repair assays with SP-containing DNA, which should be better a better substrate than SP dinucleotide or dinucleoside. First, damage on the DNA strand has to be created, which will be achieved by incorporating SP into an oligonucleotide. SP amidite (a precursor that can be used in DNA synthesis) has already been synthesized in our lab and now must be inserted into a 14-bp oligonucleotide (Scheme 4.2). To investigate the repair, the same method as for SP assays will be utilized. Briefly, *C.a.* SPL will be photo-reduced in the presence of deazariboflavin and added to SP-containing oligonucleotide under anaerobic conditions and the reaction will be quenched at different time points. The repair products will be detected by using HPLC and their identity will be further verified by co-injections of authentic compounds and by mass spectrometry.

During these repair assays SAM cleavage will also be investigated. Since SAM degradation during SP repair was previously observed, it would be interesting to investigate if it behaves as coenzyme or co-substrate during the repair of SP-containing oligonucleotide, which is the most relevant physiological substrate and should not result in SAM cleavage.

Further Experiments: SPL Binding to Undamaged and UV-Damaged Oligonucleotides

SPL specifically recognizes and repairs thymine photodimer, termed spore photoproduct (5-thyminyl-5,6-dihydrothymine) (39,44,142,146,189). Nicholson and co-workers proposed that SPL might be recognizing the DNA bend caused by the formation of SP in similar fashion DNA photolyase recognizes CPD-induced DNA bend (121,142). However there is no evidence if SPL binding is structure-specific. Therefore it would be interesting to investigate if the SP recognition happens due to SPL's higher affinity towards thymine nucleobases or due to structural differences of UV-irradiated DNA. The experiments could involve SPL binding assays with either GC-rich or AT-rich oligonucleotides in order to determine if SPL has higher affinity to one or another, providing some insight to how SPL finds damaged sites containing spore photoproduct.

Also, a new method to perform EMSA experiments could be developed that does not require oligonucleotide labeling with ^{32}P-ATP. Instead GelRed Nucleic Acid Stain (Biotium) could be employed to visualize DNA bands on the polyacrylamide gel. This method is much faster, easier and does not involve usage of radioactive materials.

Preliminary results showed that GelRed can be successfully utilized to detect protein-DNA complexes on the polyacrylamide gels (data not shown).

In order to determine the binding affinity of SPL to UV-damaged DNA, the experiments involving the SP-containing oligonucleotide and SPL could be carried out. For that purpose SP-containing DNA could be generated in two different ways. One, as mentioned previously, would involve incorporating spore photoproduct into synthetic DNA. The other method would involve UV-irradiating oligonucleotide, which carries two adjacent thymines, to create damage. HPLC then could be utilized to separate UV-damaged DNA from undamaged as described by Carell and co-workers, who carried out a similar experiment with a 6-bp oligonucleotide (49). The binding assays could then be performed by either EMSA or time-resolved fluorescence decay (as described previously) and K_d could be determined.

Other future work may include side-directed mutagenesis in order to create SPL mutants to determine which amino acids are involved in binding spore photoproduct. The mutations could involve amino acids from the predicted helix-turn-helix motif, which would clarify the role of this motif in SPL-DNA binding. Also, spore photoproduct lyase without the entire HTH region could be designed and over-expressed, and its binding properties investigated to determine if HTH is indeed involved in DNA binding.

REFERENCES CITED

1. Setlow, P. (2006) *Journal of Applied Microbiology* **101**, 514-525

2. Setlow, P. (2007) *Trends Microbiology* **15**, 172-180

3. Marquis, R. E., Shin, S.Y. (1994) *FEMS Microbiology Reviews* **14**, 375-380

4. Nicholson, W. L., Schuerger, A.C., Setlow, P. (2005) *Mutation Research* **571**, 249-264

5. Slepecky, R., Foster, J.W. (1959) *Journal of Bacteriology* **78**(1), 117-123

6. Bender, G. R., Marquis, R.E. (1985) *Applied and Environmental Microbiology*, 1414-1421

7. Ragkousi, K., Eichenberger, P., van Ooij, C., Setlow, P. (2003) *Journalof Bacteriology* **185**(7), 2315-2329

8. Paidhungat, M., Ragkousi, K., Setlow, P. (2001) *Journal of Bacteriology* **183**(16), 4886-4893

9. Setlow, B., Setlow, P. (1993) *Applied and Environmental Microbiology* **59**(2), 640-643

10. Slieman, T. A., Nicholson, W.L. (2000) *Photobiology*

11. Douki, T., Setlow, B., Setlow, P. (2005) *Photochemical and Photobiological Sciences* **4**(591-597)

12. Nicholson, W. L., Setlow, B., Setlow, P. (1991) *Proc. Natl. Acad. Sci.* **88**, 8288-8292

13. Nicholson, W. L., Setlow, B., Setlow, P. (1990) *Journal of Bacteriology* **172**(12), 6900-6906

14. Mohr, S. C., Sokolov, N.V.H., He, Ch., Setlow, P. (1991) *Proc. Natl. Acad. Sci.* **88**, 77-81

15. Francesconi, S. C., McAlister, Th.J., Setlow, B., Setlow, P. (1988) *Journal of Bacteriology* **170**(12), 5963-5967

16. Setlow, P. (2003) *Current Opinion in Microbiology* **6**, 550-556

17. Hackett, R. H., Setlow, P. (1988) *Journal of Bacteriology* **170**(3), 1403-1404

18. Douki, T., Setlow, B., Setlow, P. (2005) *Photochemistry and Photobiology* **81**, 163-169

19. Jedrzejas, M. J. (2002) *Medical Science Monitor* **8**(8), RA183-190

20. Kosman, J., Setlow, P. (2003) *Journal of Bacteriology* **185**(20), 6095-6103

21. Sohail, A., Hayes, C.S., Divvela, P., Setlow, P., Bhagwat, A.S. (2002) *Biochemistry* **41**, 11325-11330

22. Setlow, B., Sun, D., Setlow, P. (1992) *Journal of Bacteriology* **174**(7), 2312-2322

23. Nicholson, W. L., Setlow, B., Setlow, P. (1990) *Journal of Bacteriology* **172**(12), 6900-6906

24. Setlow, P. (1975) *The Journal of Biological Chemistry* **250**(20), 8168-8173

25. Hayes, C. S., Peng, Z-Y, Setlow, P. (2000) *The Journal of Biological Chemistry* **275**(45), 35040-35050

26. Lee, S. K., Bumbaca, D., Kosman, J., Setlow, P., Jedrzejas, M.J. (2008) *PNAS* **105**(8), 2806-2811

27. Hayes, C. S., Alarcon-Hernandez, E., Setlow, P. (2001) *The Journal of Biological Chemistry* **276**(3), 2267-2275

28. Frenkiel-Krispin, D., Sack, R., Englander, J., Shimoni, E., Eisenstein, E., Bullitt, E., Horowitz-Scherer, R., Hayes, C.S., Setlow, P., Minsky, A, Wolf, S.G. (2004) *Journal of Bacteriology* **186**(11), 3525-3530

29. Griffith, J., Makhov, A., Santiago-Lara, L., Setlow, P. (1994) *PNAS* **91**, 8224-8228

30. Setlow, B., Setlow, P. (1987) *Proc. Natl. Acad. Sci.* **84**(421-423)

31. Desnous, C., Guillaume, D., Clivio, P. (2009) *Chemical Reviews*

32. Moeller, R., Douki, T., Cadet, J., Stackebrandt, E., Nicholson, W.L., Rettberg, P., Reitz, G., Horneck, G. (2007) *International Microbiology* **10**, 39-46

33. Fajardo-Cavazos, P., Nicholson, W. L. (1995) *Journal of Bacteriology* **177**(15), 4402-4409

34. Munakata, N., Rupert, C.S. (1974) *Molecular Genetics and Genomics* **130**(3), 239-250

35. Fajardo-Cavazos, P., Salazar, C., Nicholson, W. L. (1993) *Journal of Bacteriology* **175**(6), 1735-1744

36. Pedraza-Reyes, M., Gutierrez-Corona, F., Nicholson, W.L. (1994) *Journal of Bacteriology* **176**, 3983-3991

37. Rebeil, R., Sun, Y., Chooback, L., Pedraza-Reyes, M., Kinsland, C., Begley, T. P., Nicholson, W. L. (1998) *Journal of Bacteriology* **180**(18), 4879-4885

38. Fajardo-Cavazos, P., Rebeil, R., Nicholson, W. L. (2005) *Current Microbiology* **51**, 331-335

39. Cheek, J., Broderick, J.B. (2002) *Journal of the American Chemical Society* **124**(12), 1860-2861

40. Guo, J.-D., Luo, Y., Himo, F. (2003) *Journal of Physical Chemistry B* **81**, 163-169

41. Himo, F. (2005) *Biochimica at Biophysica Acta* **1707**, 24-33

42. Buis, J. M., Cheek, J., Kalliri, E., Broderick, J.B. (2006) *The Journal of Biological Chemistry* **281**(36), 25994-26003

43. Chandor, A., Berteau, O., Douki, T., Gasparutto, D., Sanakis, Y., Ollagnier-de-Choudens, S., Atta, M., Fontecave, M. (2006) *Journal of Biological Chemistry* **281**(37), 26922-26931

44. Silver, S. C., Chandra, T., Zilinskas, E., Ghose, S., Broderick, W.E., Broderick, J.B. (2010) *Journal of Biological Inorganic Chemistry* **In Press**

45. Broderick, J. B., Henshaw, T.F., Cheek, J., Wojtuszewski, K., Smith, S.R., Trojan, M.R., McGhan, R.M., Kopf, A., Kibbey, M., Broderick, W.E. (2000) *Biochemical and Biophysical Research Communications* **269**, 451-456

46. Ollagnier-de Choudens, S., Fontecave, M. (1999) *FEBS Letters* **253**(1), 25-28
47. Rebeil, R., Nicholson, W. L. (2001) *PNAS* **98**(16), 9038-9043

48. Mehl, R. A., Begley, T.P. (1999) *Organic Letters* **1**(7), 1065-1066

49. Pieck, J. C., Hennecke, U., Pierik, A.J., Friedel, M.G., Carell, T. (2006) *Journal of Biological Chemistry* **281**(47), 36317-36326

50. Frey, P. A., Hegeman, A.D., Ruzicka, F.J. (2008) *Critical Reviews in Biochemistry and Molecular Biology* **43**, 63-88

51. Marsh, E. N. G., Patwardhan, A., Huhta, M.S. (2004) *Bioorganic Chemistry* **32**, 326-340

52. Sofia, H. J., Chen, G., Hetzler, B.G., Reyes-Spindola, J.F., Miller, N.E. (2001) *Nucleic Acids Research* **29**(5), 1097-1106

53. Jensen, K. P. (2006) *Journal of Inorganic Biochemistry* **100**, 1436-1439

54. Beinert, H., Holm, R.H., Munck, E. (1997) *Science* **277**, 653-658

55. Lukianova, O. A., David, S.S. (2005) *Current Opinion in Chemical Biology* **9**, 145-151

56. Johnson, D. C., Dean, D.R., Smith, A.D., Johnson, M.K. (2005) *Annual Reviews in Biochemistry* **74**, 247-281

57. Dey, A., Jenney Jr., F.E., Adams, M.W.W., Babini, E., Takahashi, Y., Fukuyama, K., Hodgson, K.O., Hedman, B., Solomon, E.I. (2007) *Solvent tuning of electrochemical potentials in the active sites of HiPIP versus ferredoxin* **318**(1464-1468)

58. Beinert, H. (2000) *Journal of Biological Inorganic Chemistry* **5**, 2-15

59. Sutton, V. R., Mettert, E.L., Beinert, H., Kiley, P.J,. (2004) *Journal of Bacteriology* **186**(23), 8018-8025

60. Crack, J. C., Gaskell, A.A., Green, J., Cheesman, M.R., Le Brun, N.E., Thomson, A.J. (2008) *Journal of the American Chemical Society* **130**, 1749-1758

61. Meyer, J. (2008) *Journal of Biological Inorganic Chemistry* **13**, 157-170

62. Peters, J. W., Szilagiy, R.K., Naumov, A., Douglas, T. (2006) *FEBS Letters* **580**, 363-367

63. Hu, Y., Corbett, M.C., Fay. A.W., Webber, J.A., Hedman, B., Hodgson, K.O., Ribbe, M.W. (2005) *Proc. Natl. Acad. Sci.* **102**(39), 1385-13830

64. Shah, V. K., Brill, W.J. (1981) *Proc. Natl. Acad. Sci.* **78**(6), 3438-3440

65. Chan, M. K., Kim, J., Rees, D.C. (1993) *Science* **260**(5109), 792-794

66. Bonam, D., Ludden, P.W. (1987) *Journal of Biological Chemistry* **262**(7), 2980-2987

67. Stripp, S., Sanganas, O., Happe, Th., Haumann, M. (2009) *Biochemistry*

68. Pandey, A. S., Harris, T.V., Giles, L.J., Peters, J.W., Szilagyi, R.K. (2008) *Journal of the American Chemical Society* **130**(13), 4533-4540

69. Ogata, O., Hirota, H., Nakahara, A., Komori, H., Shibata, N., Kato T., Kano, T., Higuchi, Y. (2005) *Structure* **13**, 1635-1642

70. Montet, Y., Garcin, E., Volbeda, A., Hatchikians, C., Frey, M., Fontecilla-Camps, J.C. (1998) *Pure and Applied Chemistry* **70**(1), 25-31

71. Walsby, C. H., Ortillo, D., Yang, J., Nnyepi, M.R., Broderick, W.E., Hoffman, B.M., Broderick, J.B. (2005) *Inorganic Chemistry* **44**(4), 727-741

72. Lotierzo, M., Raux, E., Tse Sum Bai, B., Goasdoue, N., Libot, F., Florentin, D., Warren, M.J., Marquet, A. (2006) *Biochemistry* **45**(12274-12281)

73. Ugulava, N. B., Frederick, K.K., Jarrett, J.T. (2003) *Biochemistry* **42**, 2708-2719

74. Frey, P. A., Hegeman, A.D., Reed, G.H. (2006) *Chemical Reviews* **106**, 3302-3316

75. Frey, P. A., Magnusson, O.Th. (2003) *Chemical Reviews* **103**, 2129-2148

76. Petrovich, R. M., Ruzicka, F.J., Reed, G.H., Frey, P.A. (1992) *Biochemistry* **31**(44), 10774-10781

77. Chen, D., Walsby, Ch., Hoffman, B.M., Frey, P.A. (2003) *Journal of the American Chemical Society* **125**, 11788-11789

78. Guianvarch'h, D., Florentin, D., Tse Sum Bui, B., Nunzi, F., Marquet, A. (1997) *Biochemical and Biophysical Research Communications* **236**, 402-406

79. Duschene, K. S., Veneziano, S.E., Silver, S.C., Broderick, J.B. (2009) *Current Opinion in Chemical Biology* **13**, 74-83

80. Fontecave, M., Atta, M., Mulliez, E. (2004) *TRENDS in Biochemical Sciences* **29**(5), 243-249

81. Grillo, M. A., Colombatto, S. (2005) *Amino Acids* **28**, 357-362

82. Markham, G. D. (2002) *Encyclopedia of Life Sciences*
83. Jeltsch, A. (2002) *ChemBioChem* **3**(274-293)

84. Lu, S. C. (2000) *The International Journal of Biochemistry & Cell Biology* **32**, 391-395

85. Knappe, J., Schacht, J., Mockel, W., Hopner, T., Vetter, H. J., Edenharder, R. (1969) *European Journal of Biochemistry* **11**(2), 316-327

86. Broderick, J. B., Duderstadt, R.E., Fernandez, D.C., Wojtuszewski, K., Henshaw, T.F., Johnson, M.K. (1997) *Journal of American Chemical Society* **119**(31), 7396-7387

87. Kulzer, R., Pils, Th., Kappl, R., Hutternmann, J., Knappe, J. (1998) *The Journal of Biological Chemistry* **273**(9), 4897-4903

88. Sun, X., Ollagnier, S., Schmidt, P.P., Atta, M., Mulliez, E., Lepape, L., Eliasson, R., Graslund, A., Fontecave, M., Reichard, P., Sjoberg, B-M. (1996) *The Journal of Biological Chemistry* **271**(12), 6827-6831

89. Ollagnier, S., Mulliez, E., Schmidt, P.P., Eliasson, R., Gaillard,J., Deronzier, C., Bergman, T., Graslund, A., Reichard, P., Fontecave, M. (1997) *The Journal of Biological Chemistry* **272**(39), 24216-24223

90. Chirpich, T. P., Zappia, V., Costilow, R. N., Barker, H. A. (1970) *Journal of Biological Chemistry* **245**(7), 1778-1789

91. Cosper, N. J., Booker, S.J., Ruzicka, F., Frey, P.A., Scott, R.A. (2000) *Biochemistry* **39**, 15668-15673

92. Baraniak, J., Moss, M. L., Frey, P. A. (1989) *Journal of Biological Chemistry* **264**(3), 1357-1360

93. Magnusson, O. T., Reed, G.H., Frey, P.A. (2001) *Biochemistry* **40**(26), 7773-7782

94. Magnusson, O. T., Reed, G.H., Frey, P.A. (1999) *The Journal of American Chemical Society* **121**, 9764-9765

95. Jarrett, J. T. (2005) *Archives of Biochemistry and Biophysics* **433**, 312-321

96. Fontecave, M., Ollagnier-de-Choudens, S., Mulliez, E. (2003) *Chemical Reviews* **103**, 2149-2166

97. Magnusson, O. T., Frey, P.A. (2003) *Chemical Reviews* **103**, 2129-2148

98. Hanzelman, P., Schindelin, H. (2004) *Proc. Natl. Acad. Sci.* **101**(35), 12870-12875

99. Layer, G., Moser, J., Heintz, D.W., Jahn, D., Schubert, W-D. (2003) *The EMBO Journal* **22**(23), 6214-6224

100. Curatti, L., Ludden, P.W., Rubio, L.M. (2006) *Proc. Natl. Acad. Sci.* **103**(5297-5301)

101. McGlynn, S. E., Mulder, D.W., Shepard, E.M., Broderick, J.B., Peters, J.P. (2009) *Dalton Transactions* **22**, 4274-4285

102. Cosper, M. M., Cosper, N.J., Hong, W., Shokes, J.E., Broderick, W.E., Broderick, J.B., Johnson, M.J., Scott, R.A. (2003) *Protein Science* **12**, 1573-1577

103. Hewitson, K. S., Baldwin, J.E., Shaw, M.N., Roach, P.L. (2000) *FEBS Letters* **466**, 372-376

104. Krebs, C., Henshaw, T.H., Cheek, J., Huynh,B.H., Broderick, J.B. . (2000) *Journal of the American Chemical Society* **122**(50), 12497-12506

105. Liu, A., Graslund, A. (2000) *The Journal of Biological Chemistry* **275**(17), 12367-12373

106. Ugulava, N. B., Sacanell, C.J., Jarrett, J.T. (2001) *Biochemistry* **40**, 8352-8358

107. Henshaw, T. F., Cheek, J., Broderick, J.B. (2000) *Journal of the American Chemical Society* **122**(34), 8331-8332

108. Walsby, C. H., Ortillo, D., Broderick, W.E., Broderick, J.B., Hoffman, B.M. (2002) *Journal of the American Chemical Society* **124**(38), 11270-11271

109. Walsby, C. H., Hong, W., Broderick, W.E., Cheek, J., Ortillo, D., Broderick, J.B., Hoffman, B.M. (2002) *The Journal of American Chemical Society* **124**(12), 3143-3151

110. Beinert, H., Kennedy, M.C., Stout, C.D. (1996) *Chemical Reviews* **96**, 2335-2373

111. Telser, J., Emptage, M.H., Merkle, H., Kennedy, M.C., Beinert, H., Hoffman, B.M. (1986) *The Journal of Biological Chemistry* **261**(4840-4846)

112. Werst, M. M., Kennedy, M.C., Houseman, A.L., Beinert, H., Hoffman, B.M. (1990) *Biochemistry* **29**(46), 10533-10540

113. Krebs, C., Broderick, W.E., Henshaw, T.H., Broderick, J.B., Huynh,B.H. (2002) *Journal of the American Chemical Society* **124**(6), 912-913

114. Hoffman, B. M. (2003) *Acc. Chem. Res.* **36**(7), 522-529

115. Berkovitch, F., Nicolet, Y., Wan, J.T., Jarrett, J.T., Drennan, C.L. (2004) *Science* **303**, 76-79

116. Nicolet, Y., Drennan, C.L. (2004) *Nucleic Acids Research* **32**(13), 4015-4025

117. Vey, J. L., Yang, J., Li, M., Broderick, W.E., Broderick, J.B., Drennan, C.L. (2008) *Proc. Natl. Acad. Sci.* **105**(42), 16137-16141

118. Lepore, B. W., Ruzicka, F.J., Frey, P.A., Ringe, D. (2005) *Proc. Natl. Acad. Sci.* **102**(39), 13819-13824

119. Layer, G., Kervio, E., Morlock, G., Heinz, D.W., Jahn, D., Retey J., Schubert, W-D. (2005) *Biological Chemistry* **386**, 971-980

120. Garvie, C. W., Wolberger, C. (2001) *Molecular Cell* **8**, 937-946

121. Mees, A., Klar, T., Gnau, P., Hennecke, U., Eker, A.P.M., Carell, T., Essen, L-O. (2004) *Science* **306**, 1789-1793

122. Kalodimos, C. G., Folkers, G.E., Boelens R., Kaptein R. (2001) *PNAS* **98**(11), 6039-6044

123. http://www.uniprot.org/uniprot/P37956.

124. Brennan, R. G., Mathews, B.W. (1989) *The Journal of Biological Chemistry* **264**(4), 1903-1906

125. Aravind, L., Anantharaman, V., Balaji, S., Mohan Babu, M., Iyer, L.M. (2005) *FEMS Microbiology Reviews* **29**, 231-262

126. Fromknecht, K., Vogel, P.D., Wise, J.G. (2003) *Journal of Bacteriology* **185**(2), 475-481

127. Czjzek, M., David, A.B., Bravman, T., Shoham, G., Henrissat, B., Shoham, Y. (2005) *Journal of Molecular Biology* **353**, 838-846

128. Tubbs, J. L., Pegg, A.E., Tainer, J.A. (2007) *DNA Repair* **6**, 1100-1115

129. Sancar, A. (2003) *Chemical Reviews* **103**, 2203-2237

130. Noort, v. J., Orsini, F., Eker, A., Wyman, C., Grooth, de B., Greve, J. (1999) *Nucleic Acids Research* **27**(19), 3875-3880

131. Cheng, X., Blumenthal, R.M. (1996) *Structure* **4**(6), 639-645

132. Priyakumar, U. D., MacKerell, A.D. Jr. (2006) *Chemical Reviews* **106**, 489-505

133. Scharer, O. D., Nash, H.M., Jiricny, J., Laval, J., Verdine, G.L. (1998) *The Journal of Biological Chemistry* **273**(15), 8592-8597

134. McCullough, A. K., Scharer, O., Verdine, G.L., Lloyd, R.S. (1996) *The Journal of Biological Chemistry* **271**(50), 32147-32152

135. Walker, R. K., McCullough, A.K., Lloyd, R.S. (2006) *Biochemistry* **45**(47), 14192-14200

136. Yang, C.-G., Yi, C., Duguid, E.M., Sullivan, C.T., Jian, X., Rice, Ph.A., He, Ch. (2008) *Nature* **452**(24), 961-966

137. Svoboda, D. L., Smith, C.A., Taylor, J-S.A., Sancar, A. (1993) *The Journal of Biological Chemistry* **268**(14), 10694-10700

138. Sancar, A. (1994) *Biochemistry* **33**, 2-9

139. Sancar, A., Smith, F.W., Sancar, G.B. (1984) *The Journal of Biological Chemistry* **259**(9), 6028-6032

140. Komori, H., Masui, R., Kuramitsu, S., Yokoyama, S., Shibata, T., Inoue, Y., Miki, K. (2001) *PNAS* **98**(24), 13560-13565

141. Carell, T., Burgdof, L.T., Kundu, L.M., Cichon, M. (2001) *Current Opinion in Chemical Biology* **5**, 491-498

142. Slieman, T. A., Rebeil, R., Nicholson, W.L. (2000) *Journal of Bacteriology* **182**(22), 6412-6417

143. Douki, T., Cadet, J. (2003) *Photochemical and Photobiological Sciences* **2**, 433-436

144. Kim, S. J., Lester, C., Begley, T.P. (1995) *The Journal of Organic Chemistry* **60**(20), 6256-6257

145. Friedel, M. G., Carsten Pieck, J., Klages, J., Dauth, C., Kessler, H., Carell, T. (2006) *Chemistry - A European Journal* **12**, 6081-6094

146. Chandra, T., Silver, S.C., Zilinskas, E., Shepard, E.M., Broderick, W.E., Broderick, J.B. (2009) *Journal of the American Chemical Society* **131**(7), 2420-2421

147. Chandor, A., Douki, T., Gasparutto, D., Sanakis, Y., Gambarelli, S., Sanakis, Y., Nicolet, Y., Ollagnier-de-Choudens, S., Atta, M., Fontecave, M. (2007) *Comptes Rendus Chimie* **10**, 756-765

148. Friedel, M. G., Berteau, O., Pieck, J.C., Atta, M., Ollagnier-de-Choudens, S., Fontecave, M., Carell, T. (2006) *Chemical Communications*, 445-447

149. Burckstummer, E., Carell, T. (2008) *Chemical Communications*, 4037-4039

150. Mantel, C., Chandor, A., Gasparutto, D., Douki, T., Atta, M., Fontecave, M., Bayle, P-A., Mouesca, J-M., Bardet, M. (2008) *The Journal of American Chemical Society* **130**(50), 16978-16984

151. Chandra, T., Broderick, W.E., Broderick, J.B. (2009) *Nucleosides, Nucleotides and Nucleic Acids* **28**(11), 1016-1029

152. Bradford, M. (1976) *Analytical Biochemistry* **72**, 248

153. Fish, W. W. (1988) *Methods in Enzymology* **158**, 357-364

154. Beinert, H. (1978) *Methods in Enzymology* **54**, 435-445

155. Layer, G., Grage, K., Teschner, T., Schunemann, V., Breckau, D., Masoumi, A., Jahn, M., Heathcote, P., Trautwein, A.X., Jahn, D. (2005) *The Journal of Biological Chemistry* **280**(32), 29038-29046

156. Rubach, J. K., Brazzolotto, X., Gaillard, J., Fontecave, M. (2005) *FEBS Letters* **579**, 5055-5060

157. Saito, K., Kikuchi, T., Yoshida, M. (1999) *Protein Engineering* **12**(3), 235-242

158. Chen, X. J., Wang, X., Butow, R.A. (2007) *PNAS* **104**(34), 13738-13743

159. Misteli, T. (2001) *Science* **291**(2), 843-847

160. Agback P., B. H., Kanpp S., Ladenstein R., Hard T. (1998) *Nature Structural Biology* **5**(7), 579-584

161. Noort van J., O. F., Eker A., Wyman C., Grooth de B., Greve J. (1999) *Nucleic Acids Research* **27**(19), 3875-3880

162. Yang K., S. R. J. (2006) *Biochemistry* **45**, 11239-11245

163. Weber, S., Richter, G., Schleicher, E., Bacher, A., Mobius, K., Kay, C.W.M. (2001) *Biophysical Journal* **81**, 1195-1204

164. Kalodimos, C. G., Biris, N., Bonvin, Alexandre, M.J.J., Levandovski, M.M., Guennuegues, M., Boelens, R., Kaptein, R. (2004) *Science* **305**, 386-389

165. Baer, E., Sancar, G.B. (1993) *The Journal of Biological Chemistry* **268**(22), 16717-16724

166. Sancar, G. B., Smith, F.W., Sancar, A. (1985) *Biochemistry* **24**, 1849-1855

167. Husain, I., Sancar, A. (1987) *Nucleic Acids Research* **15**(3), 1109-1120

168. Sancar, G. B., Smith, F.W., Reid, R., Payne, G., Levy, M., Sancar, A. (1987) *The Journal of Biological Chemistry* **262**(1), 478-485

169. Huai, Q., Colandene, J.D., Chen, Y., Luo, F., Zhao, Y., Topal, M.D., Ke, H. (2000) *The EMBO Journal* **19**(12), 3110-3118

170. www.scripps.edu/~cdputnam/protcalc.html.

171. Manuel, R. C., Czerwinski, E.W., Lloyd, R.S. (1996) *The Journal of Biological Chemistry* **271**(27), 16218-16226

172. Kuo, C. F., McRee, D.E., Fisher, C.L., O'Handley, S.F., Cunningham, R.P., Tainer, J.A. (1992) *Science* **258**(5081), 434-440

173. Setlow, B., McGinnis, K.A., Ragkousi, K., Setlow, P. (2000) *Journal of Bacteriology* **182**(24), 6906-6912

174. Husain, I., Sancar, G.B., Holbrook, S.R., Sancar, A. (1987) *The Journal of Biological Chemistry* **262**(27), 13188-13197

175. Kiener, A., Husain, I., Sancar, A., Walsh, C. (1989) *The Journal of Biological Chemistry* **264**(23), 13880-13887

176. Hitomi, K., Kim, S-T., Iwai, S., Harima, N., Otoshi, E., Ikenaga, M., Todo, T. (1997) *The Journal of Biological Chemistry* **272**(51), 32591-32598

177. Hitomi K., K. S.-T., Iwai S., Harima N., Otoshi E., Ikenaga M., Todo T. (1997) *The Journal of Biological Chemistry* **272**(51), 32591-32598

178. Neely, R. K., Daujotyte, D., Grazulis, S., Magennis, S.W., Dryden, D.T.F., Klimasauskas, S., Jones, A.C. (2005) *Nucleic Acids Research* **33**(22), 6953-6960

179. Christine, K. S., MacFarlane IV, A.W., Yang, K., Stanley, R.J. (2002) *The Journal of Biological Chemistry* **277**(41), 38339-38344

180. Jordan, S. P., Alderfer, J.L., Chanderkar, L.P., Jorns, M.S. (1989) *Biochemistry* **28**(20), 8149-8153

181. Jordan, S. P., Jorns, M.S. (1988) *Biochemistry* **27**, 8915-8923

182. Schlick, K. H., Lange, C.K., Gillispie, G.D., Cloninger, M.J. (2009) *The Journal of American Chemical Society* **131**, 16608-16609

183. Kim, S.-T., Sancar, A. (1991) *Biochemistry* **30**, 8623-8630

184. Busta, F. F., Ordal, Z.J. (1964) *Applied Microbiology* **12**(2), 106-110

185. Fields, M. L., Frank, H.A. (1969) *Journal of Bacteriology* **97**(1), 464-465

186. Jaye, M., Ordal, Z.J. (1965) *Journal of Bacteriology* **89**(6), 1617-1618

187. Gillispie, G. D. *Manuscript in preparation*

188. Lakowicz, J. R. (2006) *Principles of Fluorescence Spectroscopy*, 3rd Ed., Springer, New York